

Reproduced by

Armed Services Technical Information Agency

**DOCUMENT SERVICE CENTER**

KNOTT BUILDING, DAYTON, 2, OHIO

**AD -**

**3**

**0**

**7**

---

**UNCLASSIFIED**

TECHNICAL REPORT NO. 1

*An Investigation on the*  
DYNAMIC PROPERTIES OF PLASTICS AND RUBBER-LIKE MATERIALS

Contract No. N7on 3.11

Project No. NR 06-3.1

Sponsored by  
Office of Naval Research  
Department of the Navy

at  
MECHANICS DEPARTMENT  
ILLINOIS INSTITUTE OF TECHNOLOGY  
TECHNOLOGY CENTER  
CHICAGO, ILLINOIS

304

Technical Report No. 1

An Investigation on the  
DYNAMIC PROPERTIES OF PLASTICS AND RUBBER-LIKE MATERIALS

by

R. A. Eubanks, D. Muster, E. G. Volterra

Contract No. N7onr-32911  
Project No. NR 064 369

Sponsored by

Office of Naval Research  
Department of the Navy

at

Mechanics Department  
Illinois Institute of Technology  
Technology Center  
Chicago, Illinois

Dated: 14 June 1952

ARMY

Commanding Officer  
Frankford Arsenal  
Philadelphia, Pennsylvania  
Attn: Laboratory Division (1)

Commanding Officer  
Squier Signal Laboratory  
Fort Monmouth, New Jersey  
Attn: Components and Materials  
Branch (1)

NAVY

Chief, Bureau of Ships  
Department of the Navy  
Washington 25, D. C.  
Attn: Director of Research (1)  
Code 371 (2)

Commanding Officer and Director  
David Taylor Model Basin  
Washington 7, D.C.  
Attn: Structural Mechanics Div. (2)  
Library (1)  
Acoustics Division (1)

Director  
Naval Engr'g. Experiment  
Station  
Annapolis, Maryland  
Attn: Wave Mechanics Lab. (2)

Director  
Materials Laboratory  
New York Naval Shipyard  
Brooklyn, New York (2)

Chief, Bureau of Ordnance  
Department of the Navy  
Washington 25, D. C.  
Attn: Ad-3, Technical Library (1)  
Rec, P. H. Girouard (1)

Superintendent  
Naval Gun Factory  
Washington 25, D. C. (1)

NAVY

Naval Ordnance Laboratory  
White Oak, Maryland  
RFD 1, Silver Spring, Md.  
Attn: Mechanics Division (2)

Naval Ordnance Test Station  
Inyokern, California  
Attn: Scientific Officer (1)

Naval Ordnance Test Station  
Underwater Ordnance Division  
Pasadena, California  
Attn: Structures Division (1)

Chief, Bureau of Aeronautics  
Department of the Navy  
Washington 25, D. C.  
Attn: TD-41, Tech. Lib. (1)  
DE-22, C. W. Hurley (1)

Naval Air Experiment Station  
Naval Air Material Center  
Naval Base  
Philadelphia 12, Pa.  
Attn: Head, Aeronautical  
Materials Lab. (1)

Chief, Bureau of Yards and  
Docks  
Department of the Navy  
Washington 25, D. C.  
Attn: Code P-314 (1)  
Code P-313 (1)

Officer in Charge  
Naval Civil Engr'g. Research  
and Evaluation Laboratory  
Naval Station  
Port Hueneme, California (1)

Superintendent  
Post Graduate School  
U. S. Navy  
Monterey, California (1)

Chief, Bureau of Ships  
Department of the Navy  
Washington 25, D. C.  
Attn: Code 324 (2)

Commander  
Mare Island Naval Shipyard  
Vallejo, California  
Attn: Rubber Laboratory (1)

Naval Ordnance Laboratory  
White Oak, Maryland  
RFD 1, Silver Spring, Maryland  
Attn: Mr. Snavely (1)

Commanding Officer and Director  
U.S.N. Underwater Sound Lab.  
Fort Trumbull  
New London, Connecticut (1)

British Joint Services Mission  
Navy Staff  
1910 K Street, N.W.  
Washington, D. C. (1)

#### AIR FORCES

Commanding General  
U. S. Air Forces  
The Pentagon  
Washington 25, D. C.  
Attn: Research and Development  
Division (1)

Commanding General  
Wright-Patterson Air Force Base  
Wright Air Development Center  
Dayton, Ohio  
Attn: Mr. E. H. Schwartz (1)  
(WCR) Materials Lab. (1)  
Chief, Applied Mechanics (1)  
Flight Research Lab. (1)

#### OTHER GOVERNMENT AGENCIES

U. S. Atomic Energy Commission  
Division of Research  
Washington, D. C. (1)

Director  
National Bureau of Standards  
Washington, D. C.  
Attn: Mechanics Division (1)  
Sound Division (1)

National Advisory Committee  
for Aeronautics  
1724 F Street, N. W.  
Washington, D. C. (1)

National Advisory Committee  
for Aeronautics  
Langley Field, Virginia  
Attn: Mr. E. Lundquist (1)

National Advisory Committee  
for Aeronautics  
Cleveland Municipal Airport  
Cleveland, Ohio  
Attn: J. H. Collins, Jr. (1)

Commanding General  
Headquarters, Air Research  
and Development Command  
P. O. Box 1395  
Baltimore 3, Maryland  
Attn: Office of Scientific  
Research, RDRF (1)

Office of Ordnance Research  
Durham, North Carolina (1)

#### COAST GUARD

U. S. Coast Guard  
1300 E Street, N.W.  
Washington, D. C.  
Attn: Chief, Testing and  
Development Div. (1)

Contractors and Other Investigators  
Actively Engaged in Related Research

<p>Professor L. S. Jacobsen Stanford University Stanford, California</p>	<p>(1)</p>	<p>Professor T. J. Dolan Department of Theoretical and Applied Mechanics University of Illinois Urbana, Illinois</p>	<p>(1)</p>
<p>Professor W. K. Krefeld College of Engineering Columbia University New York, New York</p>	<p>(1)</p>	<p>Dr. Martin Goland Midwest Research Institute 4049 Pennsylvania Avenue Kansas City 2, Missouri</p>	<p>(1)</p>
<p>Professor N. J. Hoff, Head Department of Aeronautical Engineering and Appl. Mech. Polytechnic Institute of Brooklyn 99 Livingston Street Brooklyn 2, New York</p>	<p>(1)</p>	<p>Dr. W. H. Hoppmann Department of Applied Mechanics Johns Hopkins University Baltimore, Maryland</p>	<p>(1)</p>
<p>Dr. N. M. Newmark Department of Civil Engineering University of Illinois Urbana, Illinois</p>	<p>(1)</p>	<p>Dr. R. P. Petersen Director, Appl. Physics Div. Sandia Laboratory Albuquerque, New Mexico</p>	<p>(1)</p>
<p>Dr. J. N. Goodier School of Engineering Stanford University Stanford, California</p>	<p>(1)</p>	<p>Professor A. C. Eringen Illinois Institute of Tech- nology Technology Center Chicago 16, Illinois</p>	<p>(1)</p>
<p>Dr. A. Phillips School of Engineering Stanford University Stanford, California</p>	<p>(1)</p>	<p>Professor B. J. Lazan University of Minnesota Minneapolis, Minnesota</p>	<p>(1)</p>
<p>Dr. W. Prager Graduate Div. of Appl. Mathe- matics Brown University Providence, Rhode Island</p>	<p>(1)</p>	<p>Professor Paul Lieber Department of Aeronautical Engr'g. and Appl. Mech- anics Rensselaer Polytechnic Inst. Troy, New York</p>	<p>(1)</p>
<p>Professor P. W. Bridgeman Department of Physics Harvard University Cambridge, Massachusetts</p>	<p>(1)</p>	<p>Dr. Eugene Guth, Director Department of Physics Notre Dame University Notre Dame, Indiana</p>	<p>(1)</p>
<p>Dr. J. H. Hollomon General Electric Research Lab. 1 River Road Schenectady, New York</p>	<p>(1)</p>		

## TABLE OF CONTENTS

	Page
DISTRIBUTION LIST . . . . .	i
TABLE OF CONTENTS . . . . .	vi
LIST OF FIGURES . . . . .	viii
LIST OF TABLES . . . . .	xi
SECTION I. Introduction . . . . .	1
SECTION II. Description and Use of the Apparatus for Testing Materials at Low Rates of Straining.	5
A. General description of the apparatus . . . . .	6
B. Theory of the method . . . . .	12
C. Degree of accuracy of the mechanical and optical methods employed . . . . .	16
D. Direct computation of the dynamic stress- strain curves for a given material, with known hereditary characteristics, under impact loading . . . . .	18
1. Heredity of the first degree . . . . .	19
2. Heredity of the first degree with residual . . . . .	20
3. Heredity of the second degree . . . . .	21
4. Heredity of the second degree with residual . . . . .	22
E. Determination of the hereditary characteristics of a material from the experimental dynamic stress-strain curves . . . . .	23
SECTION III. Description and Use of Apparatus for Testing Materials at High Rates of Straining . . . . .	25
A. General description of the mechanical apparatus . . . . .	26

	Page
B. Theory of the method . . . . .	32
Boundary and initial conditions . . . . .	36
Case I - Elastic specimen . . . . .	37
Case II - Elasto-viscous specimen . . . . .	38
Case III - Hereditary specimen . . . . .	41
Case IV - Elastic specimen - approximate . . . . .	46
Case V - Elasto-viscous specimen - approximate . . . . .	48
Case VI - Hereditary specimen - approximate . . . . .	49
C. Mathematical analysis of the longitudinal impact of a round-head short bar on an infinitely long bar . . . . .	50
SECTION IV. Sample Computation and Discussion of Test Results for Natural Rubber (Hevea). . . . .	73
APPENDIX A. Mathematical Analysis of the Longitudinal Impact of a Ball on an Infinitely Long Bar . . . . .	96
APPENDIX B. Rubber Specimen Recipes . . . . .	106
BIBLIOGRAPHY . . . . .	110
CONTRIBUTING PERSONNEL . . . . .	112

## LIST OF FIGURES

	Page
Figure 1 Front View - Camera . . . . .	7
Figure 2 Back View - Camera . . . . .	8
Figure 3 Schematic Diagram of Equipment Arrangement - Optical Method . . . . .	9
Figure 4 Schematic Diagram of Optical System - Optical Method . . . . .	10
Figure 5 Static Testing Machine . . . . .	13
Figure 6 Rigid Car - Rubberlike Specimen Model . . . . .	14
Figure 7 View of Assembled Equipment - Strain-Gage Method . . . . .	27
Figure 8 Pulse-Time Relations for Figure 5 . . . . .	33
Figure 9 Schematic Diagram of Material Models . . . . .	35
Figure 10 Bromwich Contour - Viscous . . . . .	42
Figure 11 Bromwich Contour - Hereditary . . . . .	42
Figure 12 Round-Head Hammer Impact. . . . .	54
Figure 13 Stress-Time Relationships . . . . .	57
Figure 14 Stress-Time Relationships . . . . .	58
Figure 15 Stress-Time Relationships . . . . .	59
Figure 16 Stress-Time Relationships . . . . .	60
Figure 17 Stress-Time Relationships . . . . .	61
Figure 18 Stress-Time Relationships . . . . .	62
Figure 19 Stress-Time Relationships . . . . .	63
Figure 20 Stress-Time Relationships . . . . .	64
Figure 21 Stress-Time Relationships . . . . .	65

	Page
Figure 22 Stress-Time Relationships . . . . .	66
Figure 23 Stress-Time Relationships . . . . .	67
Figure 24 Stress-Time Relationships . . . . .	68
Figure 25 Stress-Time Relationships . . . . .	69
Figure 26 Stress-Time Relationships . . . . .	70
Figure 27 Stress-Time Relationships . . . . .	71
Figure 28 Stress-Time Relationships . . . . .	72
Figure 29 Displacement-Time Curves, Nominal velocity 25 cm/sec . . . . .	77
Figure 30 Displacement-Time Curves, Nominal velocity 50 cm/sec . . . . .	78
Figure 31 Displacement-Time Curves, Nominal velocity 75 cm/sec . . . . .	79
Figure 32 Static True Stress - True Strain Natural Rubber (Hevea) . . . . .	87
Figure 33 Hereditary Function, Nominal velocity 25 cm/sec . . . . .	88
Figure 34 Hereditary Function, Nominal velocity 50 cm/sec . . . . .	89
Figure 35 Stress versus Strain - Viscous Analysis Nominal velocity 25 cm/sec . . . . .	90
Figure 36 Stress versus Strain - Viscous Analysis Nominal velocity 50 cm/sec . . . . .	91
Figure 37 Stress versus Strain - Viscous Analysis Nominal velocity 75 cm/sec . . . . .	92
Figure 38 Stress versus Strain - Hereditary Analysis Nominal velocity 25 cm/sec . . . . .	93
Figure 39 Stress versus Strain - Hereditary Analysis Nominal velocity 50 cm/sec . . . . .	94

	Page
Figure 40 Ball Impact - $v_o = 45$ cm/sec . . .	100
Figure 41 Ball Impact - $v_o = 90$ cm/sec . . .	101
Figure 42 Ball Impact - $v_o = 135$ cm/sec. . .	102
Figure 43 Ball Impact - $v_o = 180$ cm/sec. . .	103
Figure 44 Ball Impact - $v_o = 220$ cm/sec. . .	104

## LIST OF TABLES

		Page
Table 1	Theoretical Time of Contact in Micro-seconds as a Function of Height of Drop and Hammer Length . . . . .	31
Table 2	Height of Drop Versus Velocity and Limiting Stress . . . . .	55
Table 3	Critical Values for Figures 13 Through 28 . . . . .	56
Table 4	Results - Viscous Case . . . . .	86
Table 5	Results - Hereditary Case . . . . .	86
Table 6	Ball Impact Values . . . . .	99
Table 7	Rubber Specimen Formulas . . . . .	107
Table 8	Summary of Physical Properties of Rubber Compounds given in Table 7 . . . . .	108

SECTION I  
INTRODUCTION

## SECTION I

### Introduction

The object of this technical report is to inform the Office of Naval Research on the present status of their Project NR 064 369, Contract No. N7onr-32911, "The Dynamic Properties of Plastics and Rubber-like Materials", which is being conducted by the Department of Mechanics at Illinois Institute of Technology.

Two apparatuses are being used to study the effects of dynamic loading on materials:

The first uses mechanical and optical devices to determine directly the stress-strain curves of plastic and rubber-like materials subjected to impact loads, the durations of which are of the order of milliseconds.

The second apparatus, which is only partially built, will use mechanical and electronic devices to determine the stress-strain curves of elastic materials subjected to impact loads, the durations of which will be of the order of microseconds.

In this report a general description of the apparatuses is presented and the theories of both methods are outlined briefly. The mechanical and optical parts of the apparatus for testing materials at low rates of compressive straining are described, the theory of the experimental method is outlined, and the influence of the principal causes of mechanical and optical

error associated with the method are evaluated. It is shown how the dynamic stress-strain curves for a given specimen under impact loading can be calculated directly, when the hereditary characteristics of the material are known. By comparing the experimental and calculated curves it is possible then to determine the accuracy of this experimental method of investigating the dynamic properties of materials. Some results are given for a natural rubber of 30-durometer hardness.

The component mechanical devices and electronic equipment for testing materials at higher rates of compressive straining are described and the theory of the method is given.

A mathematical analysis of the longitudinal impact of a round-headed, short bar on an infinitely long bar is presented. This study follows that given by W. A. Prowse [1], [2], [3], [4], but the analysis is extended so as to give final results in an explicit form more suitable for numerical computation.

The propagation of a stress wave of known characteristics through a cylindrical specimen held between the flat ends of two elastic bars is analyzed. Three specimens are considered, namely, one made of a purely elastic material, and a second and third made of materials which display elasto-viscous and hereditary characteristics, respectively. An approximate solution of the problem is given in the report for each of these specimens. Further, a more elaborate and complete theory of the same problems is indicated. In Appendix A a mathematical analysis of the

longitudinal impact of a ball on an infinitely-long cylindrical bar is given. The final results of this analysis are presented in tabular form for given initial velocities of the impinging balls.

SECTION II

DESCRIPTION AND USE OF THE APPARATUS FOR TESTING MATERIALS

AT LOW RATES OF COMPRESSIVE STRAINING

## SECTION II

### Description and Use of the Apparatus for Testing Materials at Low Rates of Straining

#### A. General description of the apparatus

The apparatus employed in these experiments is shown in Figures 1 and 2 and in the schematic diagram of Figures 3 and 4. It consists essentially of:

- 1) two 3-foot, steel bars of equal mass suspended as ballistic pendulums;
- 2) a rotating-drum camera, the drum of which rotates at a known speed, and the shutter of which is synchronized to operate with the motion of the steel bars;
- 3) an optical system which focuses the image of a very thin slit on the knife edges machined on the adjoining ends of the steel bars (a cylindrical specimen to be tested is mounted between the two bar ends on which the knife ends are machined);
- 4) an electromagnetic device which can release one or both of the bars at the same time.

The cylindrical specimens of the rubber or rubber-like materials are 1/2-inch in diameter and 1/2-inch long. The first group of specimens has been fabricated from the following materials:

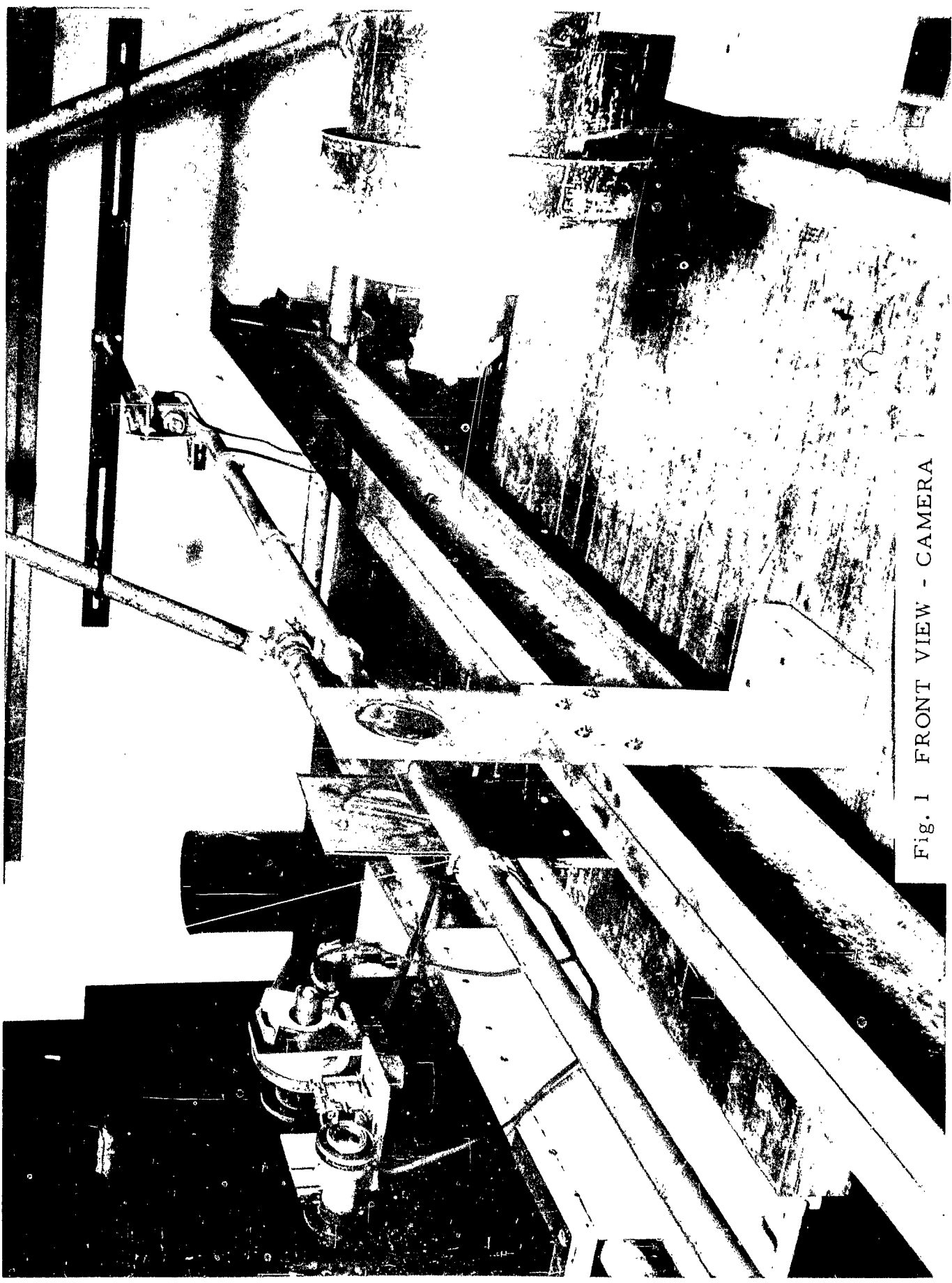
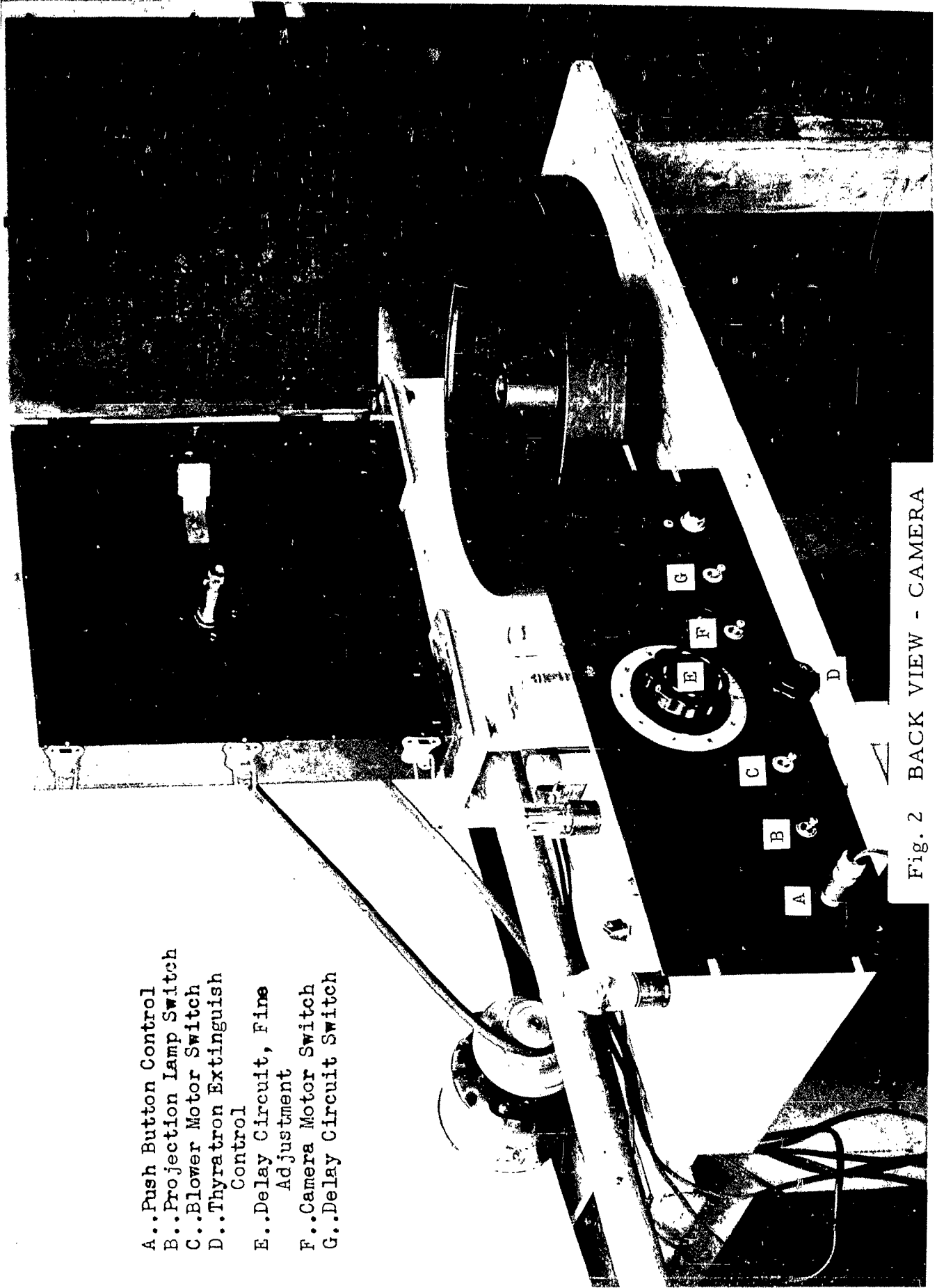


Fig. 1 FRONT VIEW - CAMERA



- A..Push Button Control
- B..Projection Lamp Switch
- C..Blower Motor Switch
- D..Thyratron Extinguish Control
- E..Delay Circuit, Fine Adjust
- F..Camera Motor Switch
- G..Delay Circuit Switch

Fig. 2 BACK VIEW - CAMERA

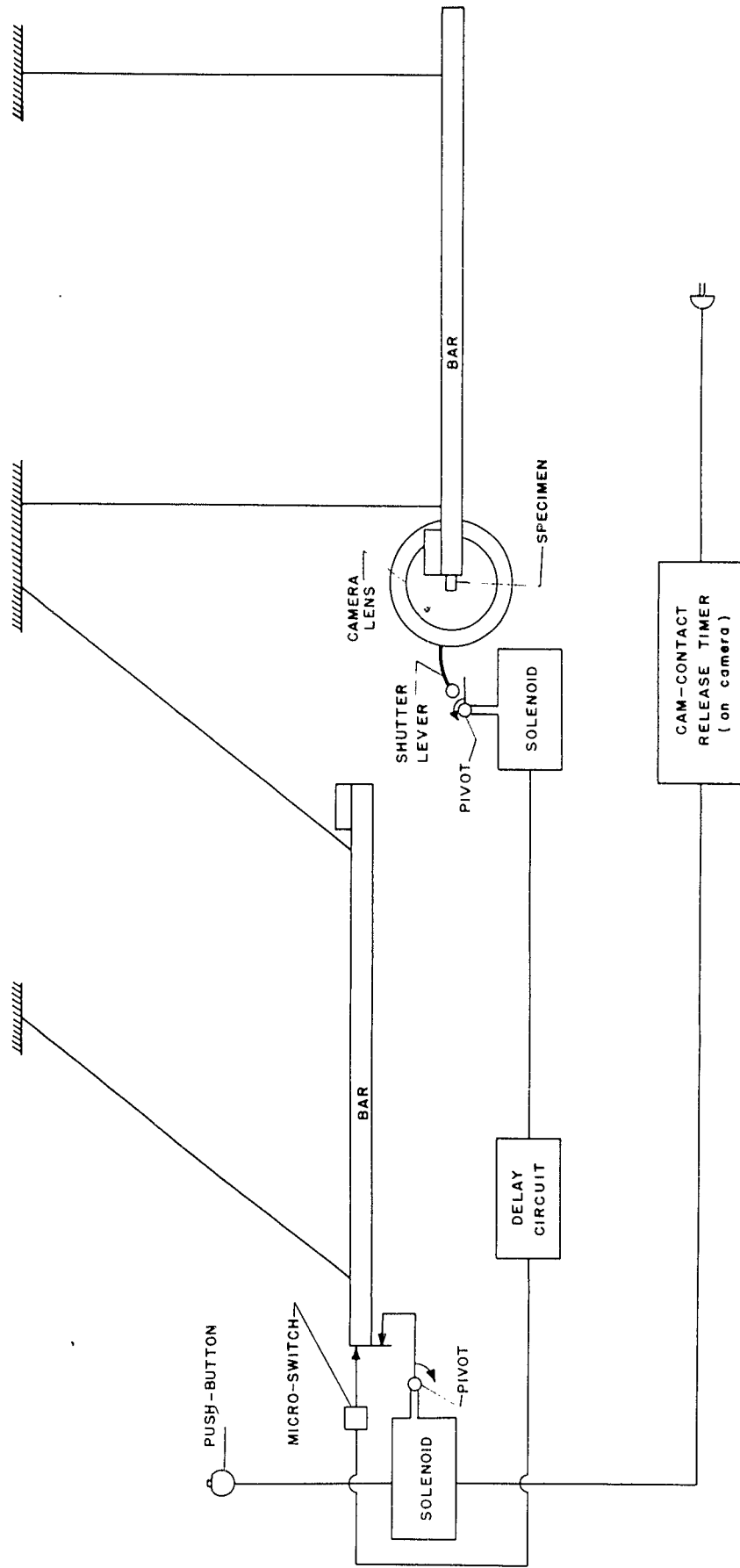


Fig. 3 SCHEMATIC DIAGRAM OF EQUIPMENT ARRANGEMENT - OPTICAL METHOD

Figure 4. Schematic diagram of optical system.

- P....Projection Lamp, GE 750T12P
- G....Ground-Glass Plate, 2 in. x 3 in.
- S....Slit, 0.001 in. x 7/8 in.
- K....Knife Edges on bars
- M....Mirror, first-surface set at  $45^\circ$   
to axis of lens arrangement
- F....Film, Kodak Linagraph Panchromatic LP421
- L<sub>1</sub>...Condensing Lens, 6 in. f/l, 4-7/16 in. diam.
- L<sub>2</sub>...Projection Lens, 75mm f/l, 49mm diam coated  
achromat
- L<sub>3</sub>...Plano Convex Field Lens, 17 in. f/l, 3-1/2 in.  
diam.
- L<sub>4</sub>...Plano Convex Field Lens, 21 in f/l, 3-1/2 in.  
diam.
- L<sub>5</sub>...Camera Lens, Color Skopar f/3.5, 105 mm f/l

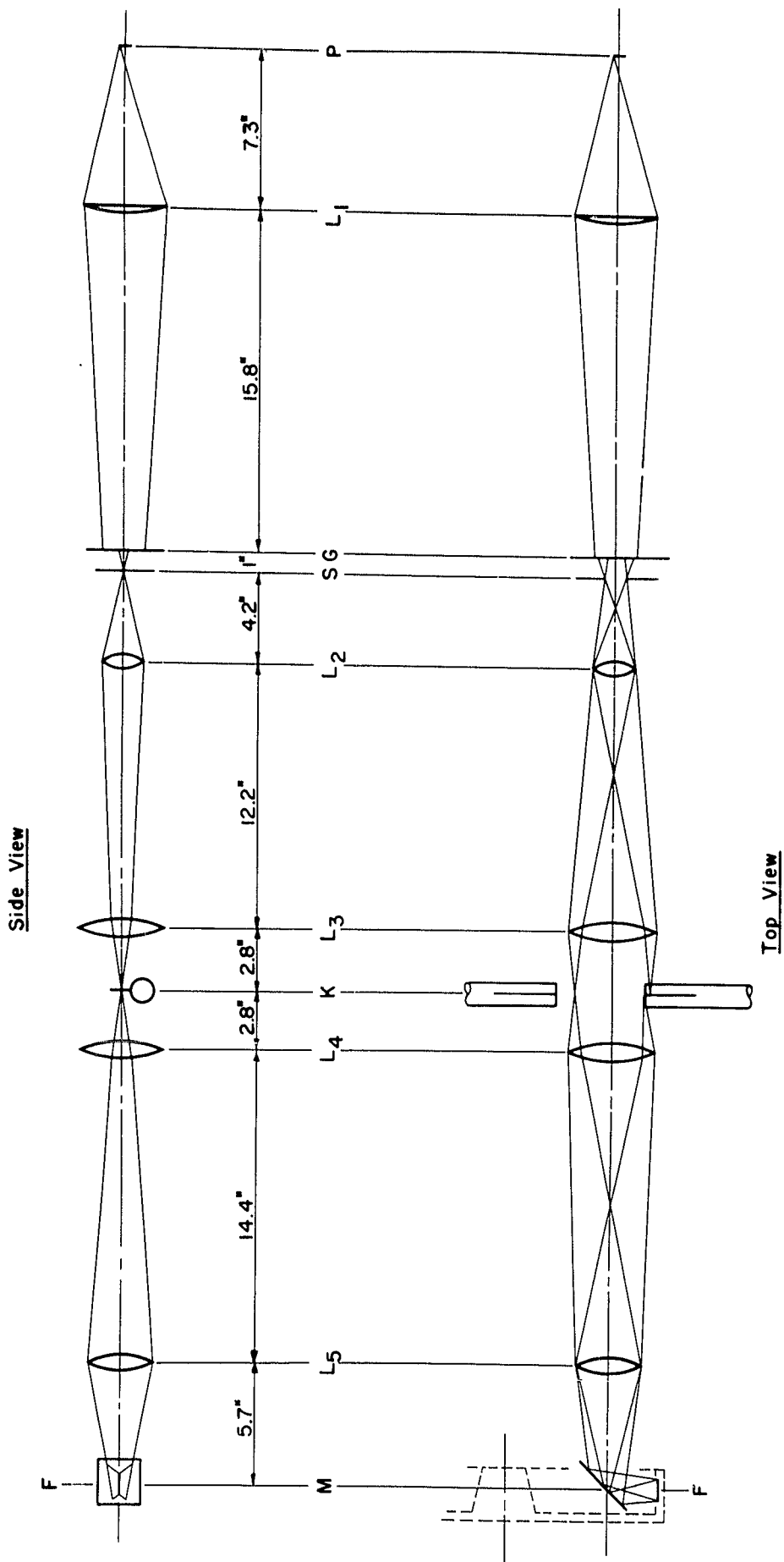


Fig. 4 SCHEMATIC DIAGRAM OF OPTICAL SYSTEM - OPTICAL METHOD

- a. Natural rubber (27-30 Durometer hardness)
- b. Butyl-25 (35-40 Durometer hardness)
- c. Neoprene GN (35-40 Durometer hardness)
- d. Hycar OR-15 (35-40 Durometer hardness)
- e. Buna-N (35-40 Durometer hardness)
- f. GRS-1585 (35-40 Durometer hardness)

The recipes for the rubber specimens are given in Appendix C. The second group will be fabricated from the same materials, but in about 70 Durometer hardness.

The specimens are placed on the plane end of one of the steel bars such that the longitudinal axis of the bar and the specimen coincide. The other steel bar is released from a predetermined height and made to impinge upon the free end of the specimen. During the impact, a photograph is taken of the interval between the knife edges which lie in the plane of the ends of the steel bars. The film is calibrated by taking a still photograph of the interval when both bars are barely in contact with the specimen.

The deformation of the specimen at succeeding instants of time is measured directly on the film by means of a traveling microscope. This instrument is fitted with two orthogonal, independent motions, each calibrated to read a total excursion of 4.5 inches in increments of 0.001 inch. From these measurements it is possible to deduce the dynamic stress-strain relationship of the specimen.

With certain modifications, the same apparatus will be used to test specimens at ambient temperatures other than room

temperature. A small chamber will be constructed which will completely enclose the specimen and yet not interfere with any of the moving parts necessary to conduct the tests. Preliminary designs of the chamber have been considered and it will be constructed when the testing program at room temperature has been completed. With acetone and dry ice (or possibly another solvent) it should be possible to conduct tests at ambient temperatures of  $-68^{\circ}\text{F}$ , and, with hot water, at  $+158^{\circ}\text{F}$ . These devices are not described in this report but will be discussed more completely in a later technical report.

A static testing device has been built and is shown in Figure 5. Static loads up to 200 pounds can be applied to the specimen and a maximum deformation of 1-inch can be measured to within 0.00025 inch. The same size specimens (1/2-inch x 1/2-inch cylinders) are used for the static tests. Compression set tests of each rubber stock are being conducted concurrently by the staff of the Rubber Laboratory, Armour Research Foundation, an affiliate of IIT.

#### B. Theory of the Method

In Figure 6 let  $F(t)$  represent the compressive force acting on the specimen at the instant  $t$  measured from the instant  $t = 0$ , at which time the impinging bar first contacts the specimen. Let  $x_1(t)$  and  $x_2(t)$  be the horizontal displacements of the two extremities of the bars measured from their position at

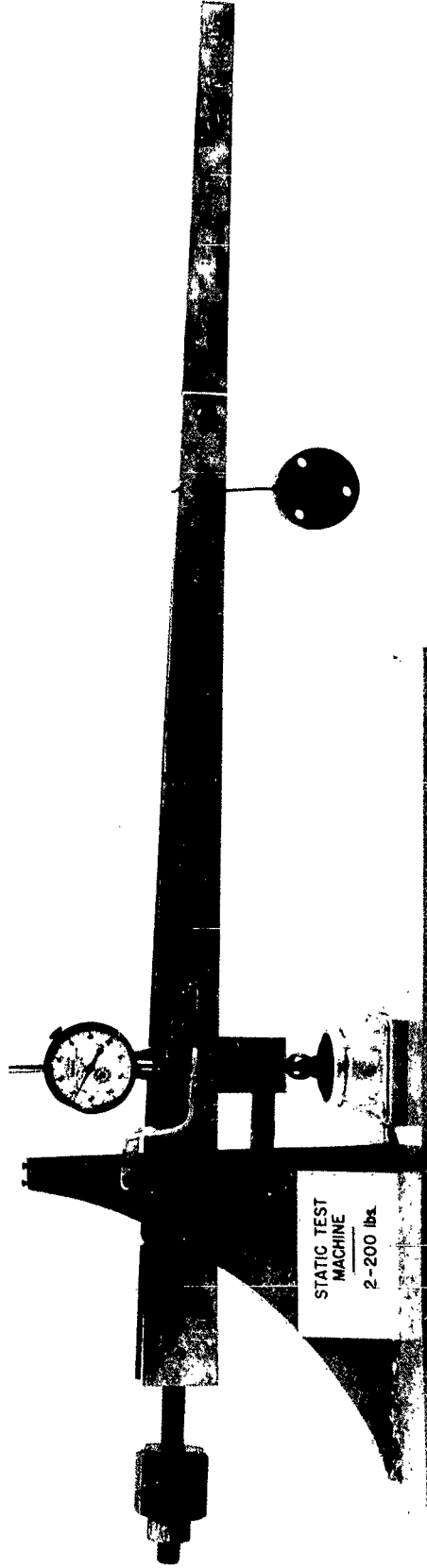


Fig. 5 STATIC TESTING MACHINE

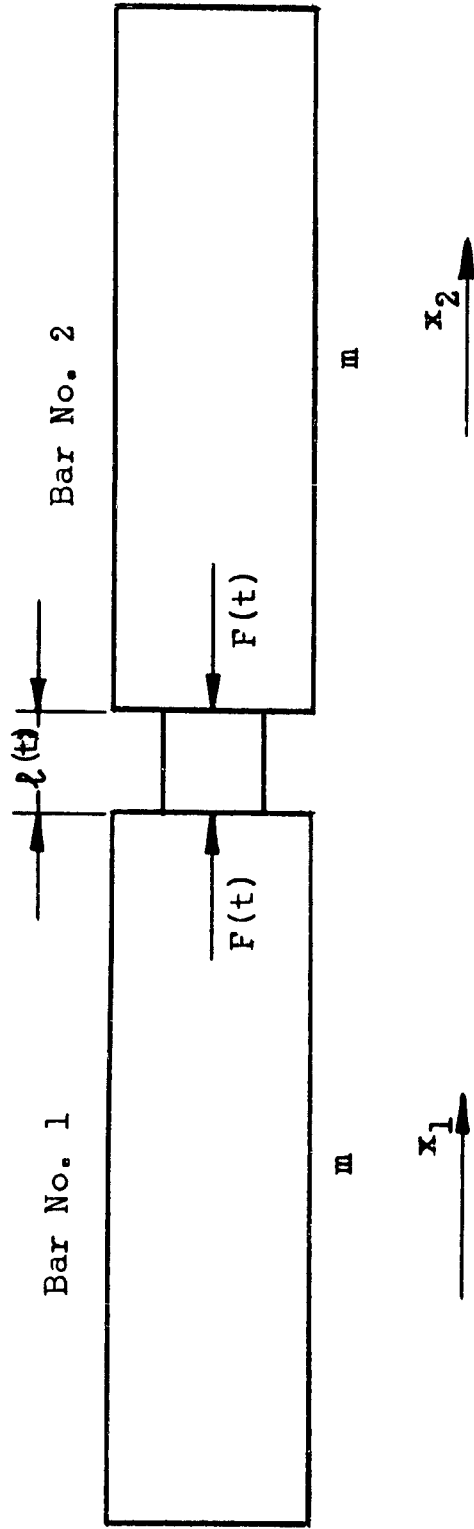


Figure 6  
Rigid Bar -- Rubberlike Specimen Model

the instant  $t = 0$  and  $m$  be the mass of each of the two equal steel bars.

The following relationship will be verified [5], [6], [7],

$$F = - m \frac{d^2(x_2 - x_1)}{dt^2} = - m \frac{d^2 s}{dt^2} \quad (2.1)$$

Call  $\ell(t)$  the actual length of the specimen at the instant  $t$  ( $\ell$  is deduced directly from the readings of the film).

Then

$$\ell(t) = \ell_0 - s(t)$$

where  $\ell_0$  is the initial length of the specimen.

By differentiating the experimental  $(s, t)$  curves twice it is possible to find the corresponding  $(F, t)$  curves by the use of equation (2.1). If we suppose that during deformation the volume of the specimen remains constant and call  $A$  and  $A_0$  the cross-section areas of the specimen at the instants  $t$  and  $t = 0$ , respectively, and  $V_0$  initial volume, we get

$$V_0 = A_0 \ell_0 = A \ell$$

The actual true stress will then be

$$\sigma(t) = \frac{F(t)}{A(t)} = \frac{F(t) \ell(t)}{V_0}$$

as compared to the engineering stress

$$\sigma(t) = \frac{F(t)}{A_0}$$

The actual true strain is defined as

$$\epsilon(t) = \ln \frac{l_0}{l(t)}$$

as compared to the engineering strain

$$\epsilon(t) = \frac{s(t)}{l_0}$$

From the readings of the photographs it is possible to determine the curves:  $l(t)$ ,  $F(t)$ ,  $\sigma(t)$ ,  $\epsilon(t)$  and finally the dynamic stress-strain curves ( $\sigma$ ,  $\epsilon$ ).

C. Degree of accuracy of the mechanical and optical methods employed

Two causes of possible error in the described experimental method have to be taken into account. The first, of a mechanical nature, is due to the elastic deformation of the steel bars during impact. The second, of an optical nature, is due to the finite dimensions of the slit.

The effect of these causes of error are negligible in the case of plastics and rubber-like materials due to the fact that during impact the forces acting on the metallic bars and the induced deformations of the bars are very small, while the total duration of impact is comparatively large. An evaluation of their effects is given below.

1) Let the following notation be used;

$\rho_1$  ..... the density of steel

$E_1$  ..... Young's modulus of steel

- $c_1$  ..... velocity of sound in steel
- $p$  ..... pressure of the longitudinal wave produced in bars by the force  $F(t)$  caused by the impact
- $\frac{d\xi}{dt}$  ..... the particle velocity of the same wave
- $a(t)$  ..... acceleration of the bar at the instant of initial impact with the specimen
- $v_0$  ..... velocity of the bar at the instant of initial impact with the specimen
- $A_1$  ..... cross-section area of the bars
- $L_1$  ..... length of the bars

The following relationships hold:

$$p = \rho_1 c_1 \frac{d\xi}{dt} \tag{2.2}$$

where

$$c_1^2 = \frac{E_1}{\rho_1}, \text{ and} \tag{2.3}$$

$$p(t) = \frac{F(t)}{A_1} = - m \frac{a(t)}{A_1}$$

From equations (2.2) and (2.3), it follows that

$$\xi(t) = - \frac{m}{\rho_1 c_1 A_1} \int_0^t a(t) dt \tag{2.4}$$

$$\xi(t) = \frac{L_1}{c_1} [v_0 - v(t)]$$

Let  $v_o'$  be the velocity (negative) of the bar after impact. Then from equation (2.4) the maximum elastic deformation in the bar is given by:

$$\xi_{\max} = \frac{L_1}{c_1} [v_o + v_o'] \leq \frac{2Lv_o}{c_1} \quad (2.5)$$

which yields an approximate value for  $\xi_{\max}$  of 0.01-inch for the bars used.

2) The finite thickness of the slit image of the film gives rise to an error in determining the instants of time for the experimental  $s(t)$  curves. The error is of the same order of magnitude as the time taken by the film on the rotating drum to move a distance equal to the thickness of the slit image on the film and can be determined as follows:

Call  $\delta$  the thickness of the image of the slit on the film,  $L$ , the total length of the film,  $n$  the number of revolutions per second of the rotating drum. It follows that a 1" length of film corresponds to  $\frac{1}{Ln}$  seconds and the thickness of the slit image corresponds to  $\frac{\delta}{Ln}$  seconds. If  $T$  is the total duration of impact, the percentage error in the evaluation of time in our measurements will be given by  $\frac{\delta}{LnT}$ , which indicates a possible error in the indicated time of approximately 0.2 percent.

D. Direct computation of the dynamic stress-strain curves for a given material, with known hereditary characteristics, under impact loading.

When the hereditary characteristics for a given material are known, as a function of time, it is possible to calculate directly

the dynamic stress-strain curve under impact. In order to simplify the calculations we shall assume that under static load conditions the material obeys Hooke's law, while under dynamic conditions the stress-strain relationship for the material is

$$\sigma = E\varepsilon + \int_0^t \psi(t - \tau) \frac{d\varepsilon(\tau)}{d\tau} d\tau \quad (2.6)$$

Suppose that such a material is subjected to an impact test. Call  $l_0$  its initial length,  $A_0$  its initial cross-sectional area,  $l(t) = l_0 - s(t)$ , its length at time  $t$ , and  $m$  the mass of the impinging bar.

The following integro-differential equation will characterize the motion during impact in the case of the assumed linear stress-strain relationship:

$$m \frac{d^2 s(t)}{dt^2} + E \frac{A_0}{l_0} s + \frac{A_0}{l_0} \int_0^t \psi(t - \tau) \frac{ds(\tau)}{d\tau} d\tau = 0 \quad (2.7)$$

The solutions of equation (2.7) will be given for different types of heredity. It is evident that if the equation is solved, i.e., the function  $s(t)$  is determined, then the stress-strain curves can be calculated by the use of the formulas given in Section II B.

1. Heredity of the first degree:  $\psi(t) = He^{-\alpha t}$

By a simple differentiation with respect to  $t$  equation (2.7) can be transformed into the following differential equation:

$$m \frac{d^3 s(t)}{dt^3} + \alpha m \frac{d^2 s(t)}{dt^2} + \frac{(E + H) A_0}{l_0} \frac{ds}{dt} + \frac{A_0 E \alpha s(t)}{l_0} = 0 \quad (2.8)$$

The solution of equation (2.8) is of the form

$$s(t) = C_1 e^{-nt} + C_2 e^{-pt} \cos qt + C_3 e^{-pt} \sin qt \quad (2.9)$$

where  $-n$ ;  $-p + iq$ ;  $-p - iq$ , are the roots of the algebraic equation:

$$x^3 + \alpha x^2 + \frac{(E + H) A_0}{l_0 m} x + \frac{A_0 E \alpha}{l_0 m} = 0 \quad (2.10)$$

From the initial conditions:

$$s = 0, \frac{ds}{dt} = v_0; \frac{d^2 s}{dt^2} = 0 \text{ for } t = 0, \text{ it follows that}$$

$$C_1 = \gamma_1 v_0, C_2 = -\gamma_1 v_0, C_3 = \gamma_2 v_0 \quad (2.11)$$

where:

$$\gamma_1 = \frac{2p}{q^2 + (p-n)^2} \quad (2.12)$$

$$\gamma_2 = \frac{q^2 + n^2 - p^2}{q(q^2 + (p-n)^2)}$$

## 2. Heredity of the first degree with residual:

$$\psi(t) = H e^{-at} + H_0$$

The solution of equation (2.8) is given by equations (2.10), (2.11), and (2.12) where, in this case,  $-n$ ,  $-p + iq$ ,  $-p - iq$  are the roots of the algebraic equation:

$$x^3 + x^2 + \frac{(E + H + H_0)A_0}{l_0 m} x + \frac{A_0(E + H_0)a}{l_0 m} = 0 \quad (2.13)$$

3. Heredity of the second degree:  $\psi(t) = H_1 e^{-\alpha_1 t} + H_2 e^{-\alpha_2 t}$

By a double differentiation with respect to  $t$  equation (2.8) can be transformed, in this case, into the following differential equation:

$$\begin{aligned} \frac{d^4 s(t)}{dt^4} + (\alpha_1 + \alpha_2) \frac{d^3 s(t)}{dt^3} + \left[ \frac{A_0}{l_0 m} (E + H_1 + H_2) + \alpha_1 \alpha_2 \right] \frac{d^2 s(t)}{dt^2} \\ + \frac{A_0}{l_0 m} [E(\alpha_1 + \alpha_2) + \alpha_1 H_2 + \alpha_2 H_1] \frac{ds}{dt} + \alpha_1 \alpha_2 \frac{EA_0}{l_0 m} = 0 \end{aligned} \quad (2.14)$$

The solution of equation (2.14) is:

$$s(t) = C_1 e^{-\eta t} + C_2 e^{-\zeta t} + C_3 e^{-pt} \cos qt + C_4 e^{-pt} \sin qt \quad (2.15)$$

where  $-\eta$ ,  $-\zeta$ ,  $-p+iq$ ,  $-p-iq$  are the roots of the algebraic equation:

$$\begin{aligned} x^4 + (\alpha_1 + \alpha_2)x^3 + \left[ \frac{A_0}{l_0 m} (E + H_1 + H_2) + \alpha_1 \alpha_2 \right] x^2 \\ + \frac{A_0}{l_0 m} [E(\alpha_1 + \alpha_2) + \alpha_1 H_2 + \alpha_2 H_1] x + \alpha_1 \alpha_2 \frac{EA_0}{l_0 m} = 0 \end{aligned} \quad (2.16)$$

The initial conditions for determining the four constants  $C_1$ ,  $C_2$ ,  $C_3$  and  $C_4$  are:

$$s = 0; \frac{ds}{dt} = v_0; \frac{d^2s}{dt^2} = 0; \frac{d^3s}{dt^3} = \frac{(E + H_1 + H_2)A_0}{m l_0} \frac{ds}{dt};$$

for  $t = 0$

The following four equations for determining the constants  $C_i$  ( $i = 1, 2, 3, 4$ ) are derived:

$$C_1 + C_2 + C_3 = 0$$

$$-\eta C_1 - \zeta C_2 - p C_3 + q C_4 = v_0$$

$$\eta^2 C_1 + \zeta^2 C_2 + (p^2 - q^2) C_3 - 2pq C_4 = 0 \tag{2.17}$$

$$-(\eta^3 + \eta B) C_1 - (\zeta^3 + \zeta B) C_2 + p(3q^2 - p^2 - B) C_3 + q(3p^2 - q^2 + B) C_4 = 0$$

where:

$$B = \frac{(E + H_1 + H_2)A_0}{l_0 m}$$

4. Heredity of the second degree with residual;

$$\psi(t) = H_1 e^{-\alpha_1 t} + H_2 e^{-\alpha_2 t} + H_0$$

The solution of equation (2.8) is given by equation (2.15) and (2.17) where:  $-\eta, -\zeta, -p + iq, -p - iq$  are the roots of the algebraic equation:

$$x^4 + (\alpha_1 + \alpha_2)x^3 + \left[ \frac{A_0}{l_0 m} (E + H_1 + H_2 + H_0) + \alpha_1 \alpha_2 \right] x^2 + \frac{A_0}{l_0 m} [ (E + H_0) (\alpha_1 + \alpha_2) + \alpha_1 H_2 + \alpha_2 H_1 ] x + \alpha_1 \alpha_2 \frac{(E + H_0) A_0}{l_0 m} = 0 \tag{2.18}$$

and B of equation (2.17) is given by:

$$B = \frac{(E + H_1 + H_2 + H_0)A_0}{l_0^m}$$

E. Determination of the hereditary characteristics of a material from the experimental dynamic stress-strain curves

We shall demonstrate the method of analysis by considering the case of heredity of the first degree with residual.

By equation (2.9) we note that  $s(t)$  can be written in the form

$$s(t) = C_1 e^{-nt} + C e^{-\beta t} + \bar{C} e^{-\bar{\beta} t} \quad (2.19)$$

where  $C_1$  and  $n$  are real,  $C$  and  $\beta$  are complex, and

$$C = \frac{(-C_1 + iC_3)}{2}, \quad \beta = p + iq \quad (2.20)$$

We assume an expression for  $s(t)$  of the form of Equation (2.19) and fit it to our experimental data by the method of least squares, following the procedure of Prony (See reference [8], page 373).

Since  $-n$ ,  $-\beta$ , and  $-\bar{\beta}$  are the roots of the equation

$$x^3 + (n + 2p)x^2 + (2pn + p^2 + q^2)x + n(p^2 + q^2) = 0 \quad (2.21)$$

We have by comparison of (2.13) and (2.21) the following three equations for determination of  $\alpha$ ,  $H_0$ , and  $H$ :

$$\alpha = n + 2p$$

$$E + H_0 + H = \frac{m l_0}{A_0} (2pn + p^2 + q^2)$$

$$\alpha(H_0 + E) = \frac{m_0^2}{A_0} (p^2 + q^2)n$$

where  $E$  is the static secant modulus of the material.

Since

$$\left. \frac{ds}{dt} \right]_{t=0} = v_0 = qC_3 - (n-p)C_1$$

we have a check on the accuracy of our calculations, as we can obtain the initial velocity directly from the experimental data.

With obvious modifications this method can also be used to analyze viscous damping.

However, it should be noted that, in the relationship

$$\sigma = D\varepsilon + \gamma \frac{d\varepsilon}{dt}$$

$D$  is a lumped parameter which is obtained directly from the dynamic test data; it may have no relationship to the static secant modulus  $E$ . A close approximation of its value is

$$D = E + H_0.$$

SECTION III

DESCRIPTION AND USE OF APPARATUS FOR TESTING MATERIALS  
AT HIGH RATES OF STRAINING

### SECTION III

#### Description and Use of Apparatus for Testing Materials At High Rates of Compressive Straining

##### A. General description of the mechanical apparatus.

The mechanical apparatus is shown in Figure 7. It consists of:

- 1) two steel bars, 1" diameter, 6 feet long, and
- 2) a short impinging bar (hammer) with a round head.

This mechanical apparatus is equipped with a system of strain gages, amplifier, radio frequency oscillator, oscilloscope and photographic camera to record the longitudinal pulses which are propagated along the two steel bars when the short bar strikes the end of one of the long bars. The details of the electronic equipment are given in the next section.

The specimens to be tested, in the form of circular discs of uniform thickness, with diameters slightly smaller than those of the adjoining bars are placed between the carefully-lapped plane ends of the two bars. For reducing friction between specimen and bars both surfaces of each specimen are lubricated before being placed in the apparatus.

The hammer is released from a known height. When it strikes the first steel bar an open ground circuit is completed which triggers one sweep of the dual-beam oscilloscope. A compression wave is propagated in the bar and its passage is recorded from an amplified strain gage signal by the camera attached to the

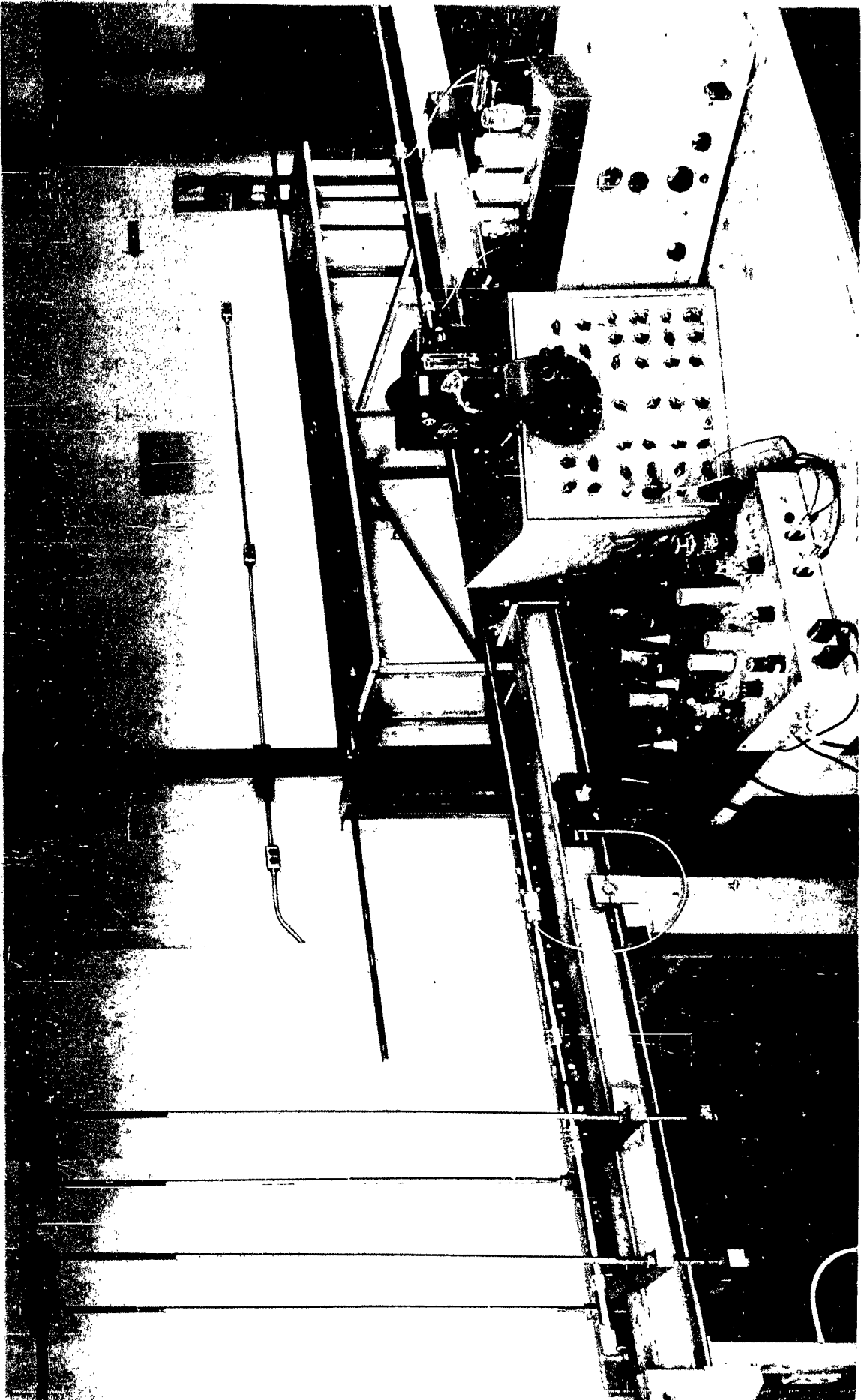


Fig. 7 VIEW OF ASSEMBLED EQUIPMENT - STRAIN-GAGE METHOD



Fig. 7 VIEW OF ASSEMBLED EQUIPMENT - STRAIN-GAGE METHOD

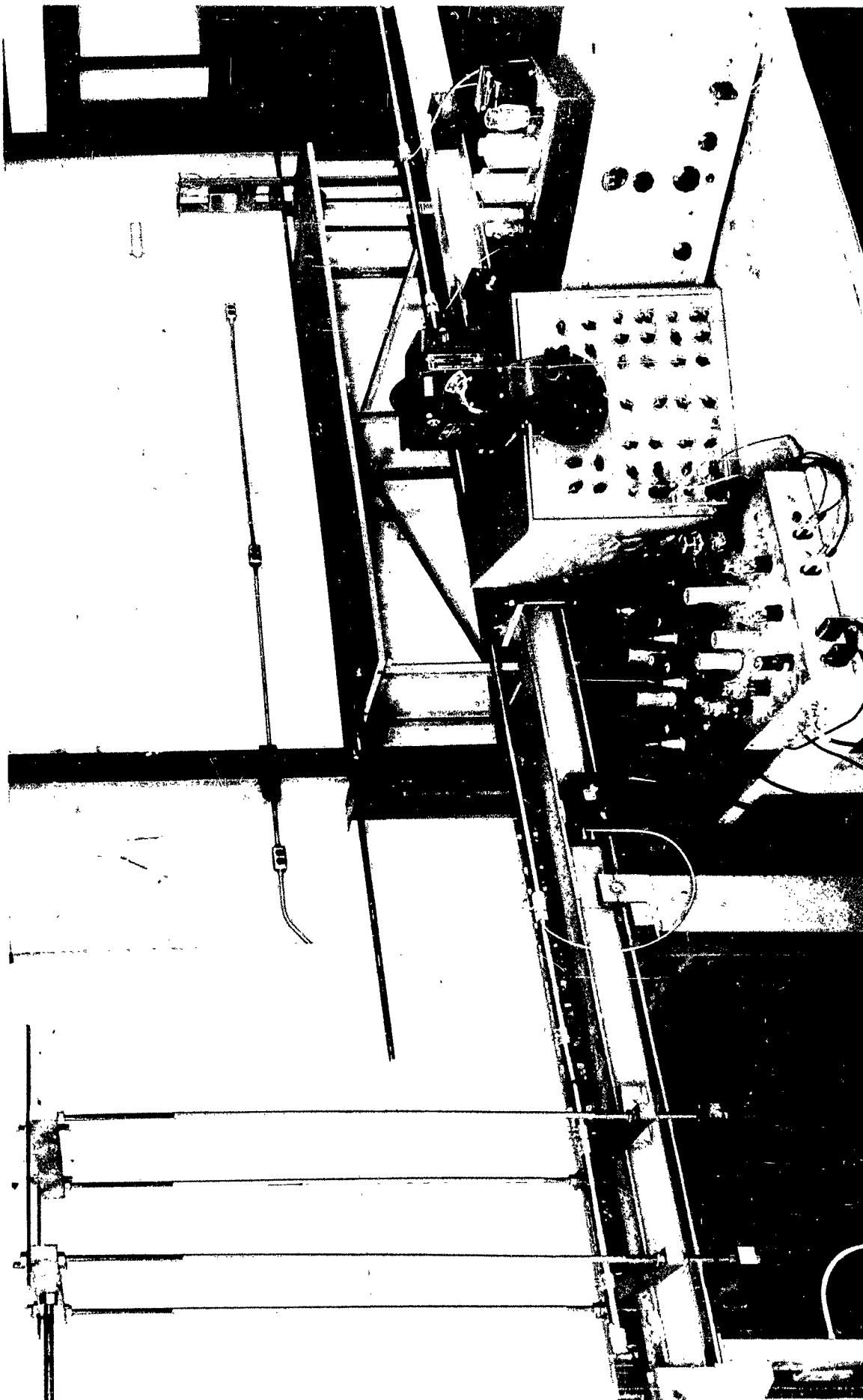


Fig. 7 VIEW OF ASSEMBLED EQUIPMENT - STRAIN-GAGE METHOD

oscilloscope. When the compression wave reaches the other end of the steel bar, a certain portion of the wave is reflected back along the bar as a tension wave and the remainder is transmitted through the specimen on to the second steel bar.

On the first steel bar, about 12 inches from the mounted specimen, a strain gage is fastened. It is connected electrically to a second trigger circuit which sets the second sweep of the dual-beam oscilloscope. Thus, when the compressive wave, which is being propagated in the second steel bar, reaches a set of strain gages about 12 inches beyond the specimen a second compressive trace is recorded by the oscilloscope camera.

From this photographic record then it is possible to calculate directly the dynamic stress-strain curve of the specimen, as will be shown later.

In this method, auxiliary electronic equipment is used to amplify a signal from a set of strain gages, to superpose a timing pulse on this signal, and finally, to indicate the magnitude and length of the impact pulses on the screen of an oscilloscope.

Essentially, there are three circuits of importance,

- 1) the strain gage circuit, which amplifies the original signal and mixes it with the timing pulse before it is fed into the signal circuit of one beam of the dual-beam oscilloscope;

- 2) the time pulse circuit, which superposes 20 microsecond pips on the strain gage signal; and

3) the trigger circuits which set the sweep of one beam of the oscilloscope to fire when they receive an external voltage pulse.

The strain gages are arranged in sets of four at equidistant points around the periphery of the steel bars (Figure 7). There are two sets, each about 12 inches from the head end of the two steel bars. Since each set is connected in series, the net effect of any bending modes will be zero and the voltage change generated will be due entirely to the compressional pulse being propagated along the steel bars.

The voltage pulse is amplified first by a four-stage triode amplifier with a wide frequency response. A timing pip at intervals of 20 microseconds is added to the output of the amplifier.

The time interval of the pip is controlled by a Hewlett-Packard audio-oscillator and can be varied if it is desired. The pulse (pip) generator consists of an 884 gas triode and a differentiating circuit. The output of the latter is formed by a clipper circuit and then fed into a wide range amplifier in order to obtain the proper phase relationship between the original pulse and the timing pip. This corrected pulse is superposed, in turn, on the amplified strain gage signal just before the latter is fed into one of the signal circuits of the oscilloscope.

The phenomenon is transient rather than steady state and as a consequence it is necessary to trigger the sweep of the oscillo-

scope just before the compressional pulse reaches the strain gages. This is accomplished by making use of the circuits within the oscilloscope and additional external circuits.

The sweep oscillator for each beam of the oscilloscope is set for a pre-determined sweep time, and then the other controls are so adjusted that neither oscillator will fire until an additional external voltage pulse is impressed upon them. Two external trigger circuits are used to insure that the oscillators will fire at the proper time.

The circuit for the first bar is energized when the hammer completes a ground circuit at the instant of initial impact; for the second, when the compressional wave passes a strain gage about 20 inches in front of the second set of recording strain gages. In either case, a voltage pulse is amplified and then applied to a sweep oscillator of the oscilloscope in order to produce a single sweep at the instant the compressional wave passes the recording strain gages. Thus, only one pulse from each set of strain gages is recorded by the camera.

This method of testing will allow determination of the stress-strain curves for rates of straining of the order of micro-seconds. The length of the direct pulse in the first long bar is governed by the length of the striking bar (hammer) and the relative magnitude of the pulse by the velocity at the time of initial impact.

In the following table we give some of the computed characteristics of the pulses.

TABLE I

Theoretical time of contact in microseconds as a function of height of drop and hammer length

Drop height Hammer length	5 cm	10 cm	15 cm	25 cm
25 cm	140	136	134	130
50 cm	239	233	231	228
75 cm	336	331	328	325
100 cm	432	427	424	421

This experimental method of determining dynamic stress-strain curves for very high rates of straining is subject to certain restrictions, as is the method based on the use of the Davies-Hopkinson pressure bar [10], [11], namely,

1) The waves propagated in the bar are assumed to be elastic waves, i.e., the stress at every point in the bar must always be within the region where the stress-strain curve is linear and reversible.

2) It is assumed that the pressure wave is propagated without distortion. This assumption is only true when the wave lengths of the elastic waves are large compared with the lateral dimensions of the bars. When this condition is not fulfilled,

the wave suffers dispersion and the form of the pulse is distorted as it travels along the bar.

3) A third assumption implicit in the method is that the pressure in the pulse is uniformly distributed over the cross-section of the bar, even when the force acting on the end is concentrated over a small area surrounding the center.

However, this method of investigation presents the following advantages in comparison with the method using the Davies-Hopkinson Bar:

1) While in the Davies method it is possible to record only the first part of the stress-strain curve, i.e., the part when the specimen is compressed but not when it recoils, with this method the complete stress-strain curve can be investigated.

2) The determination of the stress-strain curves from the experimental data is much simpler, and there is less possibility of making mistakes in the numerical computation. In fact, while in the Davies' method a numerical differentiation has to be performed, in this method the stress-strain curves are obtained through numerical integration of the experimental data, a method of computation with many inherent advantages.

#### B. Theory of the method

When the hammer hits the first bar a direct compressive wave  $\sigma_D$  (Figure 8) is transmitted undistorted along the first long steel bar with velocity  $c^2 = \frac{E}{\rho}$  [12]. When it reaches the specimen, after a time  $t = \frac{L}{c}$  (L being the length of the bar)

the wave suffers dispersion and the form of the pulse is distorted as it travels along the bar.

3) A third assumption implicit in the method is that the pressure in the pulse is uniformly distributed over the cross-section of the bar, even when the force acting on the end is concentrated over a small area surrounding the center.

However, this method of investigation presents the following advantages in comparison with the method using the Davies-Hopkinson Bar:

1) While in the Davies method it is possible to record only the first part of the stress-strain curve, i.e., the part when the specimen is compressed but not when it recoils, with this method the complete stress-strain curve can be investigated.

2) The determination of the stress-strain curves from the experimental data is much simpler, and there is less possibility of making mistakes in the numerical computation. In fact, while in the Davies' method a numerical differentiation has to be performed, in this method the stress-strain curves are obtained through numerical integration of the experimental data, a method of computation with many inherent advantages.

#### B. Theory of the method

When the hammer hits the first bar a direct compressive wave  $\sigma_D$  (Figure 8) is transmitted undistorted along the first long steel bar with velocity  $c^2 = \frac{E}{\rho}$  [12]. When it reaches the specimen, after a time  $t = \frac{L}{c}$  (L being the length of the bar)

the wave suffers dispersion and the form of the pulse is distorted as it travels along the bar.

3) A third assumption implicit in the method is that the pressure in the pulse is uniformly distributed over the cross-section of the bar, even when the force acting on the end is concentrated over a small area surrounding the center.

However, this method of investigation presents the following advantages in comparison with the method using the Davies-Hopkinson Bar:

only  
when  
this  
expe:

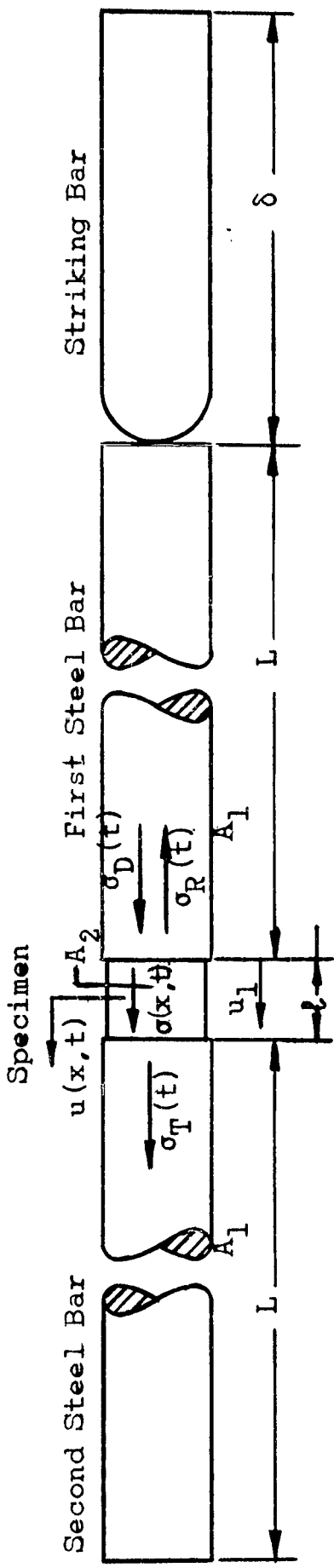
DISREGARD  
LAST PAGE

ord  
part  
ith  
igated.  
the  
bility

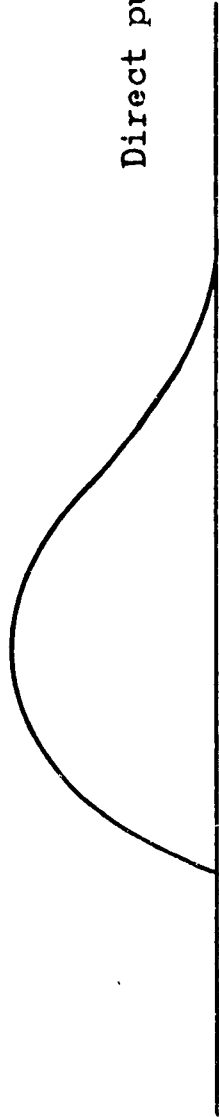
of making mistakes in the numerical computation. In fact, while in the Davies' method a numerical differentiation has to be performed, in this method the stress-strain curves are obtained through numerical integration of the experimental data, a method of computation with many inherent advantages.

B. Theory of the method

When the hammer hits the first bar a direct compressive wave  $\sigma_D$  (Figure 8) is transmitted undistorted along the first long steel bar with velocity  $c^2 = \frac{E}{\rho}$  [12]. When it reaches the specimen, after a time  $t = \frac{L}{c}$  (L being the length of the bar)



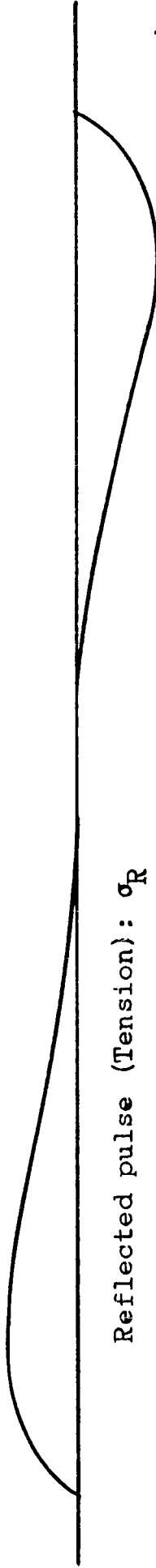
For  $0 < t \leq L/c$



Direct pulse (Compression):  $\sigma_D$

For  $L/c \leq t \leq 2L/c$

Transmitted pulse (Compression):  $\sigma_T$



Reflected pulse (Tension):  $\sigma_R$

Figure 8

Pulse-Time Relations for Figure 5

only  $\sigma_T$ , a part of the original pulse, is transmitted through the specimen and into the second bar. A tension pulse  $\sigma_R$  is reflected back along the first bar.

The theory of impact developed here can be made more realistic by considering a cylindrical specimen of a material held between the plane ends of two steel bars (Figure 8). A stress wave of known properties is propagated along the first steel bar, and the problem is to determine the characteristic stress waves induced in the specimens which follow various stress-strain relationships.

A minimum number of simplifying assumptions will be made for both a relatively realistic analysis, and later, for a more approximate theory.

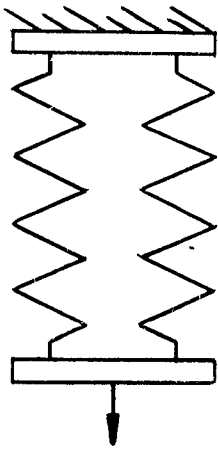
These initial assumptions for the first analysis are:

(1) The stress in the specimen is distributed uniformly across each cross section.

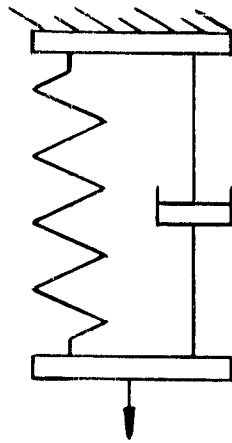
(2) There are no reflections in the specimen.

(3)  $\sigma_R(t) = \sigma_D(t) - q\sigma(o, t)$  for  $x = 0$  and all values of  $t$ ;

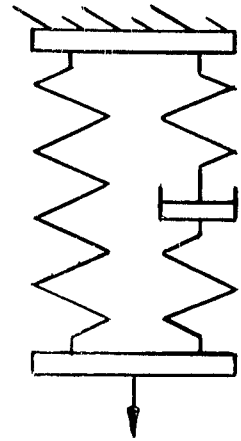
$\sigma_T(t) = q\sigma(l, t)$  for  $x = l$  and all values of  $t$ , where the specimen is of length  $l$  and cross-sectional area  $A_2$ , the steel bar has area  $A_1$  and  $q = A_2/A_1$  is the ratio of the areas.  $\sigma_D(t)$  is the wave transmitted initially along the bar on the left;  $\sigma_R(t)$  is the wave reflected from the interface of the left bar and the specimen; and  $\sigma_T(t)$  is the wave transmitted to the steel bar on the right.



(2a)  
(Hooke)



(2b)  
(Voigt)



(2c)  
(Boltzmann)

Figure 9  
Schematic Diagram of Material Models

The third assumption is, essentially, a consequence of the first two assumptions and the equilibrium of the specimen. The second of our assumptions allows us to consider the specimen infinitely extended to the right.

The stress-strain relationships for the specimen materials considered are

- (1) Elastic (Hookean Model)
- (2) Elasto-Viscous (Voigt Model) [14]
- (3) Hereditary (Boltzmann Model) [15], [16]

and the models which are characterized by each of these relationships are shown in Figure 9. In all cases the equation of motion

is

$$\frac{\partial}{\partial x} \sigma(x, t) = \rho_2 \frac{\partial^2}{\partial t^2} u(x, t) \quad (3.1)$$

where  $\rho_2$  is the mass density of the specimen.

### Boundary and Initial Conditions

The basic boundary and wave front conditions are the same for all three of the stress-strain relations considered, namely,

$$\text{For } t \leq 0; \quad 0 \leq x < \infty \quad \sigma = 0 \quad (3.2)$$

For  $t \geq 0$  the particle velocities of the specimen and the steel rod are the same, that is for  $t \geq 0, x = 0$

$$\frac{\partial u}{\partial t} = v_1 = \frac{-1}{\rho_1 c_1} [\sigma_D(t) + \sigma_R(t)] \quad (3.3)$$

where  $u(x, t)$  is the displacement of the specimen;  $\rho_1$  and  $c_1$  are the density and wave velocity of the steel rods, respectively.

The known initial wave is assumed to have the form

$$\sigma_D(t) = \begin{cases} 0 & \text{for } t \leq 0 \\ b \sin \lambda t & \text{for } 0 \leq t \leq T \\ 0 & \text{for } T \leq t \end{cases} \quad (3.4)$$

where

$$\lambda = \frac{n\pi}{T}$$

$n$  is an integer and  $T$  is the time length of the pulse. The

linearity of our equations permits superposition of solutions for different  $n$ .

Case I - Elastic Specimen

$$\sigma(x, t) = E_2 \frac{\partial}{\partial x} u(x, t) \tag{3.5}$$

where  $E_2$  is the static Young's modulus for the specimen material.

Elimination of  $u(x, t)$  between (3.1), (3.5) yields

$$\left. \begin{aligned} \frac{\partial^2 \sigma}{\partial t^2} &= c_2^2 \frac{\partial^2 \sigma}{\partial x^2} \\ c_2^2 &= \frac{E_2}{\rho_2} \end{aligned} \right\} \tag{3.6}$$

The first assumption together with conditions (3.2), (3.3) and equation (3.5) yield the boundary conditions.

Our system becomes

$$\left. \begin{aligned} \frac{\partial^2 \sigma}{\partial t^2} &= c_2^2 \frac{\partial^2 \sigma}{\partial x^2} \\ \left. \begin{aligned} t - \frac{x}{c_2} &\leq 0 \\ 0 \leq x &\leq l \end{aligned} \right\} & \sigma &= 0 \\ \left. \begin{aligned} t &\geq 0 \\ x &= 0 \end{aligned} \right\} & \sigma(0, t) &= \frac{\theta}{q} \sigma_D(t) \\ & \theta &= \frac{2q \frac{\rho_2 c_2}{\rho_1 c_1}}{1 + \frac{\rho_2 c_2}{\rho_1 c_1}} \end{aligned} \right\} \tag{3.7}$$

In view of our assumption of no reflections in the specimen, the solution of (3.7) is

$$\left. \begin{aligned} \sigma(x, t) &= 0 \quad \text{for } t - \frac{x}{c_2} \leq 0, \quad 0 \leq x \leq l \\ \sigma(x, t) &= \frac{\theta}{q} \sigma_D(t - \frac{x}{c_2}) \quad \text{for } t \geq 0, \quad 0 \leq x \leq l \end{aligned} \right\} \quad (3.8)$$

Since the transmitted stress  $\sigma_T$  is given by  $\sigma_T(t) = q\sigma(l, t)$  we have the transmitted wave as an immediate consequence of (3.8).

For the initial wave given in (3.4) we have

$$\left. \begin{aligned} \sigma_T(t) &= 0 \quad \text{for } t - \frac{l}{c_2} \leq 0 \\ \sigma_T(t) &= \theta b \sin \lambda(t - \frac{l}{c_2}) \quad \text{for } 0 \leq t \leq T \\ \sigma_T(t) &= 0 \quad \text{for } T \leq t \end{aligned} \right\} \quad (3.9)$$

Case II: Elasto-Viscous Specimen

$$\sigma(x, t) = D_2 \frac{\partial u(x, t)}{\partial x} + \gamma \frac{\partial^2 u(x, t)}{\partial t \partial x} \quad (3.10)$$

where  $\gamma$  is the coefficient of viscosity. The initial conditions are:

$$\left. \begin{aligned} t = 0: \quad u(x, 0) &= \frac{\partial u}{\partial x}(x, 0) = \frac{\partial u}{\partial t}(x, 0) = 0 \\ \sigma(x, 0) &= \frac{\partial \sigma(x, 0)}{\partial x} = 0 \end{aligned} \right\} \quad (3.11)$$

The boundary conditions are:

$$x = 0: \quad \frac{\partial}{\partial t} u(0, t) = -\frac{1}{p_1 c_1} [2\sigma_D(t) - q\sigma(0, t)] \quad (3.12)$$

where  $\sigma_D(t)$  is given by (3.4)

$$\begin{aligned} x \rightarrow \infty: \quad u(x, t) &\rightarrow 0 \\ \sigma(x, t) &\rightarrow 0 \end{aligned} \tag{3.12} \text{ cont.}$$

We attack this problem by means of the Laplace Transform [17], [18]. We denote the transform of a sufficiently regular function  $f(x, t)$  by  $\bar{F}(x, z)$ , i.e.,

$$\begin{aligned} \bar{F}(x, z) &= \int_0^{\infty} f(x, t) e^{-zt} dt \\ \text{or} \quad f(x, t) &\xrightarrow{\cdot} \bar{F}(x, z) \end{aligned} \tag{3.13}$$

By Section 4, [17] (3.1), (3.10), (3.11), (3.12), imply

$$\begin{aligned} \bar{\sigma}(x, z) &= (D_2 + \gamma z) \frac{\partial}{\partial x} \bar{u}(x, z) & (a) \\ \frac{\partial}{\partial x} \bar{\sigma}(x, z) &= z^2 \rho_2 \bar{u}(x, z) & (b) \\ x = 0: \quad z \bar{u}(0, z) &= - \frac{1}{\rho_1 c_1} [2\bar{\sigma}_D - q\bar{\sigma}(0, z)] & (c) \\ x \rightarrow \infty: \quad \bar{u}(x, z) &\rightarrow 0 & (d) \\ \bar{\sigma}(x, z) &\rightarrow 0 & (e) \end{aligned} \tag{3.14}$$

where, by (3.4)

$$\sigma_D(z) = \frac{\lambda b [1 - (-1)^n e^{-zt}]}{\lambda^2 + z^2} \tag{3.15}$$

The solution of (3.14) is

$$\left. \begin{aligned} \bar{\sigma}(x, z) &= \frac{2\rho_2 z \bar{\sigma}_1 e^{-\omega_0 x}}{\omega_0 \rho_1 c_1 + \rho_2 z q} \\ \bar{u}(x, z) &= - \frac{2\omega_0 \bar{\sigma}_1 e^{-\omega_0 x}}{\omega_0 \rho_1 c_1 + \rho_2 z q} \end{aligned} \right\} \quad (3.16)$$

where  $\omega_0$  is the branch of  $\sqrt{\frac{\rho_2 z^2}{D_2 + \gamma z}}$  which has positive real part.  
If

$$F(x, t) \rightarrow \frac{D_2 z e^{-\omega_0 x}}{\gamma c_2 \left[ \frac{q \rho_2 z}{\rho_1 c_1} + \omega_0 \right] (\lambda^2 + z^2)} \quad (3.17)$$

then, by section 10, [17],

$$\sigma(x, t) = \frac{2b\lambda\gamma}{\rho_1 c_1 c_2} \begin{cases} F(x, t) & \text{for } 0 \leq t \leq T \\ F(x, t) - (-1)^n F(x, t-T) & \text{for } t \geq T \end{cases} \quad (3.18)$$

where

$$c_2 = \sqrt{\frac{D_2}{\rho_2}} \quad (3.19)$$

by Chapter VI, [17],

$$F(x, t) = \frac{D_2}{2\pi i \gamma c_2} \int_{c-i\infty}^{c+i\infty} \frac{z e^{-\omega_0 x} e^{-z t} dz}{\left[ \frac{q \rho_2 z}{\rho_1 c_1} + \omega_0 \right] (\lambda^2 + z^2)} \quad (3.20)$$

Let

$$\begin{aligned} \tau &= \frac{D_2}{\gamma} t; & \zeta &= \frac{\gamma}{D_2} z; & \xi &= \frac{\rho_2 c_2 x}{\gamma} \\ g &= \frac{\lambda \gamma}{D_2}; & h &= \frac{q \rho_2 c_2}{p_1 c_1}; & \omega^2 &= \frac{\zeta^2}{1+\zeta} \end{aligned} \quad (3.21)$$

then

$$F(x, t) = \frac{1}{2\pi i} \int_{T_1} \frac{\zeta \exp(\zeta \tau - \omega \xi) d\zeta}{(g^2 + \zeta^2)(h\zeta + \omega)} d\zeta \quad (3.22)^*$$

where  $T_1$  is the Bromwich contour (see Figure 10) and the branch

of  $\frac{\zeta^2}{1+\zeta} = \omega$  which has positive (or zero) real part is chosen.

This implies that the only real root of  $h\zeta + \omega = 0$  for  $h > 0$

is  $\zeta = 0$ .

### Case III: Hereditary Specimen

$$\sigma(x, t) = E_2 \frac{\partial u}{\partial x} + H \int_0^t e^{-\alpha(t-\tau)} \frac{\partial^2 u(x, \tau)}{\partial x \partial \tau} d\tau \quad (3.23)$$

\*A method similar to the above was followed by I. N. Zverev [19].

His solution is given in the form of a double integral which must, in general, be evaluated numerically. For the purpose of this report, numerical evaluation of the single integral (3.22) is much more convenient.

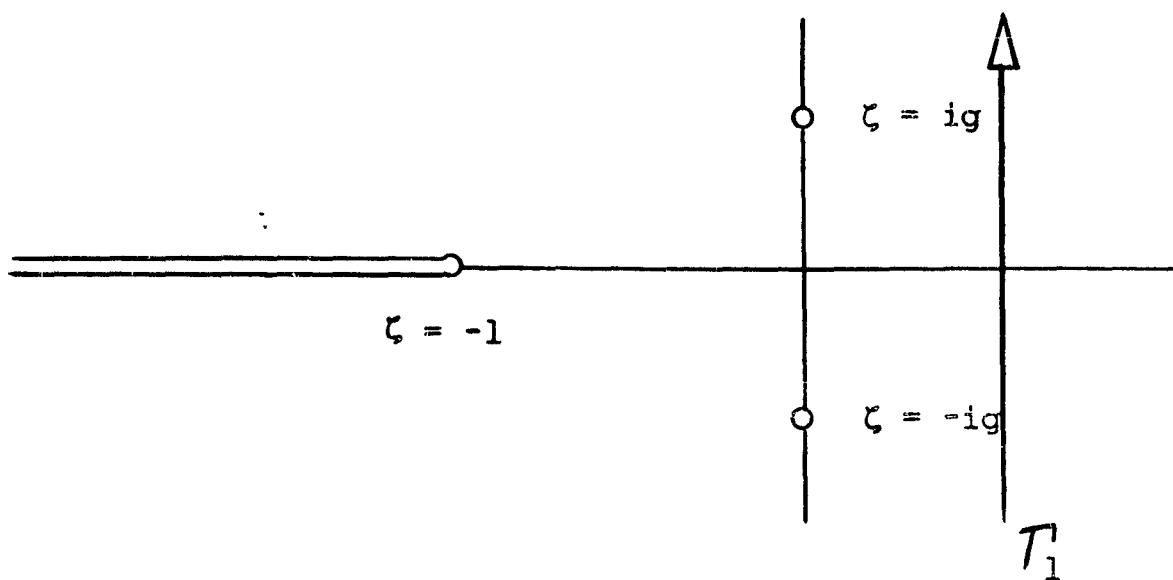


Figure 10  
Bromwich Contour - Viscous

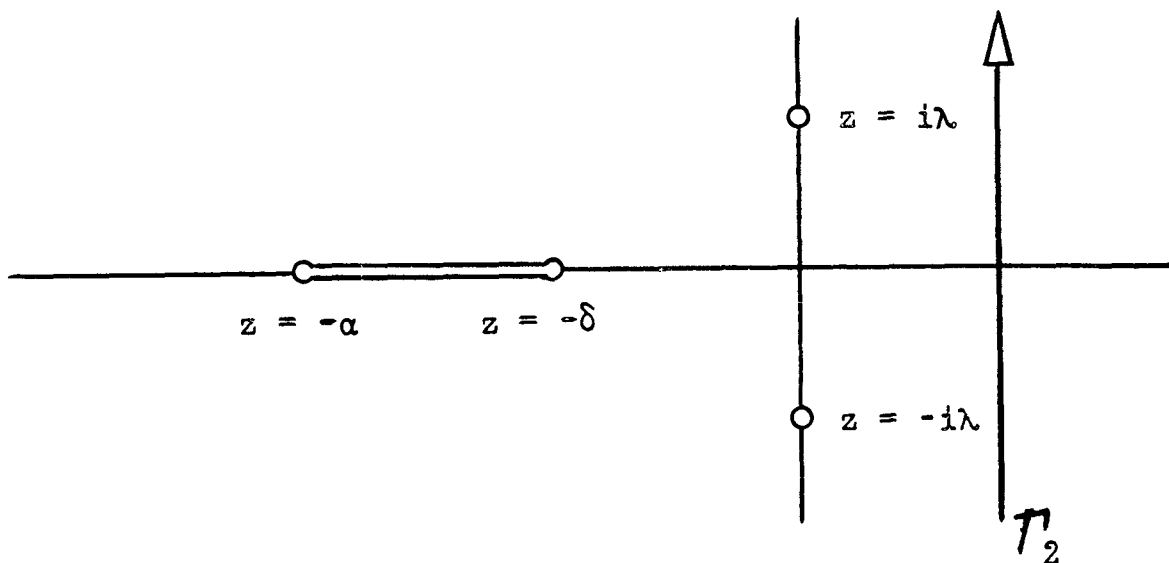


Figure 11  
Bromwich Contour - Hereditary

where  $E_2 + H$  is the dynamic Young's modulus and  $\alpha, A$  are Boltzmann constants for the material. The initial conditions are:

$$\left. \begin{aligned} t = 0: \quad u(x, 0) = \frac{\partial u}{\partial x}(x, 0) = \frac{\partial u}{\partial t}(x, 0) = 0 \\ \sigma(x, 0) = \frac{\partial \sigma}{\partial x}(x, 0) = 0 \end{aligned} \right\} (3.24)$$

The boundary conditions are:

$$\left. \begin{aligned} x = 0: \quad \frac{\partial}{\partial t} u(0, t) = - \frac{2}{\rho_1 c_1} \sigma_D(t) + \frac{q}{\rho_1 c_1} \sigma(0, t) \\ \text{where } \sigma_D(t) \text{ is given by (3.4)} \\ x \rightarrow \infty: \quad u(x, t) \rightarrow 0 \\ \sigma(x, t) \rightarrow 0 \end{aligned} \right\} (3.25)$$

We take the Laplace transform of (3.1), and (3.23). By sections 4, [17] and by (3.24), (3.25) we have:

$$\left. \begin{aligned} \bar{\sigma}(x, z) &= (E_2 + \frac{Hz}{z+\alpha}) \frac{\partial \bar{u}(x, z)}{\partial x} & (a) \\ \frac{\partial}{\partial x} \bar{\sigma}(x, z) &= \rho_2 z^2 \bar{u}(x, z) & (b) \\ x = 0: \quad z \bar{u}(0, z) &= - \frac{1}{\rho_1 c_1} [2 \bar{\sigma}_D(z) - q \bar{\sigma}(0, z)] & (c) \\ x \rightarrow \infty: \quad \bar{u}(x, z) &\rightarrow 0 & (d) \\ \bar{\sigma}(x, z) &\rightarrow 0 & (e) \end{aligned} \right\} (3.26)$$

and  $\bar{\sigma}_D(z)$  is given by (3.15).

The solution for (3.1) and (3.24) is

$$\left. \begin{aligned} \bar{\sigma}(x, z) &= \frac{2\rho_2\beta\bar{\sigma}_D e^{-\omega_0 \frac{x}{\beta}}}{\rho_1 c_1 \omega_0 + q\rho_2\beta z} \\ \bar{u}(x, z) &= -\frac{2\omega_0\bar{\sigma}_D e^{-\omega_0 \frac{x}{\beta}}}{z^2(\rho_1 c_1 \omega_0 + q\rho_2\beta z)} \end{aligned} \right\} \quad (3.27)$$

where

$$\omega_0^2 = \frac{z^2(z + \alpha)}{z + \delta}; \quad \beta^2 = \frac{E_2 + H}{\rho_2}; \quad \delta = \frac{E_2 \alpha}{E_2 + H} \quad (3.28)$$

and the branch of  $\omega_0$  which has positive real part is taken.

If

$$F(x, t) \rightarrow \frac{ze^{-\xi\omega_0}}{(\lambda^2 + z^2)(\omega_0 + zd)} \quad (3.29)$$

Then, by section 10, [17]

$$\sigma(x, t) = \frac{2b\lambda\rho_2\beta}{\rho_1 c_1} \begin{cases} F(x, t) & \text{for } 0 \leq t \leq T \\ F(x, t) - (-1)^n F(x, t-\tau) & \text{for } t \geq T \end{cases} \quad (3.30)$$

where  $\xi = \frac{x}{\beta}$  and  $d = \frac{q\rho_2\beta}{\rho_1 c_1}$ . By the inversion theorem

$$F(x, t) = \frac{1}{2\pi i} \int_{\Gamma_2} \frac{\exp[zt - \xi\omega_0]z dz}{(\lambda^2 + z^2)(\omega_0 + zd)} \quad (3.31)^*$$

where  $\Gamma_2$  is the Bromwich contour. We note, that, for  $d > 0$  the only root of  $zd + \omega_0 = 0$  is  $z = 0$ . (See Figure 11).

### Approximate Theory

In the following subsections we make various physically-plausible assumptions which lead to solutions more amenable to numerical computation.

### Approximate Assumptions

1. The stress in the specimen is uniformly distributed across each cross-section.
2. There are no reflections in the specimen.
3. The strain in the specimen is uniform.

$$\epsilon = \frac{u_2 - u_1}{l}$$

4. The stress in the specimen is independent of  $x$ , the longitudinal position in the specimen.

---

\* In a recent paper [20], H. Charles presented a solution to the problem of one-dimensional hereditary wave transmission which involves the evaluation of a fourfold iterated integral. For the purpose of this report, numerical evaluation of the single integral (3.31) is much more convenient.

$$5. \quad \sigma_R(t) = \sigma_D(t) - q \sigma(t)$$

$$\sigma_T(t) = q \sigma(t)$$

Case IV: Elastic-Specimen - Approximate

$$\dot{\sigma}(t) = E_2 \dot{\epsilon} = \frac{E_2}{L} (u_2 - u_1) \quad (3.32)$$

by assumption 3.

The particle velocity is given by

$$v = \frac{1}{\rho c} \sigma \quad (3.33)$$

(see equation 6, [12]). Now the particle velocity of the left bar is

$$v_1 = - \frac{1}{\rho_1 c_1} (\sigma_D + \sigma_R) \quad (3.34)$$

while the particle velocity of the right bar is

$$v_2 = - \frac{1}{\rho_1 c_1} \sigma_T \quad (3.35)$$

Thus

$$v_2 - v_1 = \frac{d}{dt} (u_2 - u_1) = \frac{1}{\rho_1 c_1} (\sigma_D + \sigma_R - \sigma_T) \quad (3.36)$$

By assumption (5) we have

$$v_2 - v_1 = \frac{2}{\rho_1 c_1} (\sigma_D - q\sigma) \quad (3.37)$$

Differentiating (3.32) and using (3.37) we obtain

$$\frac{d\sigma}{dt} + \frac{2E_2 q}{l\rho_1 c_1} \sigma = \frac{2E_2}{l\rho_1 c_1} \sigma_D \quad (3.38)$$

Let

$$\frac{2E_2 q}{l\rho_1 c_1} = \omega \quad (3.39)$$

then  $t > 0$  implies

$$\sigma = \frac{\omega}{q} e^{-\omega t} \int_0^t e^{\omega \tau} \sigma_D(\tau) d\tau \quad (3.40)$$

Now

$$\int_0^t e^{\omega \tau} \sin \lambda \tau d\tau = \frac{1}{\omega^2 + \lambda^2} [\omega e^{\omega t} \sin \lambda t - \lambda e^{\omega t} \cos \lambda t + \lambda] \quad (3.41)$$

Thus

$$\sigma(t) = \begin{cases} 0 & \text{for } t \leq 0 \\ \frac{\omega b}{q(\omega^2 + \lambda^2)} [\omega \sin \lambda t - \lambda \cos \lambda t + \lambda e^{-\omega t}] & \text{for } 0 \leq t \leq T \\ \frac{\omega \lambda b}{q(\omega^2 + \lambda^2)} [1 - (-1)^n e^{\omega t}] e^{-\omega t} & \text{for } t \geq T \end{cases} \quad (3.42)$$

where

$$\omega = \frac{2E_2 q}{l\rho_1 c_1} \quad (3.43)$$

The transmitted stress is, thus

$$\sigma_T = q\sigma \quad (3.44)$$

Case V: Elasto-Viscous Specimen - Approximate

$$\sigma(t) = \frac{D_2}{l} (u_2 - u_1) + \frac{\gamma}{l} (v_2 - v_1) \quad (3.45)$$

by assumption 3. Differentiate (3.45) and use (3.37) obtaining

$$\frac{d\sigma}{dt} + \frac{2D_2 q \sigma}{l \rho_1 c_1 + 2\gamma q} = \frac{2D_2 \sigma_D}{l \rho_1 c_1 + 2\gamma q} + \frac{2\gamma}{l \rho_1 c_1 + 2\gamma q} \frac{d\sigma_D}{dt} \quad (3.46)$$

Let

$$\omega = \frac{2D_2 q}{l \rho_1 c_1 + 2\gamma q}; \quad \mu = \frac{2\gamma q}{l \rho_1 c_1 + 2\gamma q} \quad (3.47)$$

Thus

$$q\sigma(t) = \mu \sigma_D + (1 - \mu) \omega e^{-\omega t} \int_0^t e^{\omega \tau} \sigma_D(\tau) d\tau \quad (3.48)$$

Hence, using (3.41)

$$\sigma(t) = \begin{cases} 0 & \text{for } t \leq 0 \\ \frac{b}{q} \left[ \mu \sin \lambda t + \frac{(1-\mu)}{\omega^2 + \lambda^2} (\omega \sin \lambda t - \lambda \cos \lambda t + \lambda e^{-\omega t}) \right] & \text{for } 0 \leq t \leq T \\ \frac{b}{q} \frac{(1-\mu)\omega\lambda}{\omega^2 + \lambda^2} [1 - (-1)^n e^{\omega t}] e^{-\omega t} & \text{for } t \geq T \end{cases} \quad (3.49)$$

Case VI: Hereditary Specimen - Approximate

$$\sigma(t) = \frac{E_2}{l} (u_2 - u_1) + \frac{H}{l} \int_0^t e^{-\alpha(t-\tau)} (v_2 - v_1) d\tau \quad (3.50)$$

by assumption 3.

Eliminate the integral between (3.50) and its derivative with respect to time. Then use (3.37) obtaining

$$\frac{d^2\sigma}{dt^2} + \left[ \alpha + \frac{2q(E_2 + H)}{l\rho_1 c_1} \right] \frac{d\sigma}{dt} + \frac{2q\alpha E_2}{l\rho_1 c_1} \sigma = \frac{2(E_2 + H)}{l\rho_1 c_1} \frac{d\sigma_D}{dt} + \frac{2E_2\alpha}{l\rho_1 c_1} \sigma_D \quad (3.51)$$

Let

$$\left. \begin{aligned} \zeta &= \frac{2q(E_2 + H)}{\rho_1 c_1} \\ \mu &= \frac{1}{2} (\alpha + \zeta) \\ \eta &= \sqrt{\mu^2 - \frac{2E_2 H q}{l\rho_1 c_1}} \end{aligned} \right\} \quad (3.52)$$

then

$$\frac{d^2\sigma}{dt^2} + 2\mu \frac{d\sigma}{dt} + (\mu^2 - \eta^2) \sigma = \begin{cases} 0 & \text{for } t \leq 0 \\ \frac{b}{q} [(\mu^2 - \eta^2) \sin \lambda t + \lambda \zeta \cos \lambda t] & \text{for } 0 \leq t \leq T \\ 0 & \text{for } t \geq T \end{cases} \quad (3.53)$$

$$\left. \begin{aligned} \sigma &= \frac{d\sigma}{dt} = 0 \quad \text{for } t = 0 \\ \sigma, \frac{d\sigma}{dt} &\text{ continuous for } t = T \end{aligned} \right\} \quad (3.54)$$

Thus

$$q\sigma = \sigma_T = \begin{cases} 0 & \text{for } t \leq 0 \\ -b[g \cosh\eta t + \frac{1}{\eta}(\mu g + \lambda h) \sinh\eta t]e^{-\mu t} \\ +b[g \cos\lambda t + h \sin\lambda t] & \text{for } 0 \leq t \leq T \\ be^{-\mu t} \left\{ \frac{(\mu g + \mu h)}{\eta} [(-1)^n e^{\mu t} \sinh\eta(t-T) - \sinh\eta t] \right. \\ \left. +g[(-1)^n e^{\mu T} \cosh(t-T) - \cosh\eta t] \right\} & \text{for } t \geq T \end{cases} \quad (3.55)$$

$$g = \frac{\lambda\zeta(\mu^2 - \eta^2 - \lambda^2) - 2\mu\lambda(\mu^2 - \eta^2)}{(\mu^2 - \eta^2 - \lambda^2)^2 + (2\lambda\mu)^2} \quad (3.56)$$

$$h = \frac{(\mu^2 - \eta^2)(\mu^2 - \eta^2 - \lambda^2) + 2\lambda^2\mu\zeta}{(\mu^2 - \eta^2 - \lambda^2)^2 + (2\lambda\mu)^2}$$

C. Mathematical analysis of the longitudinal impact of a round head short bar on an infinitely long bar.

This discussion follows that of W. A. Prowse [1] (see Figure 12).

Let the round-head anvil strike the plane surface with velocity  $v$ . Let  $\beta(t)$  be the total indentation of the anvil and surface combined. Then, for steady pressure  $p$ , the Hertz law [13] gives

$$p = k_2\beta^{3/2} \quad (3.57)$$

where

$$k_2 = \frac{2E}{3(1+\nu)(1-\nu)} r^{1/2} \quad (3.58)$$

E and  $\nu$  are the Young's modulus and Poisson ratio of the anvil and surface while  $r$  is the radius of the anvil head.

Prowse considers a section of the anvil of length  $\Delta x$ , traversed by the wave with velocity  $c$  in time  $\Delta t$ . The resultant force acting on the face AB of this section is equal to the time rate of change of momentum of the section.

The resultant force is

$$- \frac{dp}{dt} \Delta t \quad (3.59)$$

while Prowse considers the time rate of change of momentum as

$$\frac{d}{dt} \left( A \rho \Delta x \frac{1}{2} \frac{d\beta}{dt} \right) = \frac{1}{2} \rho c A \Delta t \frac{d^2\beta}{dt^2} \quad (3.60)$$

where  $A$  is the cross-sectional area of the anvil.

Thus, equaling (3.59) and (3.60)

$$\frac{d}{dt} \left( p + \frac{1}{2} \rho c A \frac{d\beta}{dt} \right) = 0$$

Using (3.57) this yields

$$k_2 \beta^{3/2} + \frac{1}{2} \rho c A \frac{d\beta}{dt} = C_1 \quad (3.61)$$

We may use either initial or final conditions for the determination of the constant of integration. First we follow

Prowse and designate the maximum indentation by  $\beta_1$ . Thus when

$$\frac{d\beta}{dt} = 0 \quad (3.62)$$

$$\beta = \beta_1$$

and it follows from (3.61) that

$$\frac{1}{2} \rho c A \frac{d\beta}{dt} = k_2 (\beta_1^{3/2} - \beta^{3/2}) \quad (3.63)$$

Since the initial indentation is zero, the solution is

$$t = \frac{\rho c A}{2k_2 \beta_1^{1/2}} \int_0^{\beta/\beta_1} \frac{dy}{1 - y^{3/2}} \quad (3.64)$$

Prowse left the result in this form and evaluated the integral numerically. For our purposes it is better to evaluate the integral analytically before starting numerical computations.

Define

$$\delta = \sqrt{\beta/\beta_1} \quad (3.65)$$

$$\tau = \frac{6v}{\beta_1} t$$

where  $v$  is the initial velocity. Then we have from (3.64)

$$\tau - \frac{\pi}{\sqrt{3}} = \ln \left[ \frac{1 + \delta + \delta^2}{(1 - \delta)^2} \right] - 2\sqrt{3} \tan^{-1} \left( \frac{2\delta + 1}{\sqrt{3}} \right) \quad (3.66)$$

From the Prowse condition

$$\frac{1}{2} \frac{d\beta}{dt} = v \text{ for } \beta = 0$$

we obtain an expression for the limiting indentation  $\beta_1$  in terms of the initial velocity, from (3.57)

$$\beta_1^{3/2} = \frac{\rho c A v}{k_2} \quad (3.67)$$

Note that the limiting stress  $\sigma_1$  is

$$\sigma_1 = \frac{k_2 \beta_1^{3/2}}{A} \quad (3.68)$$

Consequently, by (3.67) and (3.68)

$$\sigma_1 = \rho c v \quad (3.69)$$

which is the stress-velocity relation of the theory of impact due to St. Venant [12], [13].

It is possible to construct stress-time curves based on equation (3.66) and Table 2. This has been done in Figures 13 through 28 for steel hammers with hemispherical ends. The critical values for these figures are given in Table 3.

- L.....the hammer length
- h.....the height of drop
- $t_1$ .....base time =  $\frac{2L}{c}$  (time-length of corresponding St. Venant pulse)
- T.....time-length of pulse
- $cT$ .....liner pulse-length
- $\sigma_m$ .....maximum stress attained

The velocity of the hammer at time of contact and the theoretical limiting stress, are independent of the length of the hammer and are given as a function of the height of drop in Table 3.

For these computations the following values were assumed:

$$E = 2.073 \times 10^{12} \text{ dynes/cm}^2$$

$$v = 3 \times 10^{-1}$$

$$\rho = 7.7 \text{ gm/cm}^3$$

Hammer diameter = 2.5 cm

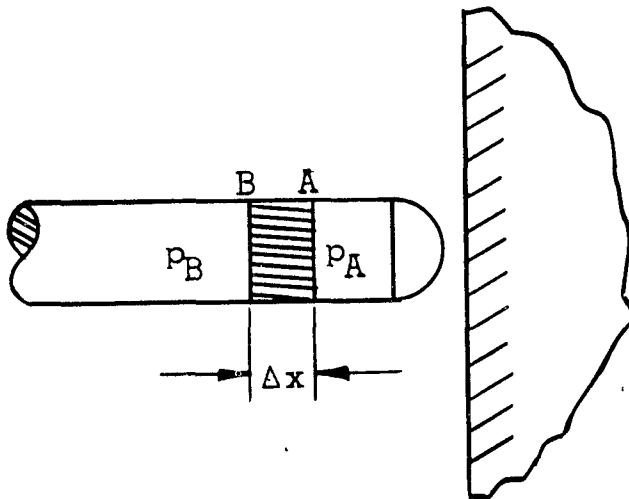


Figure 12  
Round-Head Hammer Impact

TABLE 2

Height of Drop versus Velocity and  
Limiting Stress

h (cm)	v (cm/sec)	$\sigma_1$ (kgF/cm <sup>2</sup> )
5	99.0454	408.94
10	140.071	578.33
15	171.552	708.30
20	198.091	817.88
25	221.472	914.41

TABLE 3  
Critical Values for Figures 13 through 28

Fig.	L (cm)	h (cm)	$t_1$ (micro sec)	T (micro sec)	cT (cm)	$\sigma_n$ (KgF/cm <sup>2</sup> )
10	25	5	96.5	140	72.5	348
11	25	10	96.5	136	70.5	514
12	25	15	96.5	134	69.2	644
13	25	25	96.5	130	67.5	850
14	50	5	193	239	124	405
15	50	10	193	233	121	575
16	50	15	193	231	120	708
17	50	25	193	228	118	914
18	75	5	290	336	174	409
19	75	10	290	331	171	578
20	75	15	290	328	170	708
21	75	25	290	325	168	914
22	100	5	386	432	224	409
23	100	10	386	427	221	578
24	100	15	386	424	220	708
25	100	25	385	421	218	914

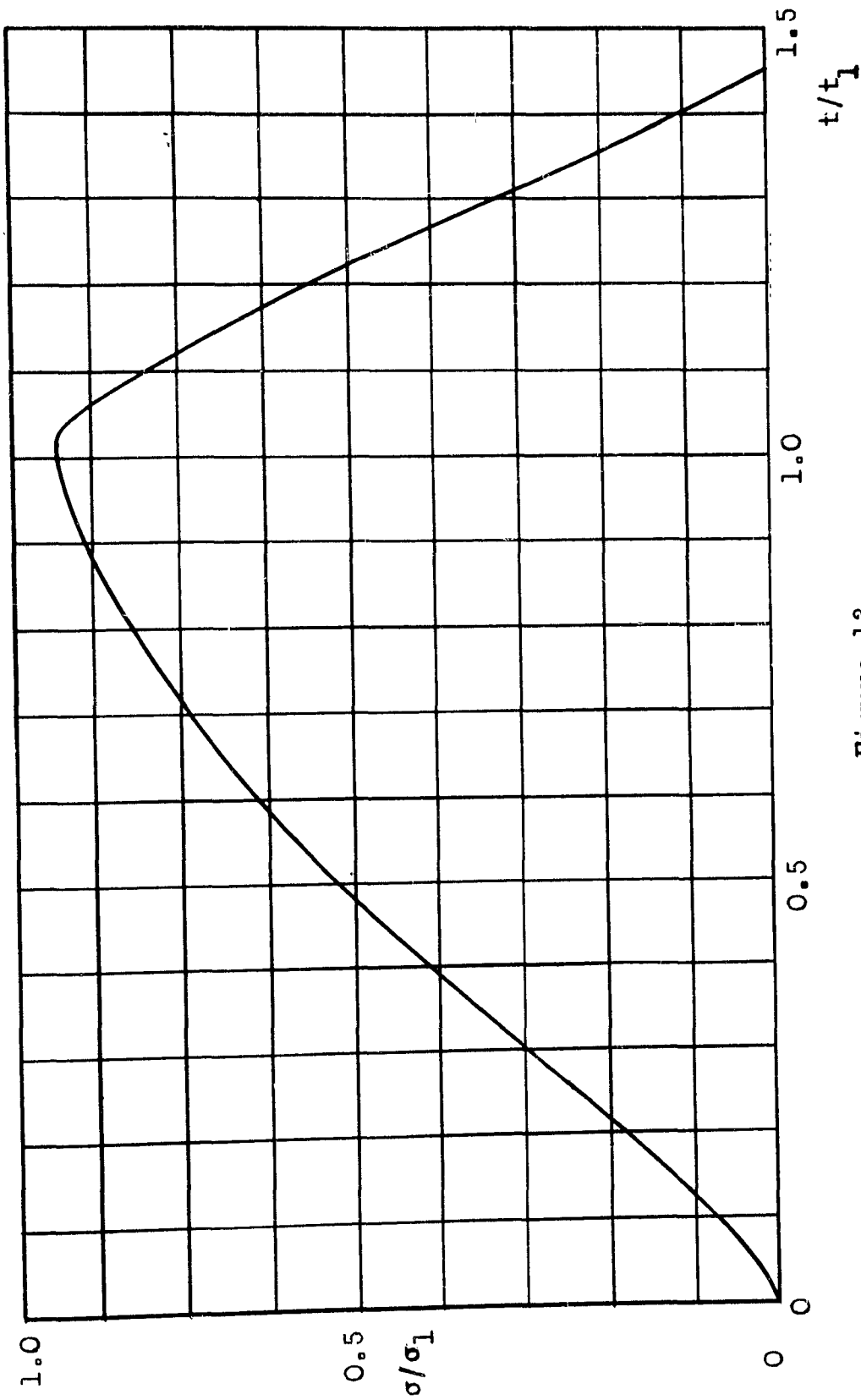


Figure 13  
Stress-Time Relationships  
(See Table 3)

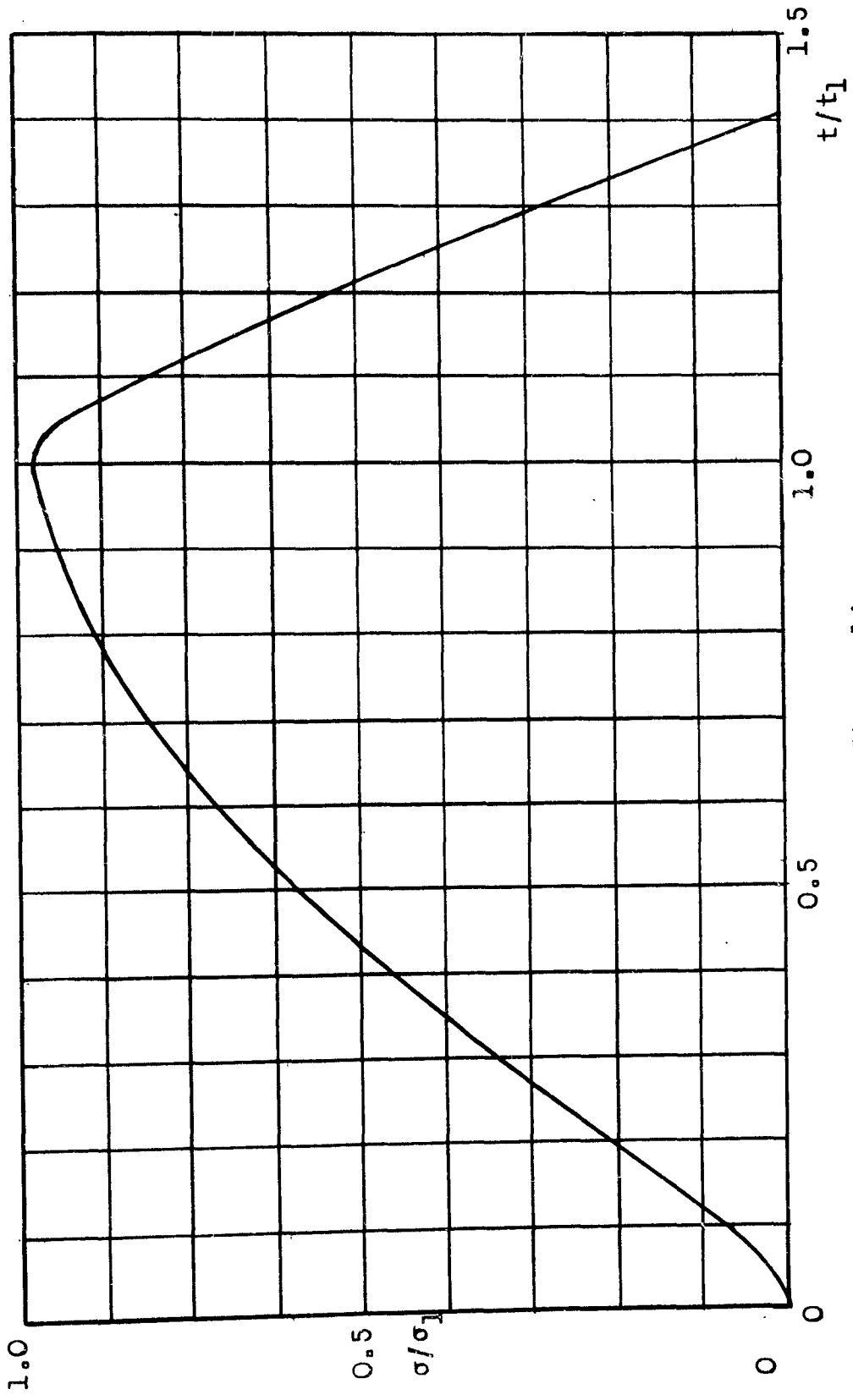


Figure 14  
Stress-Time Relationships  
(See Table 3)

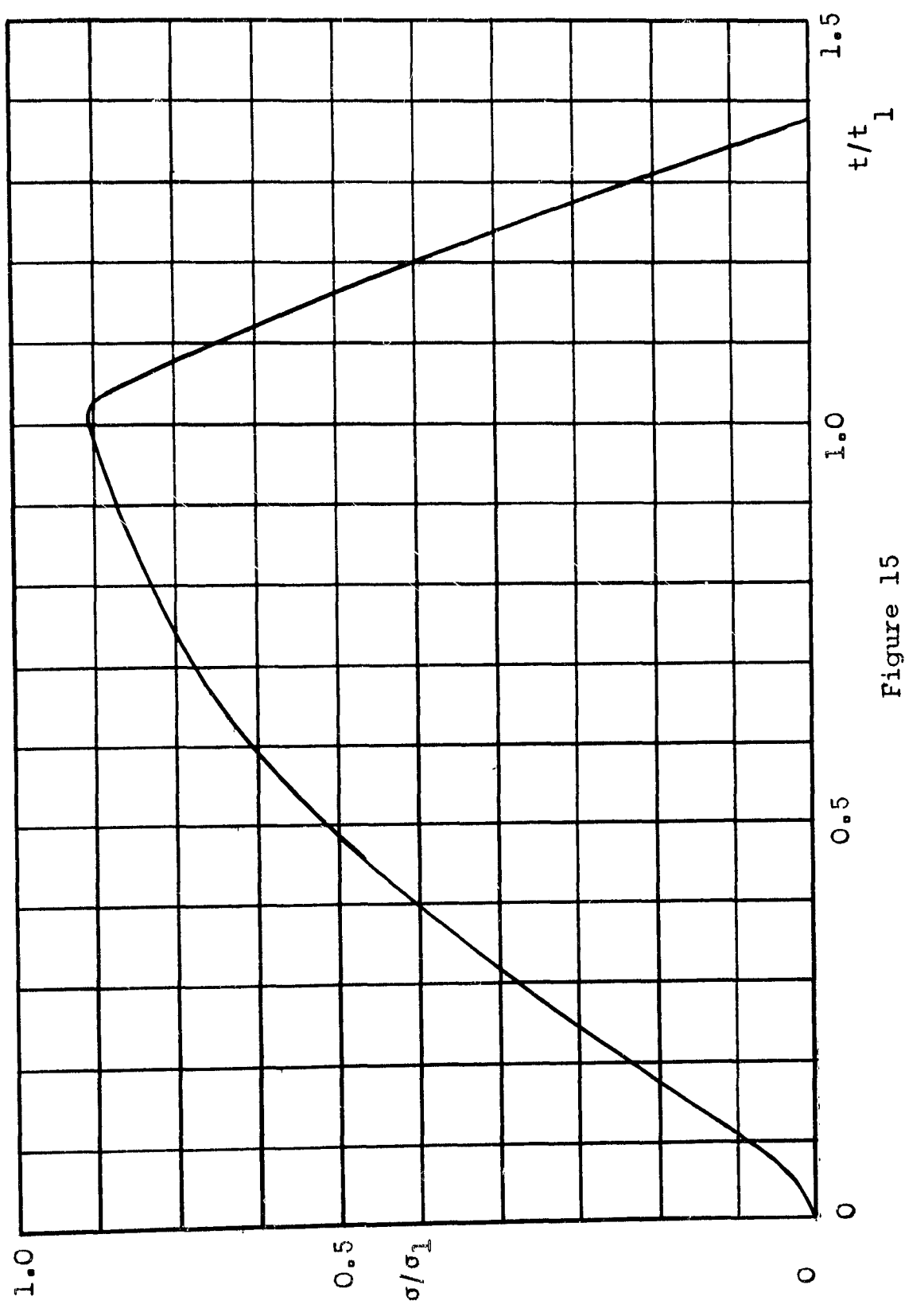


Figure 15  
Stress-Time Relationships  
(See Table 3)

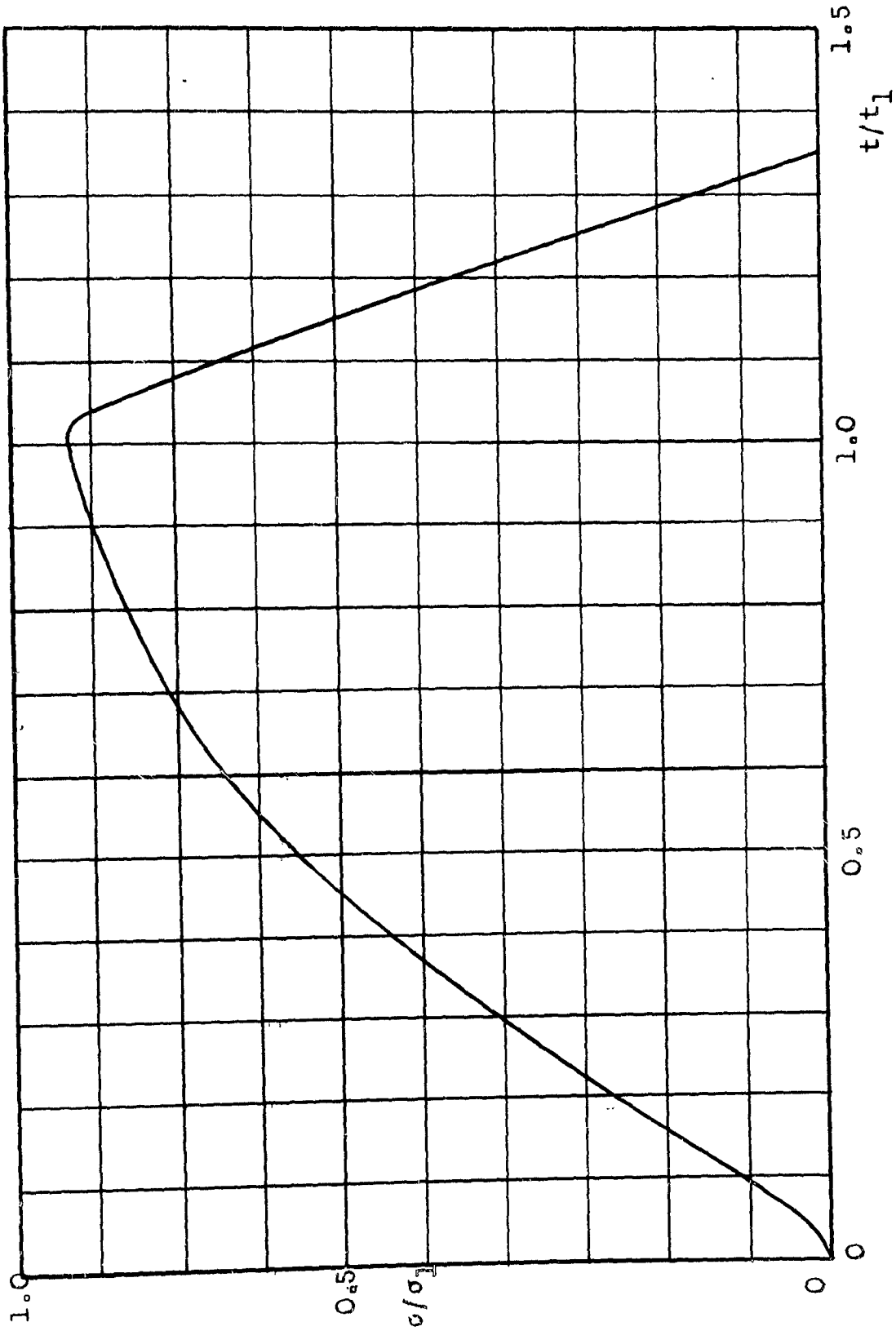


Figure 16  
Stress-Time Relationships  
(See Table 3)

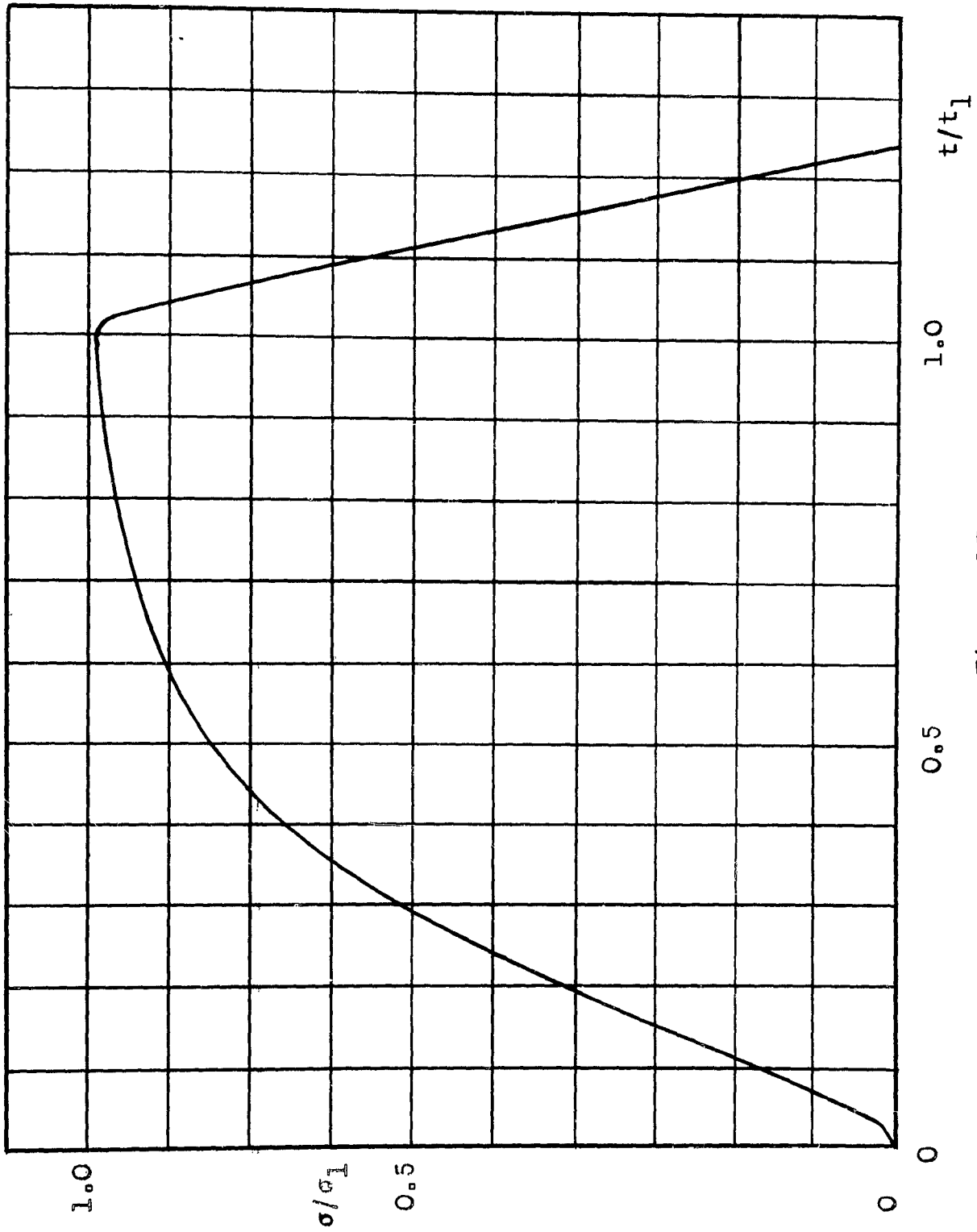


Figure 17  
Stress-Time Relationships  
(See Table 3)

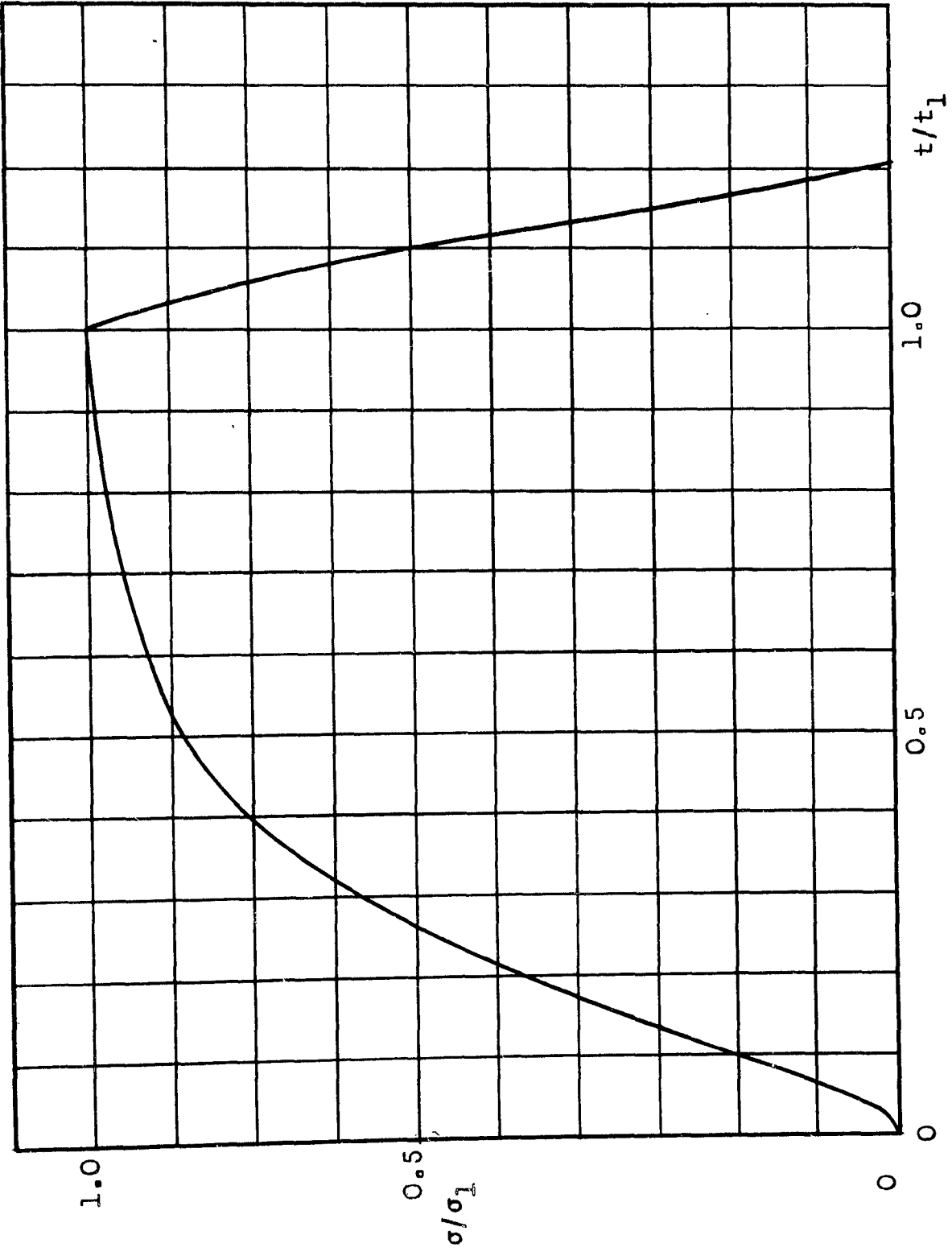


Figure 18  
Stress-Time Relationships  
(See Table 3)

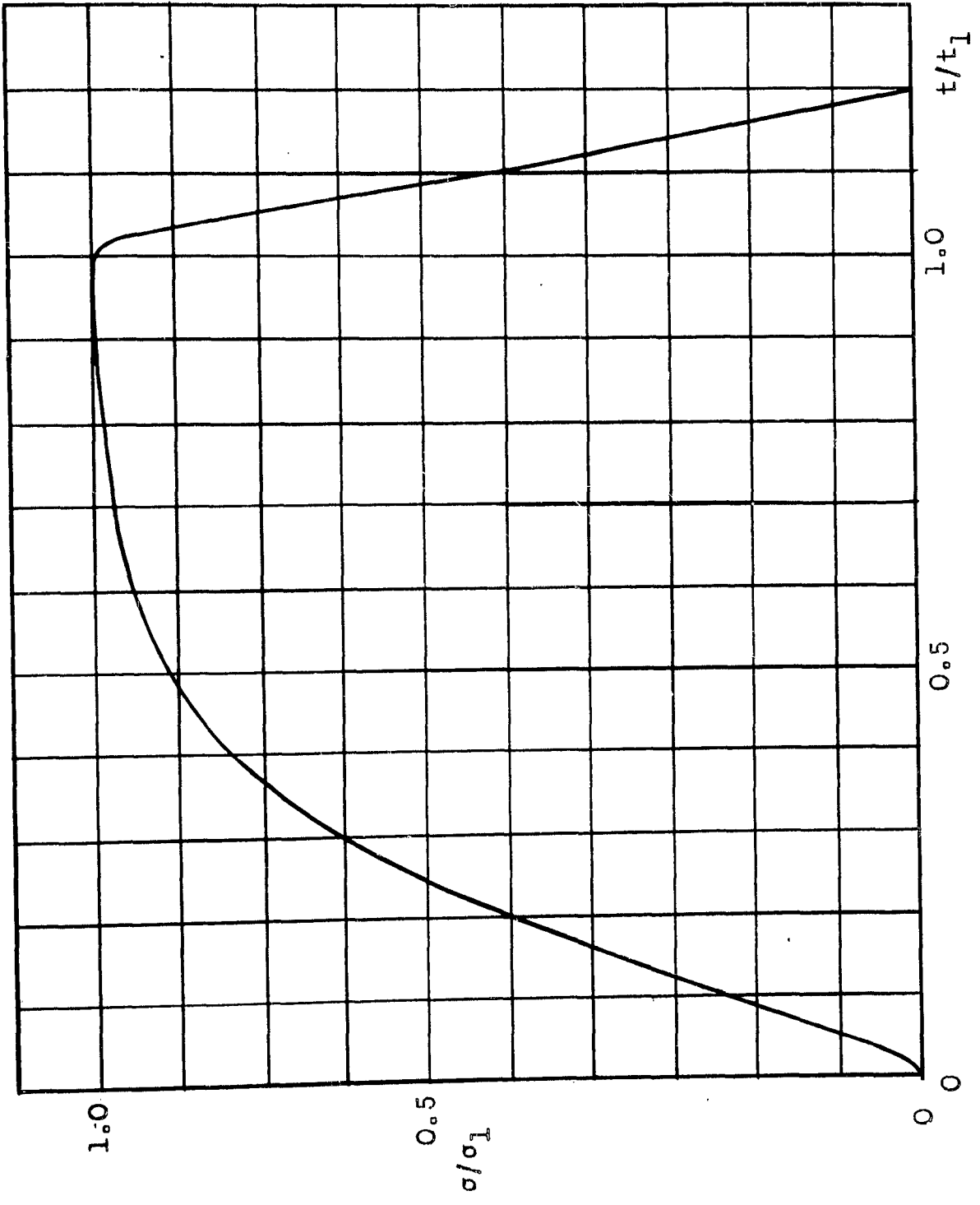


Figure 19  
Stress-Time Relationships  
(See Table 3)

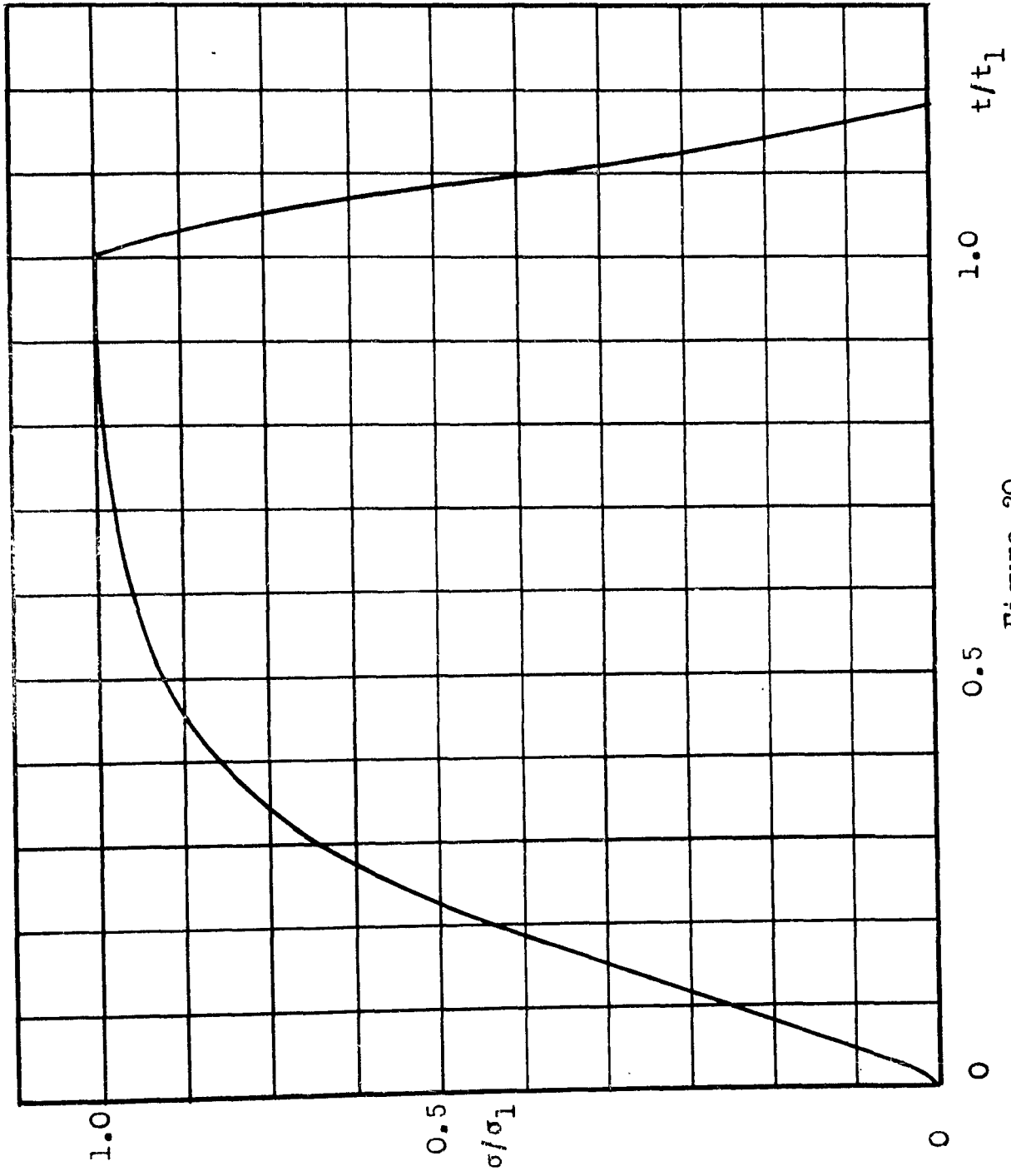


Figure 20

Stress-Time Relationships

(See Table 3)

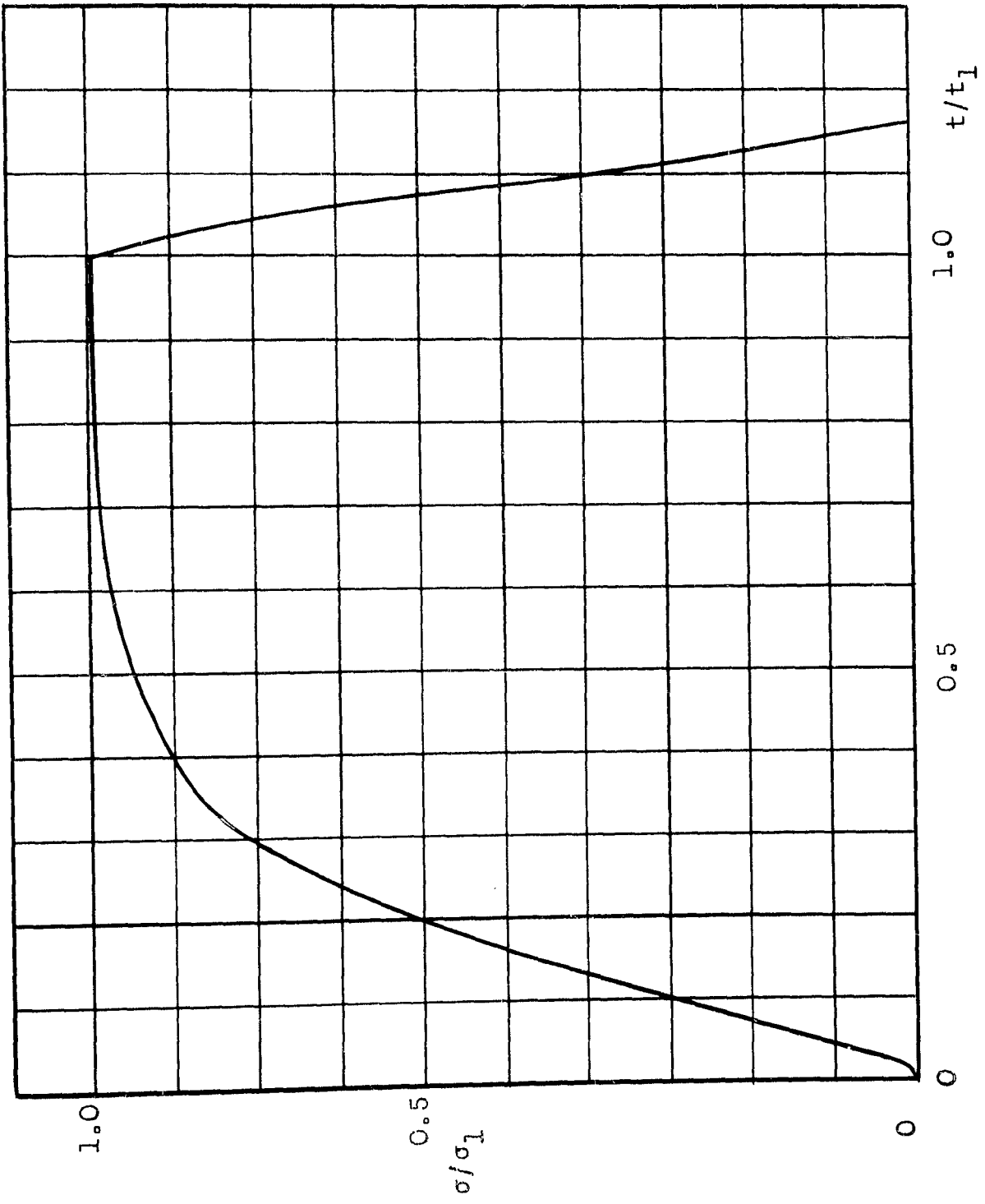


Figure 21  
Stress-Time Relationships  
(See Table 3)

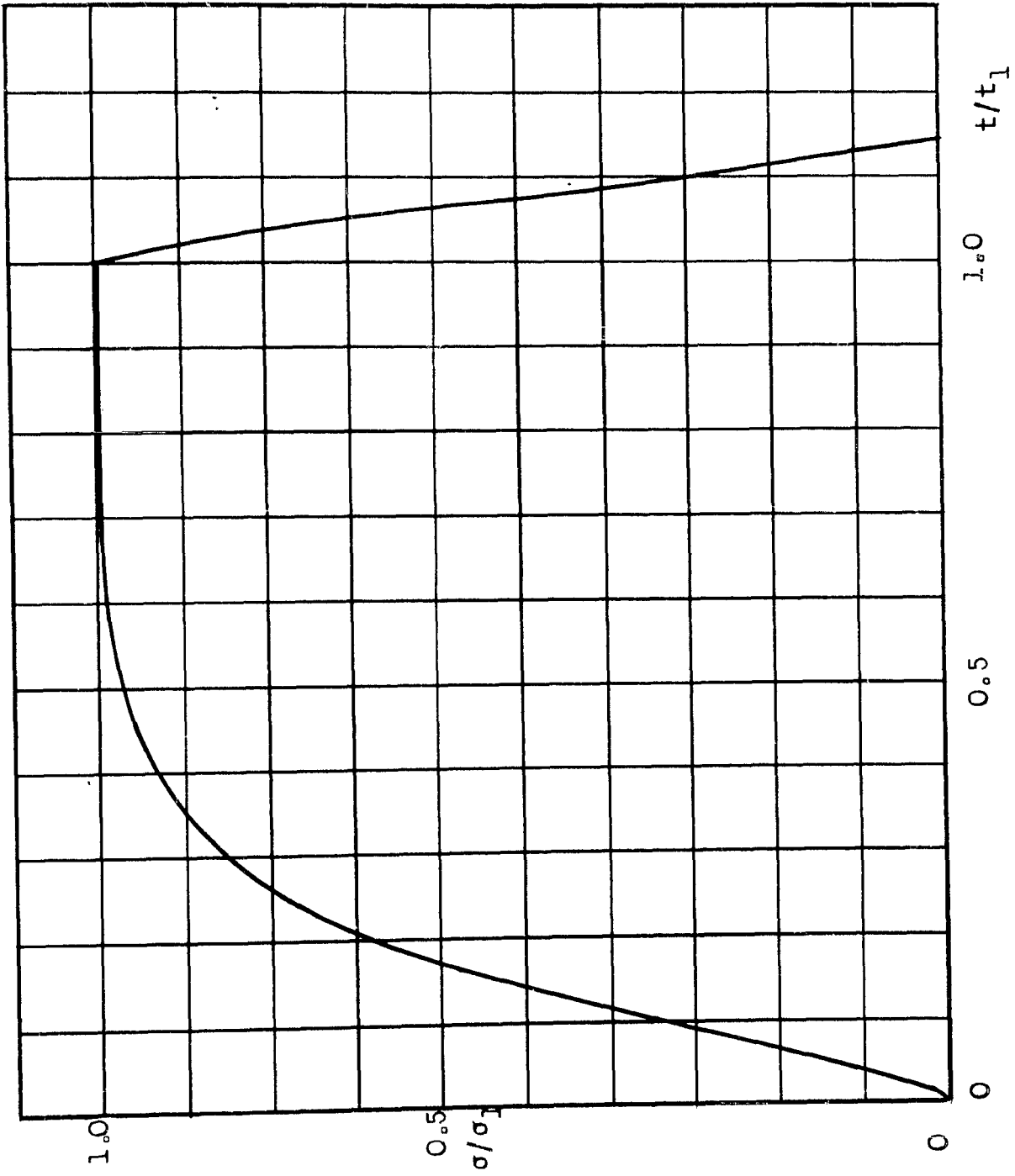


Figure 22  
Stress-Time Relationships  
(See Table 3)

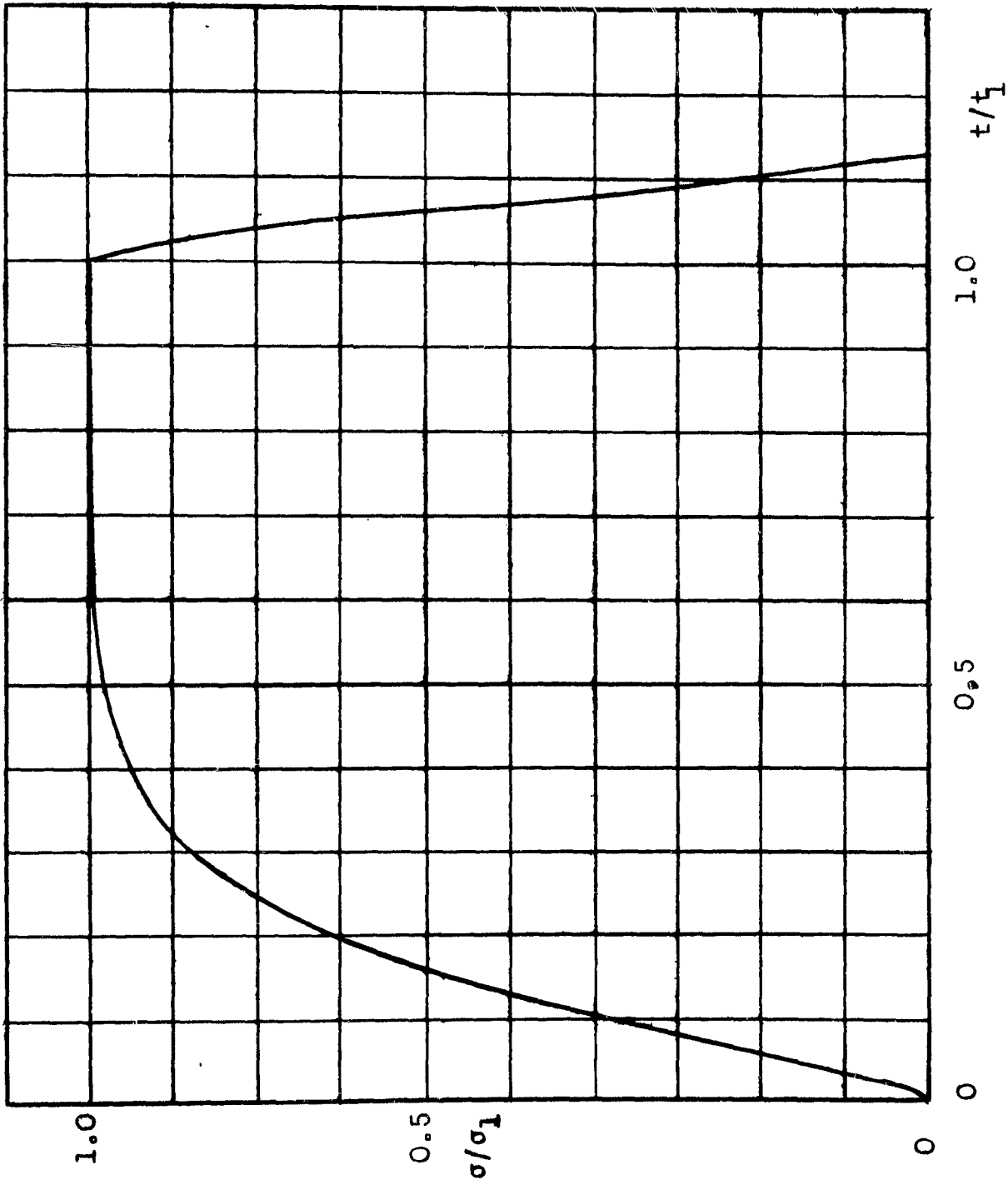


Figure 23  
Stress-Time Relationships  
(See Table 3)

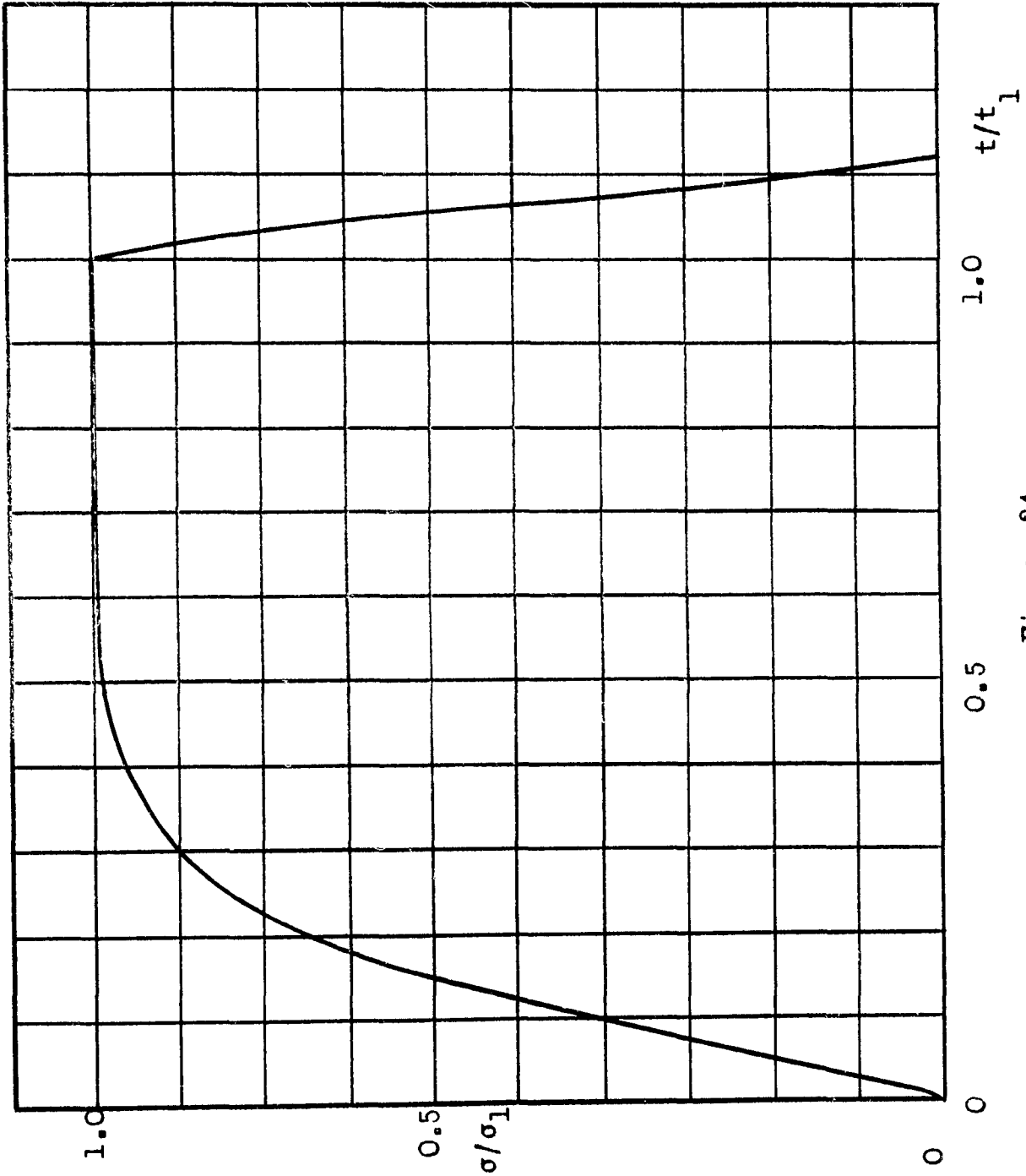


Figure 24  
Stress-Time Relationships  
(See Table 3)

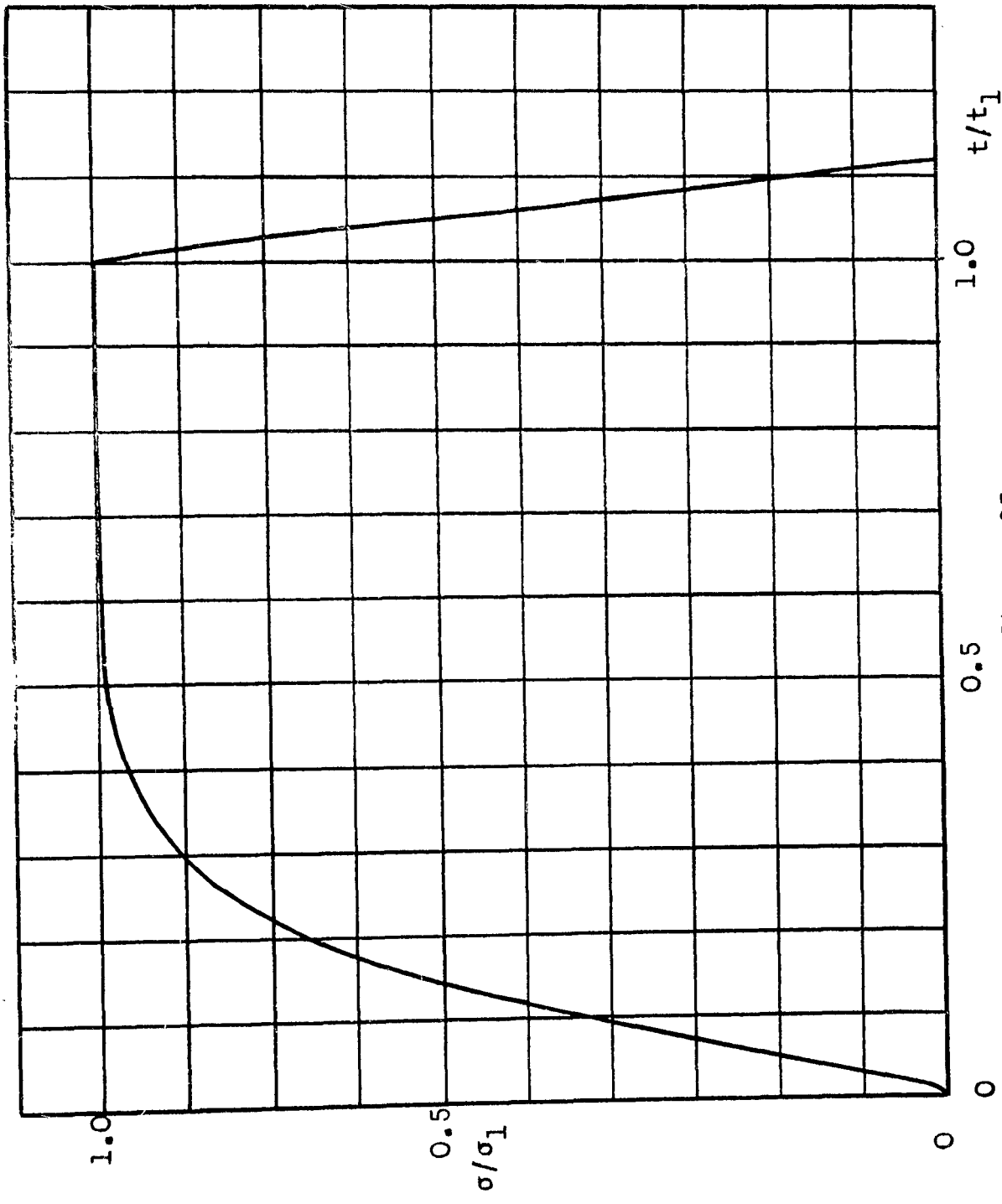


Figure 25

Stress-Time Relationships

(See Table 3)

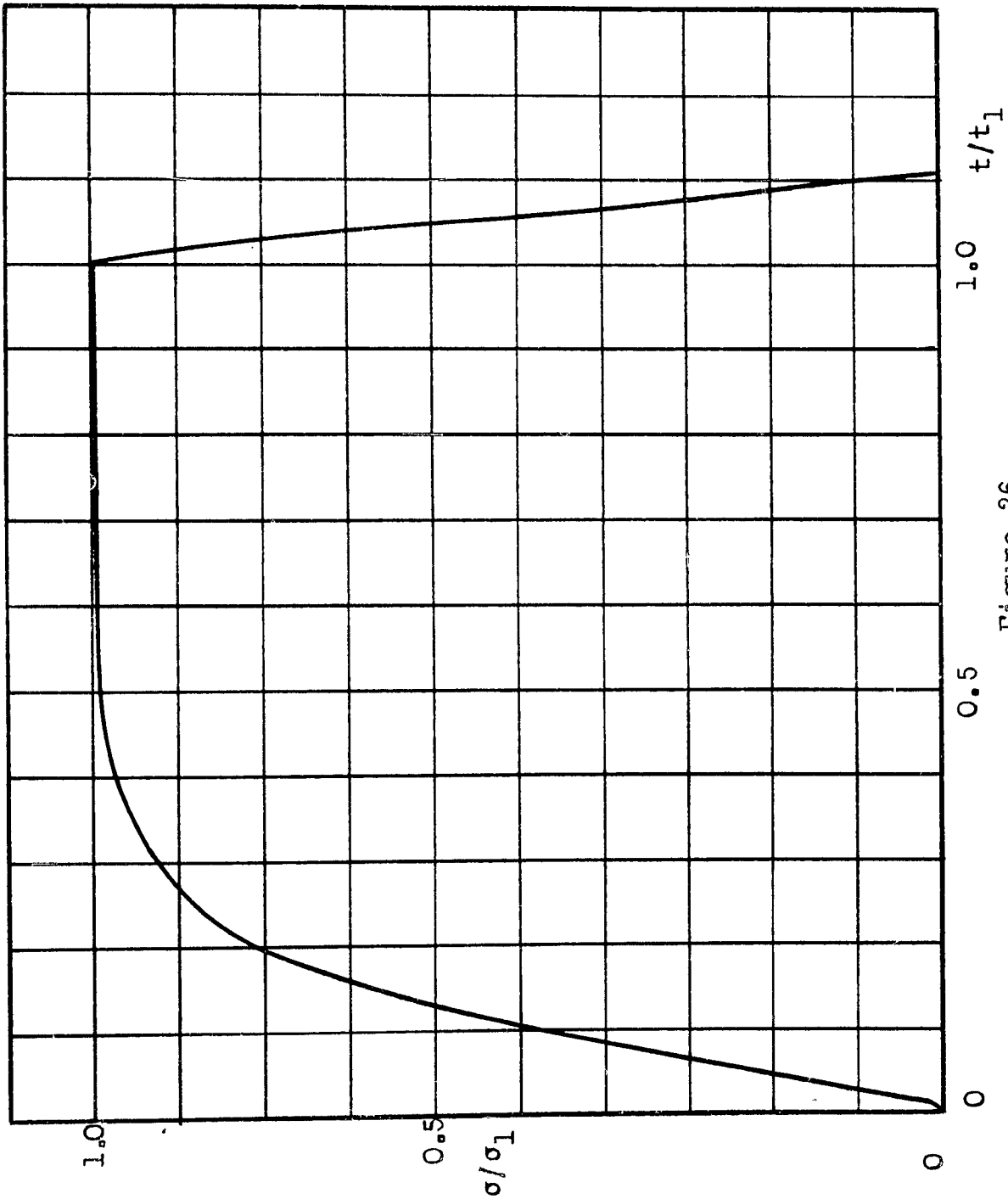


Figure 26

Stress-Time Relationships

(See Table 3)

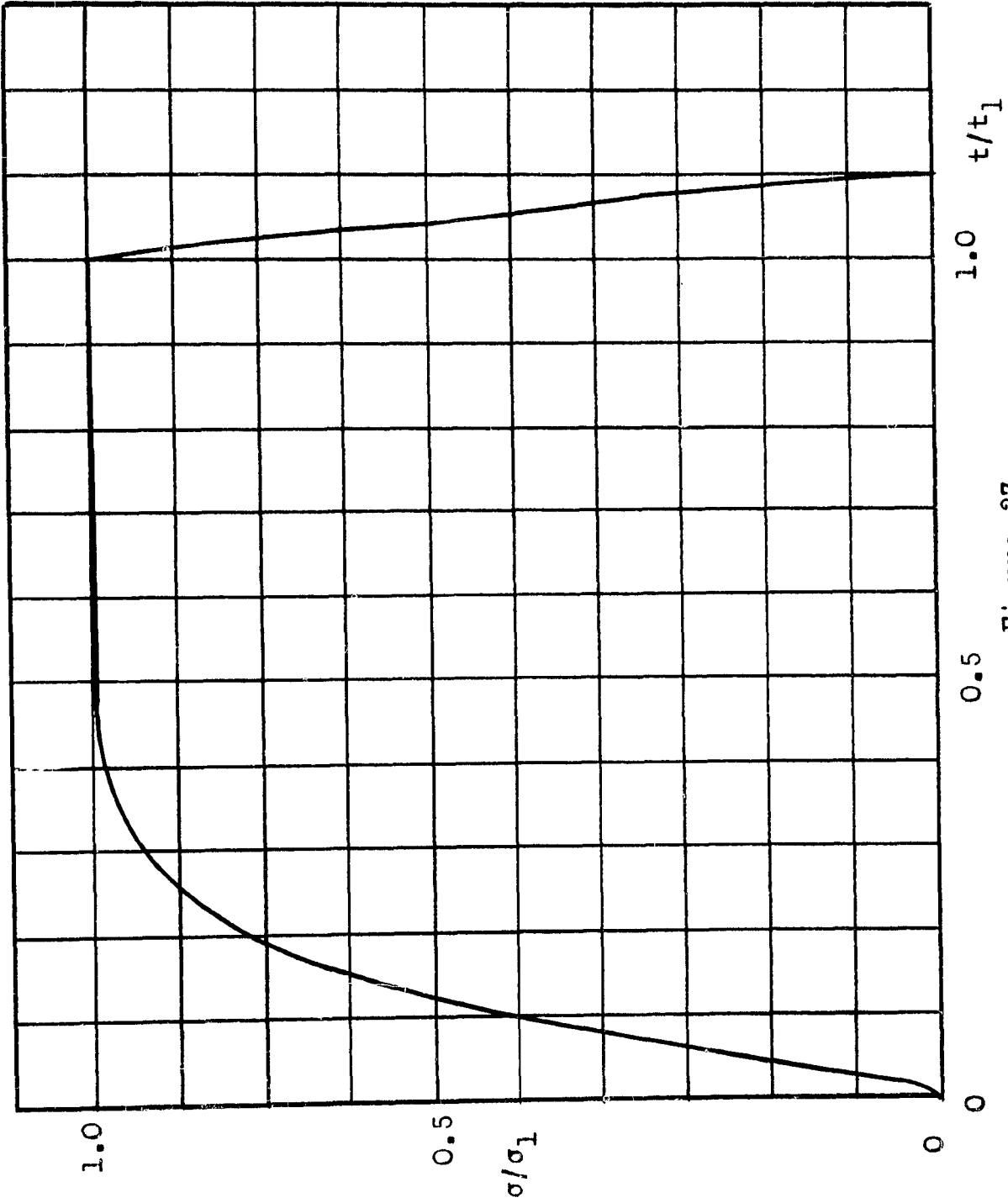


Figure 27

Stress-Time Relationships

(See Table 3)

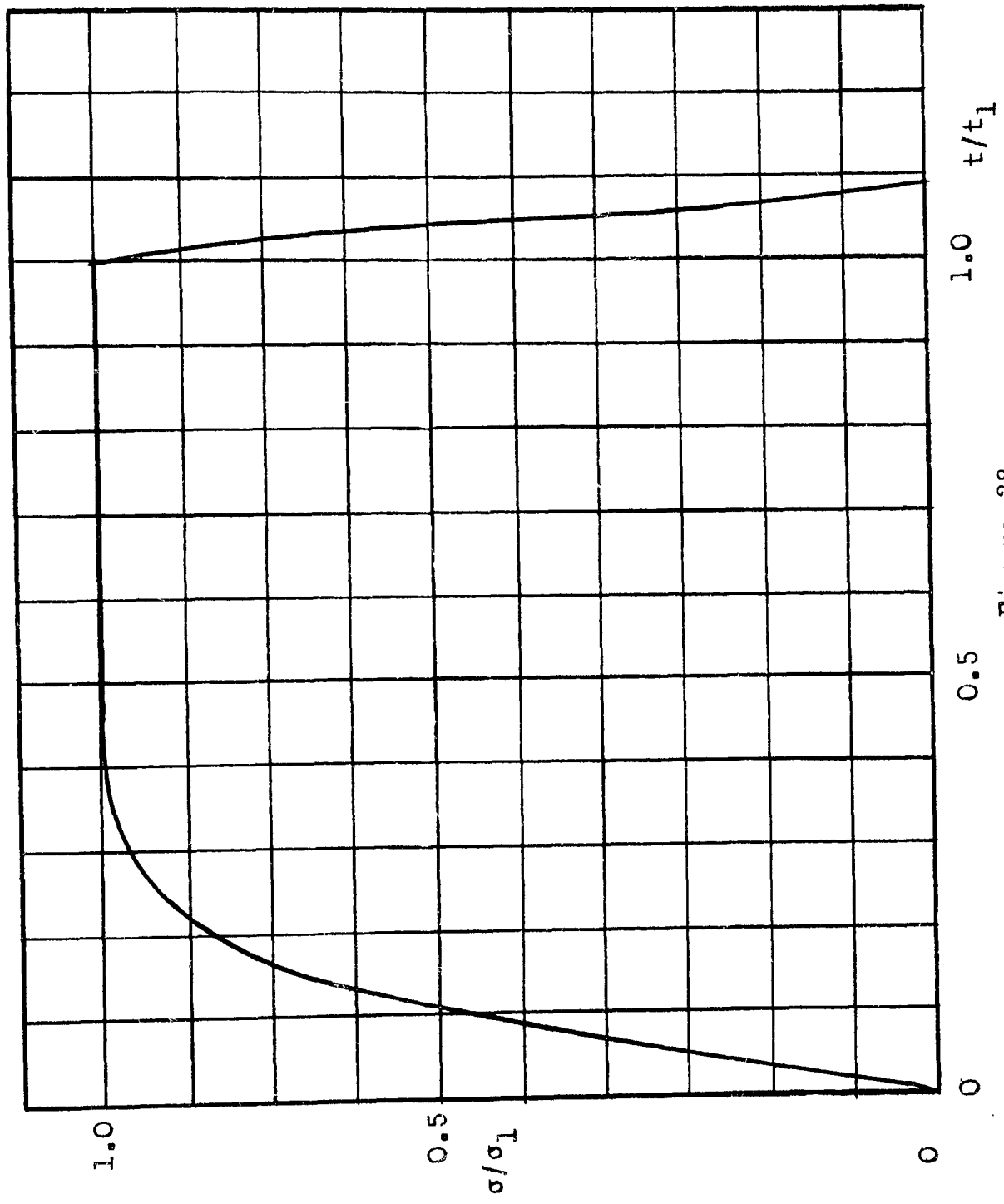


Figure 28

Stress-Time Relationships

(See Table 3)

SECTION IV  
SAMPLE COMPUTATION AND DISCUSSION OF TEST RESULTS  
FOR NATURAL RUBBER (HEVEA)

## SECTION IV

### Sample Computation and Discussion of Test Results

#### for Natural Rubber (Hevea)

We consider the case of normal (approximate) velocity of 50 cm/sec. The material is natural rubber.

The raw data obtained by averaging readings from film strips for ten separate runs are as follows

Calibration: (initial length) 185.3

Average drum speed: 121.17 rpm

Readings:

<u>Lengthwise (<math>10^{-3}</math> in.)</u>	<u>Transverse</u>	<u>d (Calibration) - (Width)</u>
0	185.3	0
100	179.3	6.0
200	172.9	12.4
300	167.0	18.3
400	160.9	24.4
500	154.8	30.5
600	149.6	35.7
700	144.1	41.2
800	139.2	46.1
900	134.9	50.4
1000	131.2	54.1
1100	127.8	57.5
1200	125.3	60.0
1300	123.4	61.9
1400	122.4	62.9
1500	123.1	62.2
1600	124.0	61.3
1700	125.7	59.6
1800	128.9	56.4
1900	132.7	52.6
2000	137.0	48.3
2100	142.0	43.3
2200	148.0	37.3
2300	154.0	31.3
2400	160.7	24.6
2500	167.9	17.4
2600	175.2	10.1
2700	182.6	2.7
2745	185.3	0
2800	190.0	-4.7

These results are then plotted and a smooth curve drawn through the points (Figure 29, 30, 31).

The scale of the curve is changed into the physically-meaningful parameters, time and displacement, through the following computations.

The inside diameter of the drum is 15.06 inches, its average rotational speed is 121.17 rpm. Hence the time corresponding to a given horizontal distance  $h$  in inches on the film is

$$t = \frac{60 h}{121.17 \times 15.06\pi}$$

hence the total time of contact is

$$T = \frac{60 \times 2.745}{121.17 \times 15.06\pi} = 2.87244 \times 10^{-2} \text{ sec}$$

The length of the specimen is 1.27 cm. The calibration measurement yields 185.3. Thus our change of scale on the displacement is given by

$$S = \frac{1.27}{185.3} d$$

We divide the abscissa of the graph into 10 divisions of length  $2.87244 \times 10^{-3}$  sec and take the values of

$$S(k) = S\left(\frac{kT}{10}\right) = S_k$$

from the graph. We have

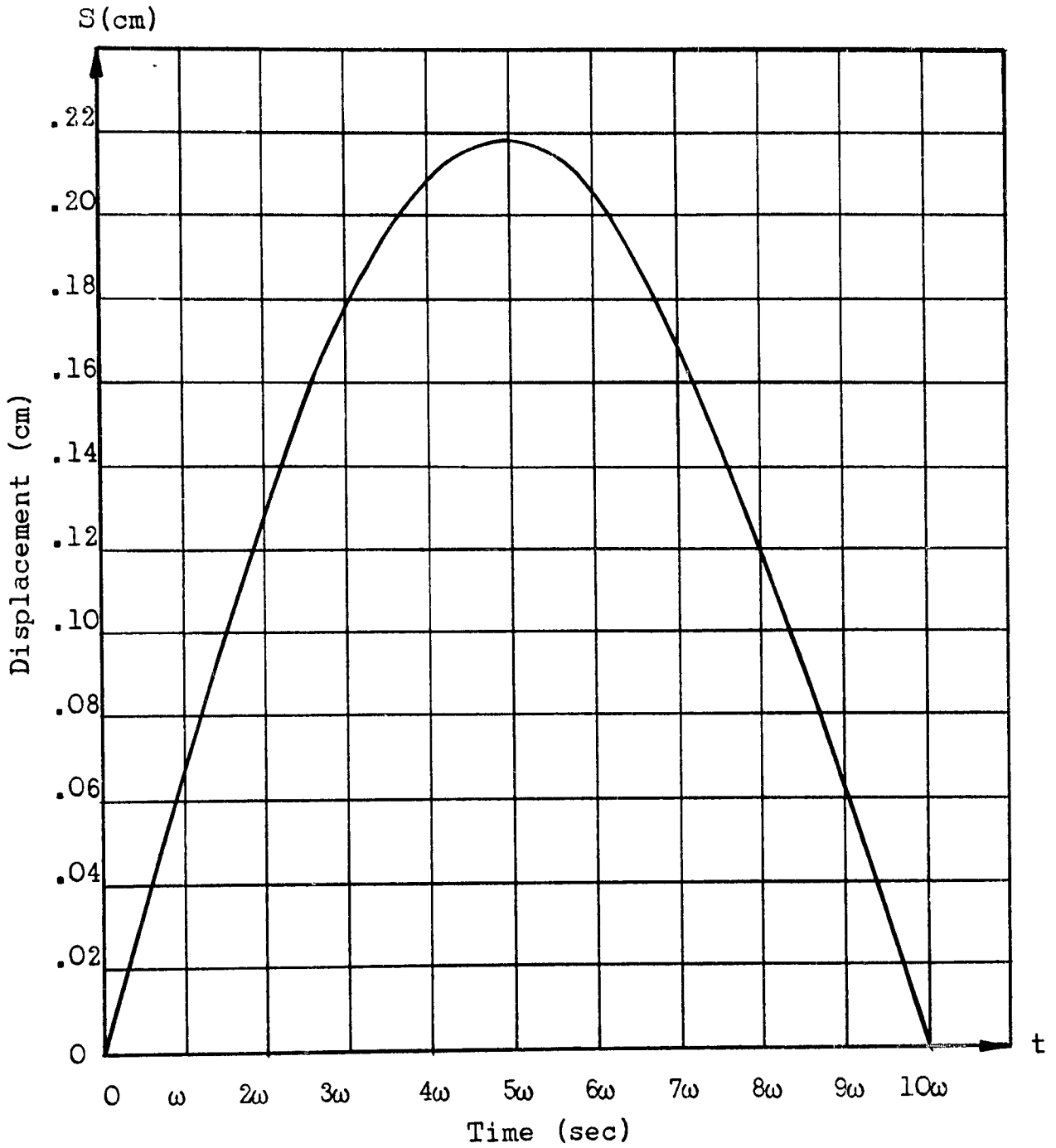


Figure 29

Displacement-Time Curves

Nominal velocity 25 cm/sec;  $\omega = 3.088 \times 10^{-3}$  sec

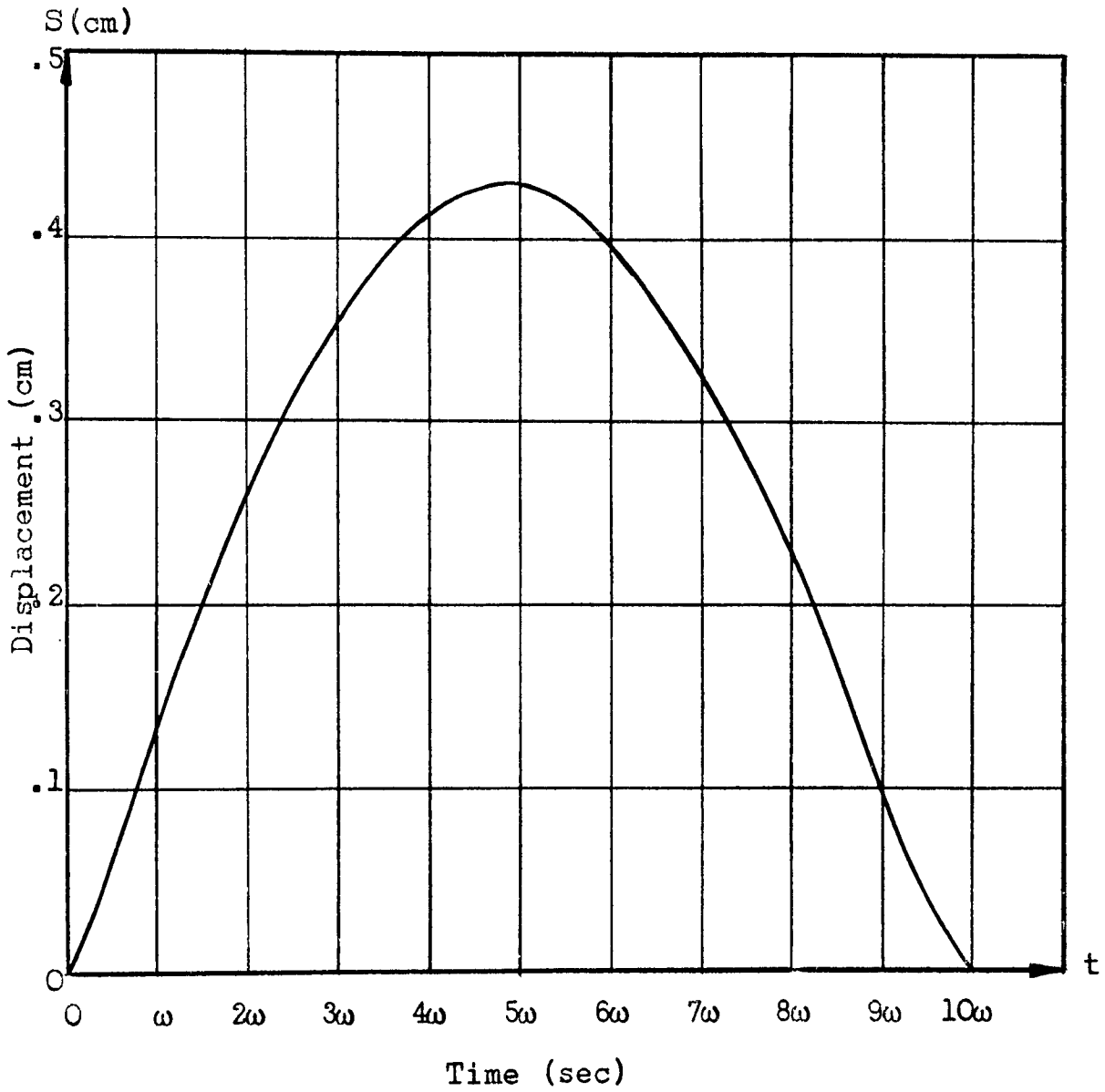


Figure 30

Displacement-Time Curves

Nominal velocity 50 cm/sec;  $\omega = 2.872 \times 10^{-3}$  sec

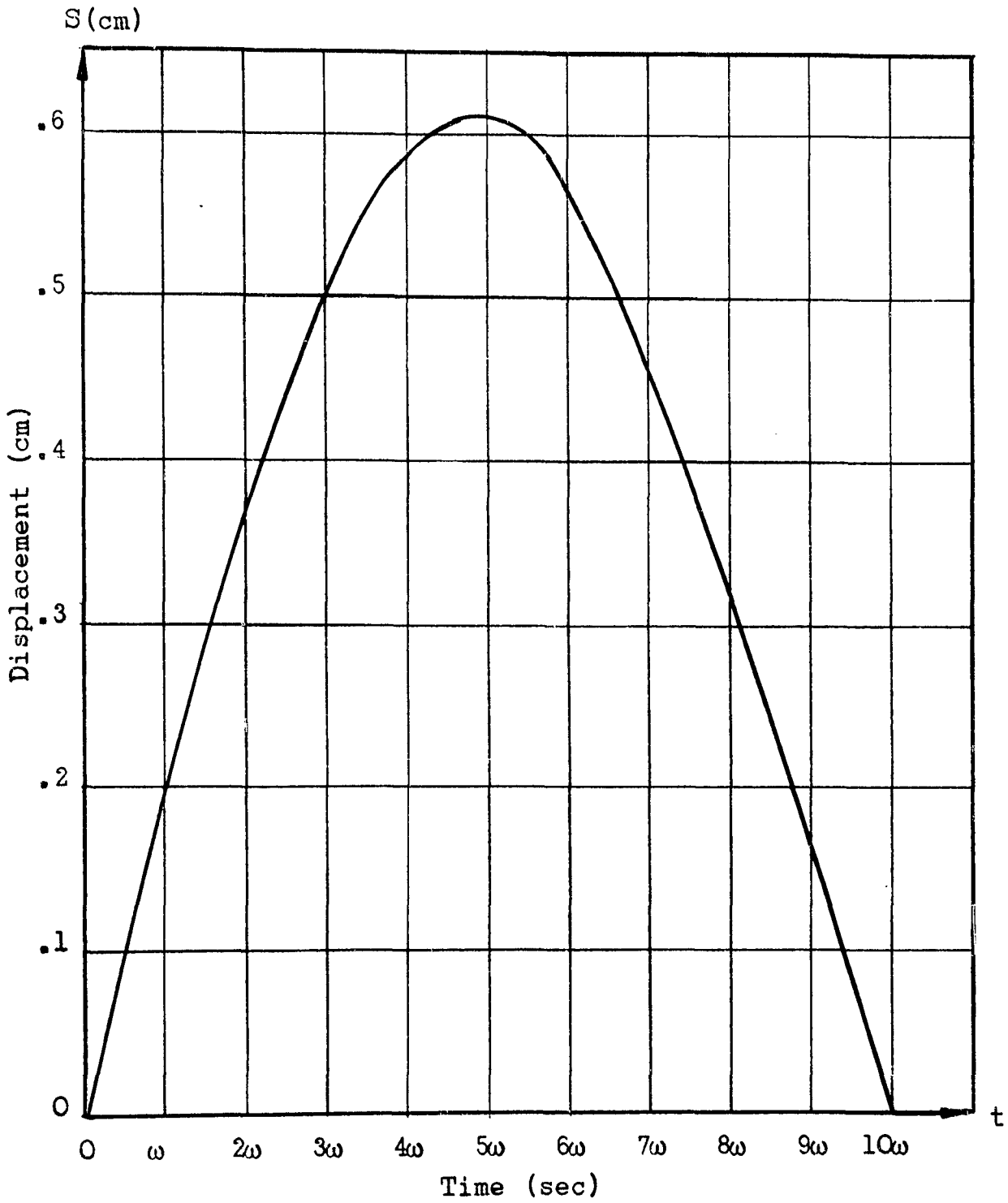


Figure 31

Displacement-Time Curves

Nominal velocity 75 cm/sec;  $\omega = 2.645 \times 10^{-3}$  sec



This procedure leads to the system of equations

$$7.338,1605 D_2 + 8.181,983,5 D_1 + 8.235,692,7 D_0 = -5.816,025,7$$

$$8.448,673,3 D_2 + 8.747,357,1 D_1 + 8.181,983,5 D_0 = -7.338,160,5$$

$$8.709,471,2 D_0 + 8.448,673,3 D_1 - 7.338,160,5 D_2 = -8.107,794,3$$

which has the solution

$$D_2 = - 2.068,220,275$$

$$D_1 = 1.350,660,495$$

$$D_0 = -0.205,225,635,7$$

We now solve the equation

$$x^3 + D_2 x^2 + D_1 x + D_0 = 0$$

for its roots

$$x_1 = e^{-n\omega}, x_2 = e^{-(p + iq)\omega}, x_3 = e^{-(p - iq)\omega}$$

and find, after obvious calculations, that

$$n = 5.337,880 \times 10^2, p = 8.771,98, q = 1.107,459 \times 10^2$$

Now that we have  $n$ ,  $p$ , and  $q$ , we can write

$$s(t) = C[e^{-nt} - e^{-pt} \cos qt + \frac{(n^2 + q^2 - p^2)}{2qp} e^{-pt} \sin qt]$$

and determine the value of  $C$  which best satisfies the equations

$$s_1 = C[e^{-n\omega} - e^{-p\omega} \cos q\omega + \frac{(n^2 + q^2 - p^2)}{2qp} e^{-p\omega} \sin q\omega]$$

$$s_2 = C[e^{-2n\omega} - e^{-2p\omega} \cos 2q\omega + \frac{(n^2 + q^2 - p^2)}{2qp} e^{-2p\omega} \sin 2q\omega]$$

.....

$$s_{10} = C[e^{-10n\omega} - e^{-10p\omega} \cos 10q\omega + \frac{(n^2 + q^2 - p^2)}{2qp} e^{-10p\omega} \sin 10q\omega]$$

We again use the method of least squares, finding this time that

$$C = 0.002,915,748$$

The hereditary constants  $\alpha$ ,  $H_0$  and  $H$  are obtained directly with the use of the secant modulus for this material and maximum deformation  $E_2 = 2.81 \times 10^7$  dynes/cm<sup>2</sup>. Hence we have

$$\alpha = n + 2p = 5.513,320 \times 10^2$$

$$H_0 = \frac{m\dot{v}_0}{\alpha A_0} (p^2 + q^2)n - E_2 = 1.626,555 \times 10^7 \text{ dynes/cm}^2$$

$$H = \frac{m\dot{v}_0}{A_0} (2pn + p^2 + q^2) - H_0 - E_2 = 3.662,901 \times 10^7 \text{ dynes/cm}^2$$

We have two checks on the accuracy of our computations. The first is a comparison of the initial velocity obtained from the graph:  $v_0 = 47.5$  cm/sec with the value obtained from the computation

$$\left. \frac{ds}{dt} \right|_{t=0} = C[p-n + \frac{n^2 + q^2 - p^2}{2p}] = 47.849 \text{ cm/sec}$$

The second check is a straight comparison of the experimental values  $s_k$  with the values  $s(k\omega)$  obtained from the equation. The latter check yields an error of less than 4 percent over the entire range of time. Further, all values were rounded off only after the computation was completed rather than at any intermediate stages.

Whittaker's summary (Reference 8) of the Prony method of approximating a function with a finite number of exponentials is quoted below. The notation has been altered to agree with that of this report as much as possible.

"Although Prony's method is more than a century old, it does not appear to be widely known or to have found its way into any text-book; and, as his original paper is perhaps not accessible to many readers, I may be justified in giving here a brief notice of it."

"Suppose that  $s(t)$  is given numerically for a certain range of values of  $t$ . Take any set of values of  $t$  equally spaced within this range, say  $t = 0, \omega, 2\omega, 3\omega, 4\omega, \dots$ , and let the corresponding values of  $s(t)$  be  $s_0, s_1, s_2, s_3, \dots$ . Now if  $s(t)$  could be represented exactly in the form of a sum of  $k$  exponentials, say,

$$Pe^{pt} + Qe^{qt} + Re^{rt} + \dots + Ve^{vt},$$

then  $s(t)$  would satisfy a linear difference-equation of the form

$$As_{n+k} + Bs_{n+k-1} + Cs_{n+k-2} + \dots + Ms_n = 0$$

where the roots of the algebraic equation

$$At^k + Bt^{k-1} + Ct^{k-2} + \dots + M = 0$$

would be

$$e^p, e^q, e^r, \dots, e^v."$$

"Prony's method, which is based on this fact, is to write down a set of linear equations,

$$As_k + Bs_{k-1} + Cs_{k-2} + \dots + Ms_0 = 0$$

$$As_{k+1} + Bs_k + Cs_{k-1} + \dots + Ms_1 = 0$$

$$As_{k+2} + Bs_{k+1} + Cs_k + \dots + Ms_2 = 0$$

$$As_{k+3} + Bs_{k+2} + Cs_{k+1} + \dots + Ms_3 = 0$$

where the quantities  $s_0, s_1, s_2, s_3, \dots$ , are known, since  $s(t)$  is a known tabulated function, and by the ordinary method of Least Squares to find the values of  $A, B, C, \dots, M$ , which most nearly satisfy the equations; then with these values of  $A, B, C, \dots, M$ , to form the algebraic equation

$$As^k + Bs^{k-1} + Cs^{k-2} + \dots + M = 0,$$

and find its roots; these roots will be  $e^p, e^q, e^r, \dots, e^v$ , and thus  $p, q, r, \dots, v$ , are determined.

Knowing  $p, q, r, \dots, v$ , we have a set of linear equations to determine the coefficients  $P, Q, R, \dots, V$ , and these also are to be solved by the method of Least Squares."

#### Discussion of Test Results for Natural Rubber (Hevea)

The data obtained from a series of tests on a natural rubber 27-30 durometer hardness were analyzed, by use of the procedure outlined above, for three initial speeds of the striking bar. It was found, as might be expected, that the phenomena were essentially viscous for nominal speeds of approximately 25, 50, and 75 centimeters per second. Indeed, in the case of the highest initial speed (and, correspondingly, the greatest distortion), the hereditary effect was so small as to be obscured by inaccuracies of the data.

The pertinent results of the investigation are given in Tables 4 and 5, which follow. For the analysis which was made under the assumption of a viscous stress-strain law:

$$\sigma = D\varepsilon + \frac{d\varepsilon}{dt} \tag{4.1}$$

$$s(t) = Ce^{-pt} \sin qt$$

We list in Table 4 the parameters,  $p, q, C, D$ , and  $\gamma$ ; as well as the time of contact  $T$ , the actual initial velocity  $v_0$ , and the maximum strain,  $\varepsilon_m$ .

The slight hereditary effect displayed by the hevea indicated that it would be pointless to carry the analysis further than

heredity of the first degree with residual; which is characterized by

$$\sigma = E\varepsilon + \int_0^t [H_0 + He^{-\alpha(t-\tau)}] \frac{d\varepsilon}{d\tau} d\tau \quad (4.2)$$

The parameters  $E, H_0, H, \alpha, C, n, p, q,$  of (4.2), are listed in Table 5. Note that  $E$  is the static secant modulus for natural rubber.

We finally remark upon an interesting connection between these two analyses. Comparison of Tables 4 and 5 reveals that, for a given initial velocity, we have approximately

$$D = E + H_0$$

Thus, it can be concluded that

$$\gamma \frac{d\varepsilon}{dt} \approx \int_0^t He^{-\alpha(t-\tau)} \frac{d\varepsilon}{d\tau} d\tau$$

for the hevea specimen.

Since we know that

$$\lim_{\alpha \rightarrow \infty} \alpha \int_0^t e^{-\alpha(t-\tau)} \frac{d\varepsilon}{d\tau} d\tau = \frac{d\varepsilon}{d\tau}$$

we expect that the approximate relation

$$H = \alpha\sigma$$

will hold.

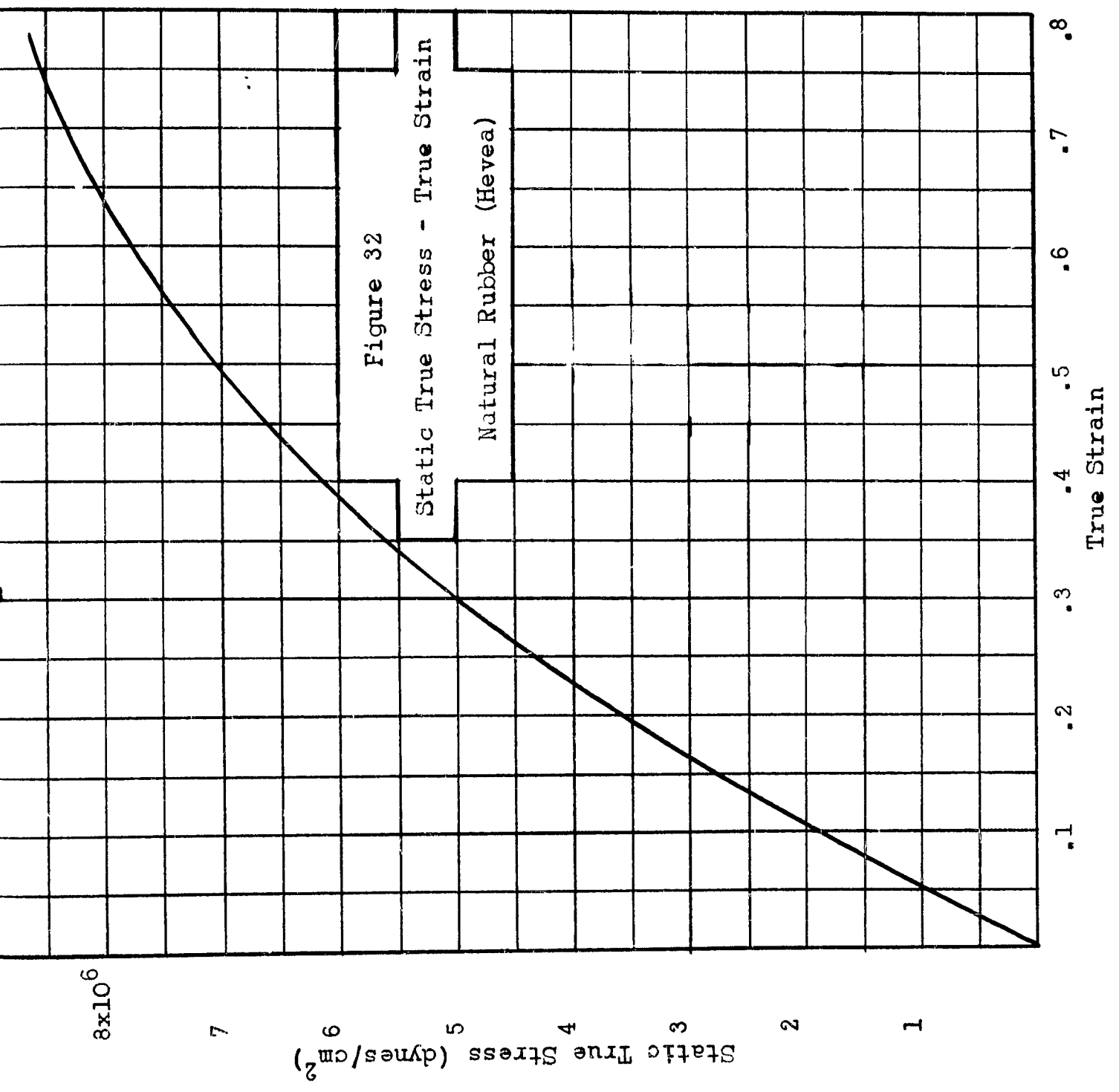
TABLE 4  
Results - Viscous Case

Nominal Velocity cm/sec	$\tau$ sec	$v_o$ cm/sec	$\epsilon_m$	p	q	C cm	D dynes/cm <sup>2</sup>	$\frac{\gamma}{\text{cm}^2}$ dyne-sec
25	$3.09 \times 10^{-2}$	23.7	0.172	5.15	102	0.233	$3.86 \times 10^7$	$4.02 \times 10^4$
50	$2.87 \times 10^{-2}$	47.8	0.338	5.05	110	0.453	$4.47 \times 10^7$	$3.75 \times 10^4$
75	$2.65 \times 10^{-2}$	77.3	0.481	6.08	119	0.650	$5.27 \times 10^7$	$4.52 \times 10^4$

TABLE 5  
Results - Hereditary Case

Nominal Velocity cm/sec	n	p	q	E dynes/cm <sup>2</sup>	H <sub>o</sub> dynes/cm <sup>2</sup>	H dynes/cm <sup>2</sup>	$\alpha$ sec <sup>-1</sup>	C cm
25	642	5.36	102	$2.44 \times 10^7$	$1.36 \times 10^7$	$2.62 \times 10^7$	653	$6.02 \times 10^{-4}$
50	543	8.77	111	$2.81 \times 10^7$	$1.63 \times 10^7$	$3.62 \times 10^7$	551	$2.92 \times 10^{-3}$

These results are shown graphically in Figs. 32 through 39.



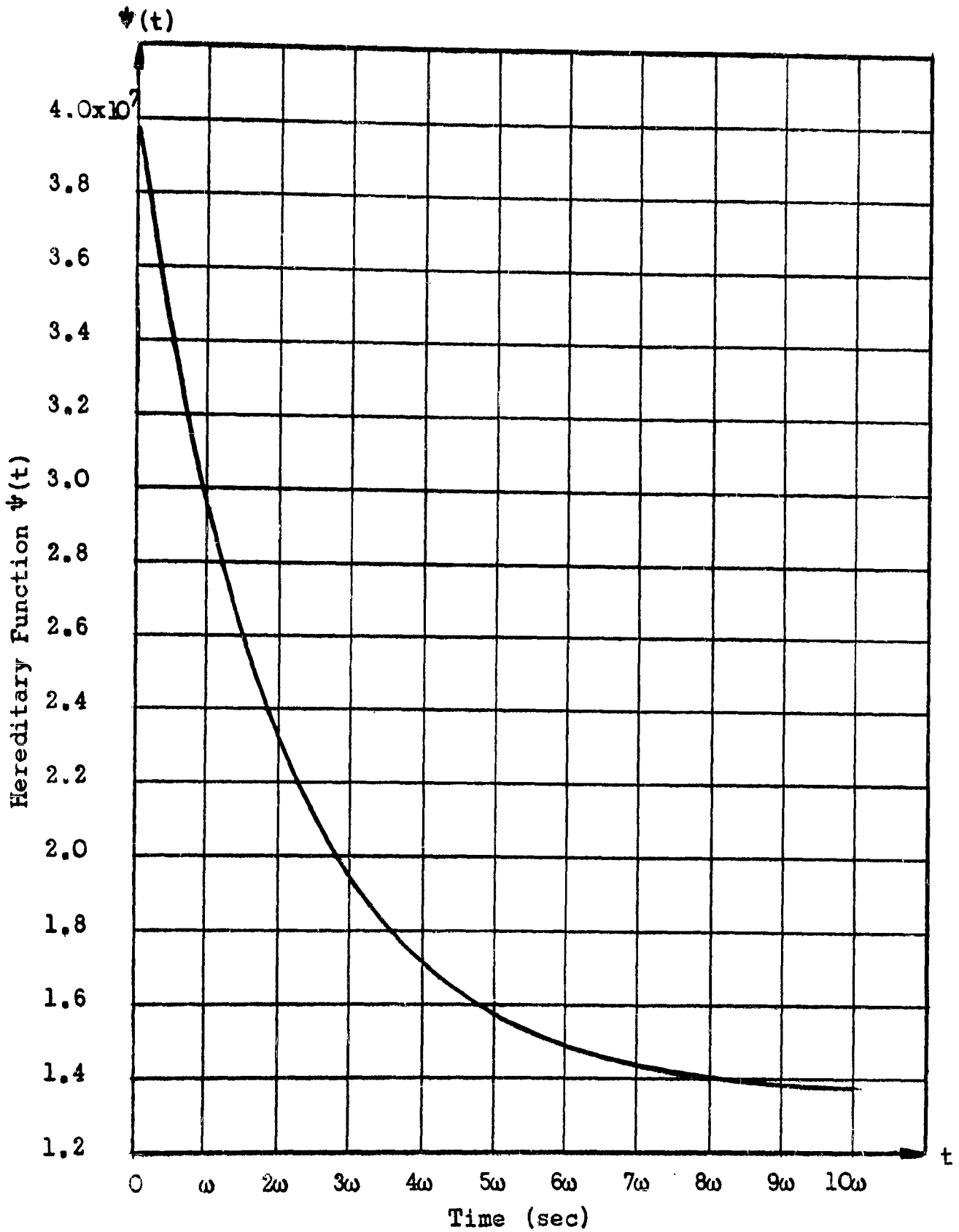


Figure 33

Hereditary Function

Nominal velocity 25 cm/sec;  $\omega = 3.088 \times 10^{-3}$  sec

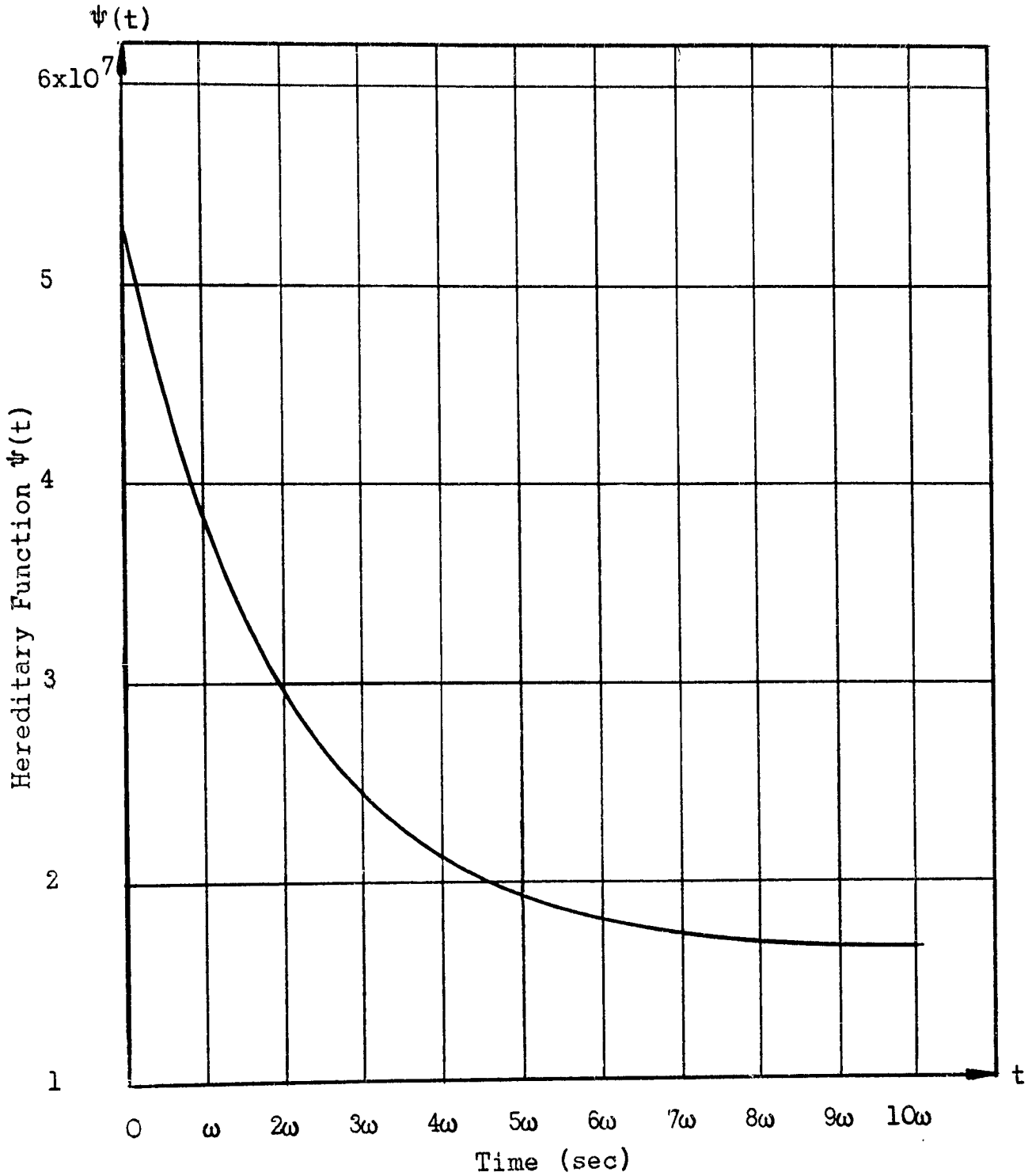


Figure 34

Hereditary Function

Nominal velocity 50 cm/sec;  $\omega = 2.872 \times 10^{-2}$  sec

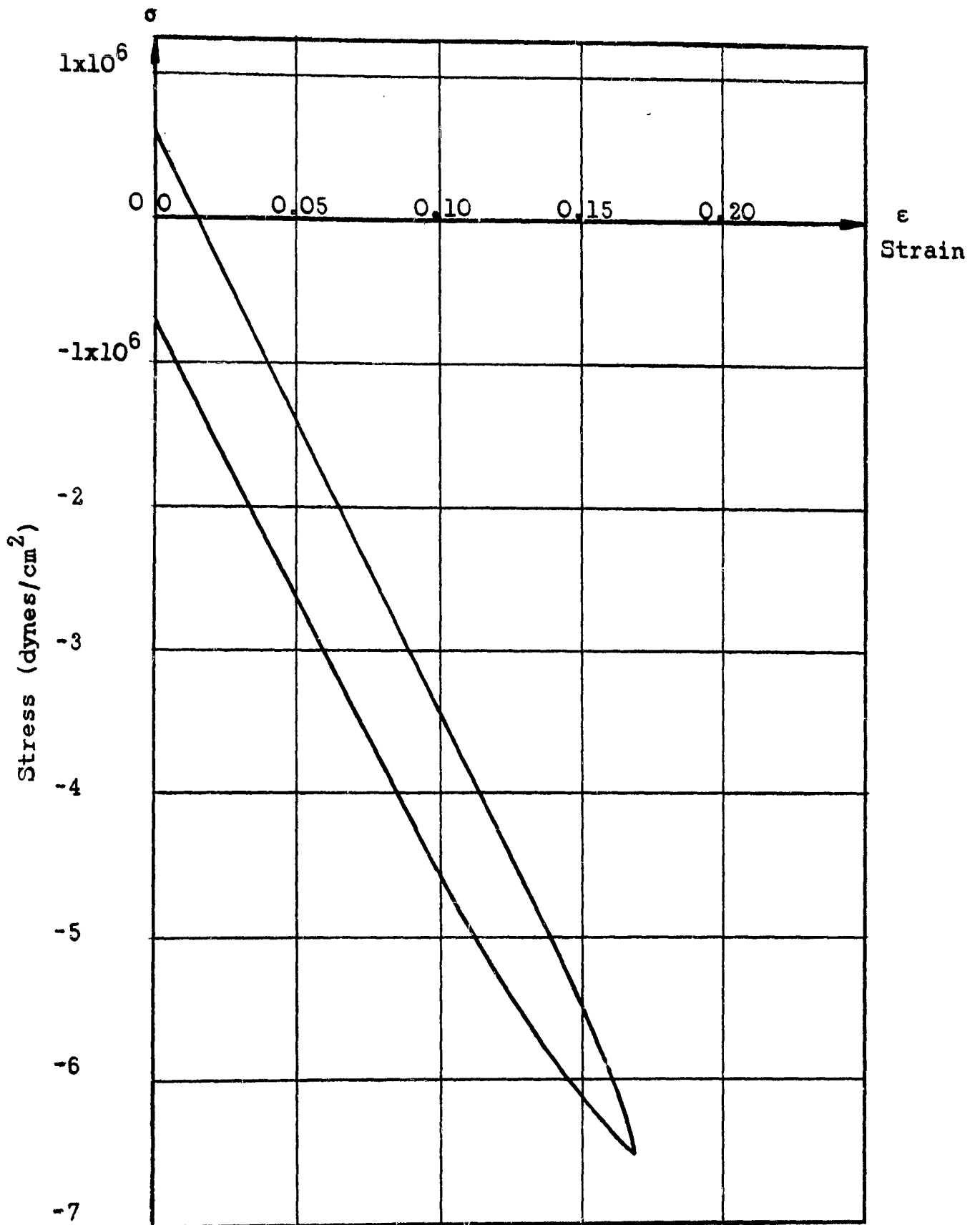


Figure 35

Stress versus Strain - Viscous Analysis

Nominal velocity 25 cm/sec

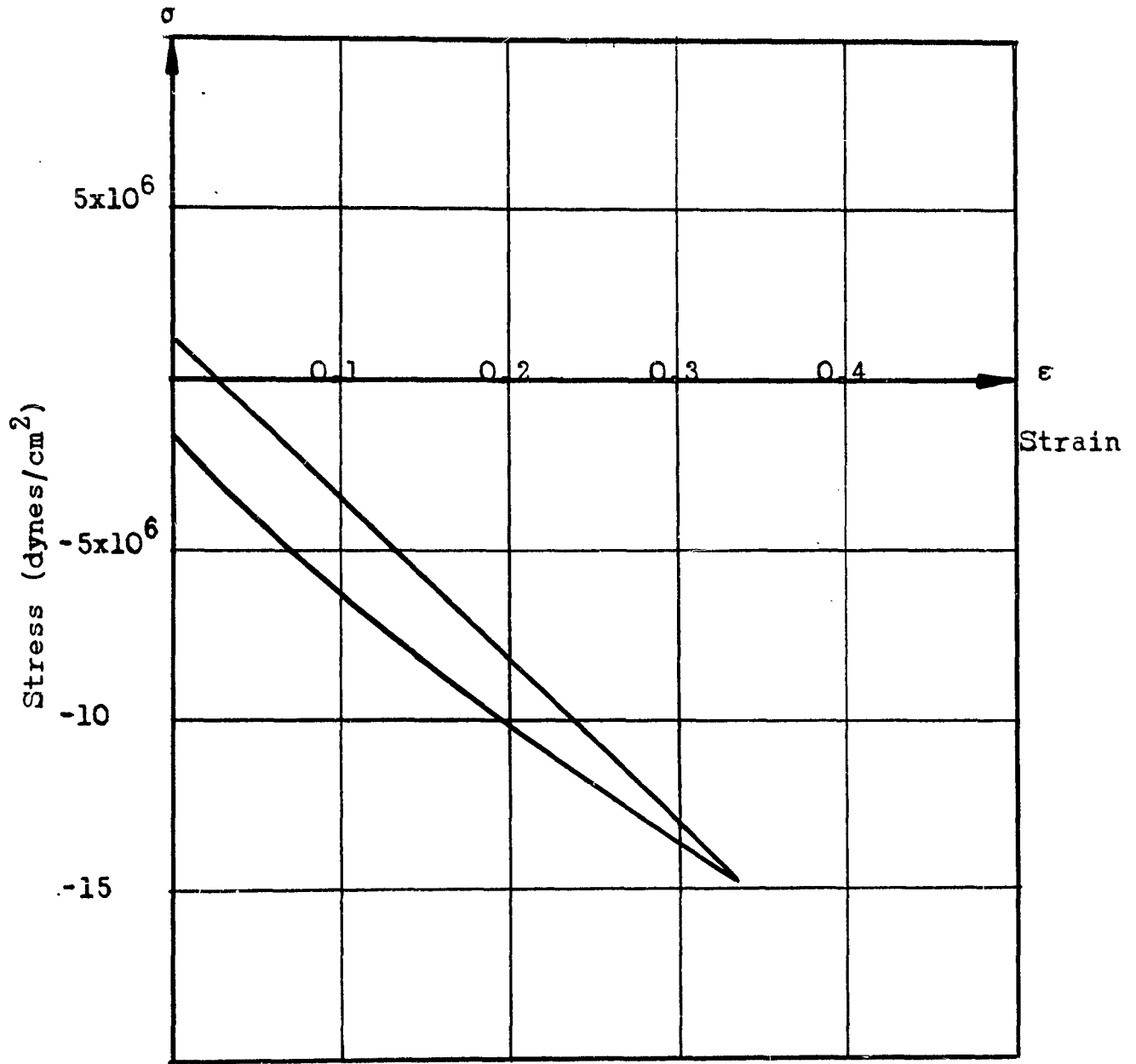


Figure 36

Stress versus Strain - Viscous Analysis

Nominal velocity 50 cm/sec

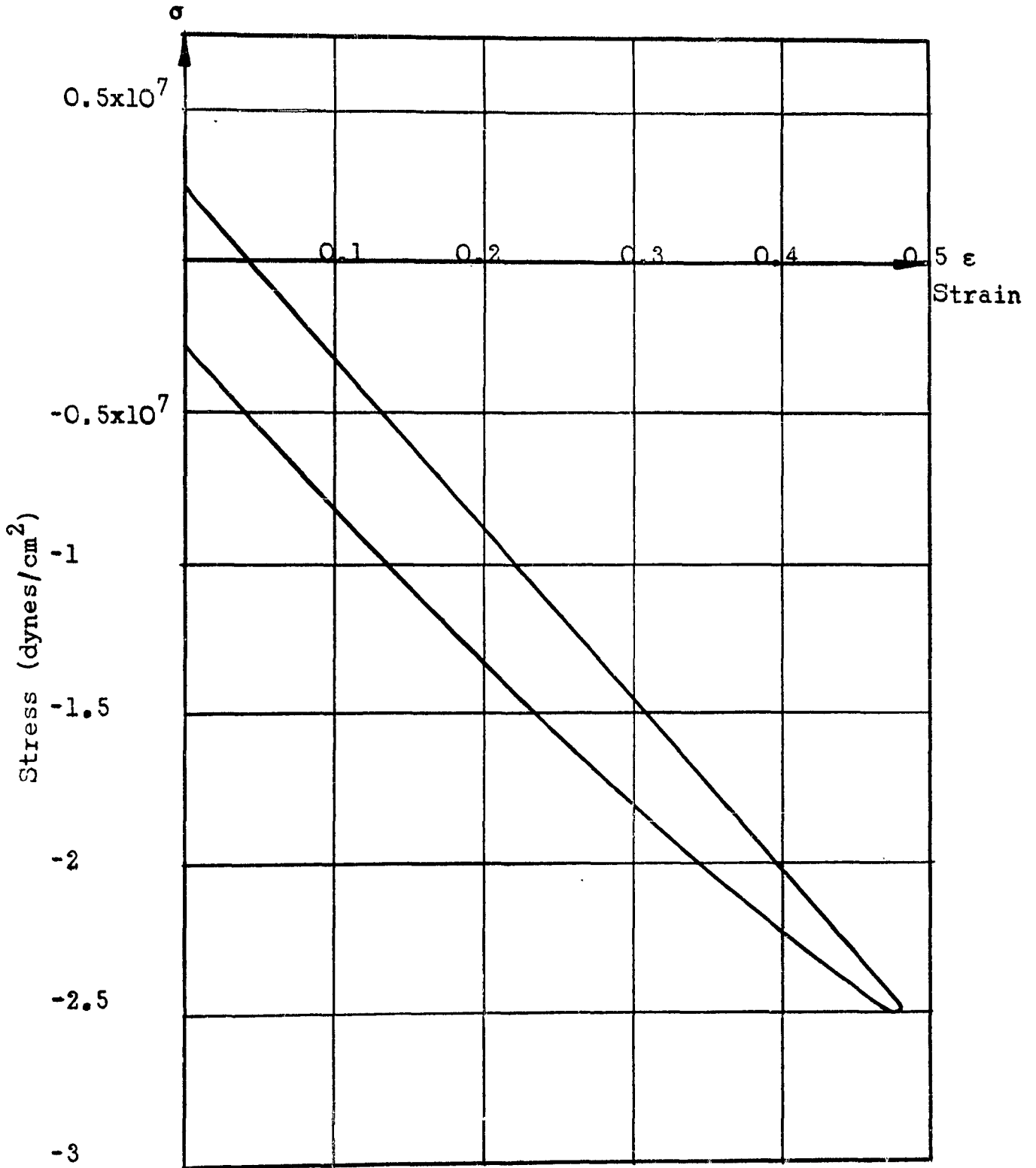


Figure 37

Stress versus Strain - Viscous Analysis

Nominal Velocity 75 cm/sec

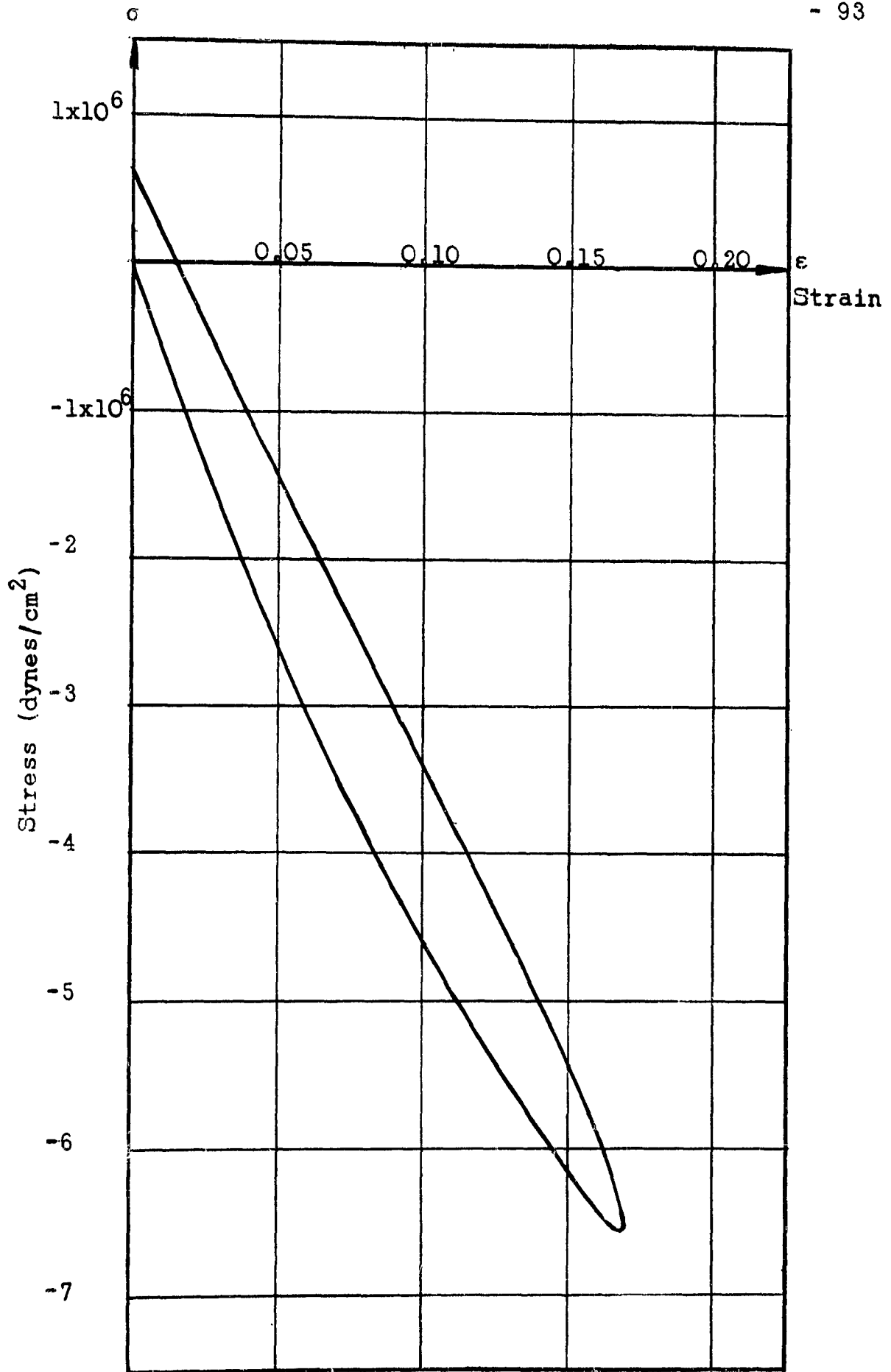


Figure 38

Stress versus Strain - Hereditary Analysis  
Nominal velocity 25 cm/sec

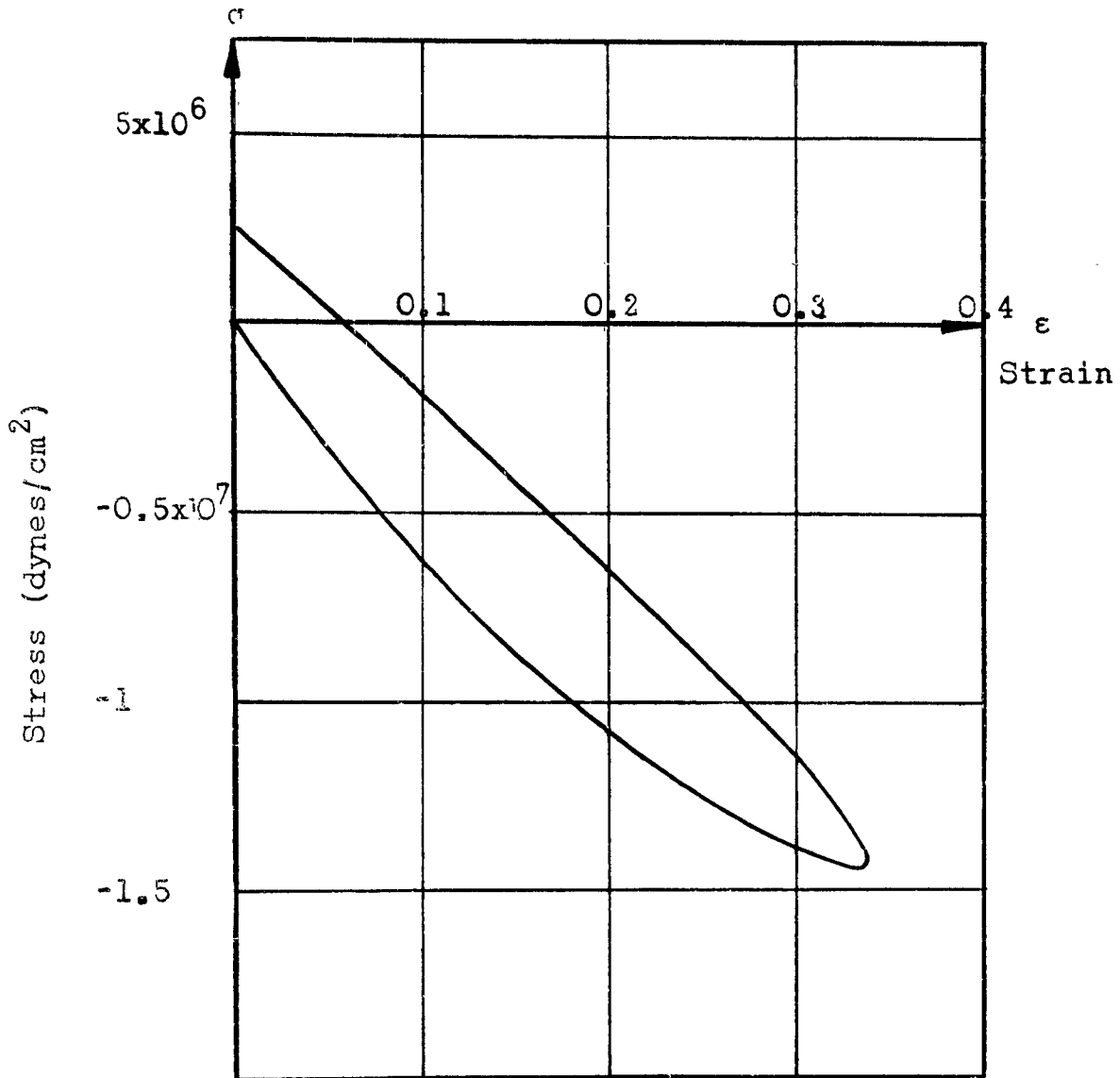


Figure 39  
Stress versus Strain - Hereditary Analysis  
Nominal velocity 50 cm/sec

At present, a series of tests has been completed on the Butyl-25 and Neoprene GNA. The computation of the results is now underway. These tests will be followed by a series on

1. Nylon
2. Polythene
3. GRS artic.

The results of these tests will appear in a final report in June 1953.

APPENDIX A

MATHEMATICAL ANALYSIS OF THE LONGITUDINAL IMPACT  
OF A BALL ON AN INFINITELY LONG BAR

## APPENDIX A

### Mathematical Analysis of the Longitudinal Impact of a Ball on an Infinitely Long Bar

A steel bar of mass  $m$ , radius  $r$ , and velocity  $v_0$  strikes the end of an infinitely long bar. We wish to find the pressure at the end of the bar as a function of time.

We take the stresses positive in compression and the displacement positive directed into the bar.

For an arbitrary force  $F(t)$  applied uniformly over the end of the bar:

$$\sigma(x, t) = \frac{1}{A} F\left(t - \frac{x}{c}\right)$$

where

$$c = \sqrt{\frac{E}{\rho}}$$

Since  $u = u\left(t - \frac{x}{c}\right)$  we have

$$\sigma(x, t) = -E \frac{\partial u}{\partial x} = \rho c \frac{\partial u}{\partial t}$$

The complete displacement due to the impact is

$$d = \beta + u$$

where  $\beta$  is the total indentation and  $u$  is the elastic deformation due to the force  $F(t)$ . The velocity is

$$v = \frac{\partial d}{\partial t} = \frac{\partial \beta}{\partial t} + \frac{\partial u}{\partial t}$$

By the law of impulse and momentum, we have at  $x = 0$

$$v = v_0 - \frac{1}{n} \int_0^t F(t) dt$$

thus

$$v_0 - \frac{1}{n} \int_0^t F(t) dt = \frac{d\beta}{dt} + \frac{1}{\rho c A} F(t)$$

Assume the Hertz law [13], i.e.,

$$F = k_2 \beta^{3/2}$$

$$k_2 = \frac{2E}{3(1+\nu)(1-\nu)} r^{1/2}$$

thus

$$\frac{d^2\beta}{dt^2} + \frac{k_2}{\rho c A} \frac{d}{dt} (\beta^{3/2}) + \frac{k_2}{n} \beta^{3/2} = 0$$

This differential equation is not easily integrated. Numerical solutions for boundary conditions of the type

$$\left. \begin{array}{l} \beta = 0 \\ v = v_0 \end{array} \right\} \text{for } t = 0$$

are available, however, for specific values of  $v_0$  and the constants of the equation.

Assume

$$k_2 = 1.73 \times 10^{12} \frac{\text{dynes}}{\text{cm}^{3/2}} \quad m = 365.1 \text{ gms}$$

$$\rho c = 4.05 \times 10^6 \frac{\text{gm-sec}}{\text{cm}^2} \quad A = 5.07 \text{ cm}^2$$

then for

$$\frac{d^2\beta}{dt^2} + b \frac{d}{dt} (\beta^{3/2}) + d \beta^{3/2} = 0$$

where

$$b = \frac{k_2}{pcA}; \quad d = \frac{k_2}{m}$$

we have

$$b = 8.44 \times 10^4 \text{ (cm}^{1/2}\text{sec)}^{-1}$$

$$d = 4.75 \times 10^9 \text{ (cm}^{1/2}\text{sec}^2)^{-1}$$

Initial conditions:

$$t = 0; \quad \beta = 0; \quad \frac{d\beta}{dt} = v_0$$

For  $m = 365.1$  gms, five cases were considered:

TABLE VI  
Ball Impact Values

$v_0$ (cm/sec)	T ( $\mu$ sec)	$\beta_{max}$ (mm)	$F_{max}$ ( $\times 10^9$ dynes)	$\sigma_{max}$ (Kg F/cm <sup>2</sup> )
45	245	0.0224	5.80	1166
90	192	0.0367	1.22	2453
135	176	0.0484	1.84	3704
180	164	0.0598	2.53	5088
220	157	0.0699	3.20	6435

The graphical solutions are given in Figures 40 through 44.

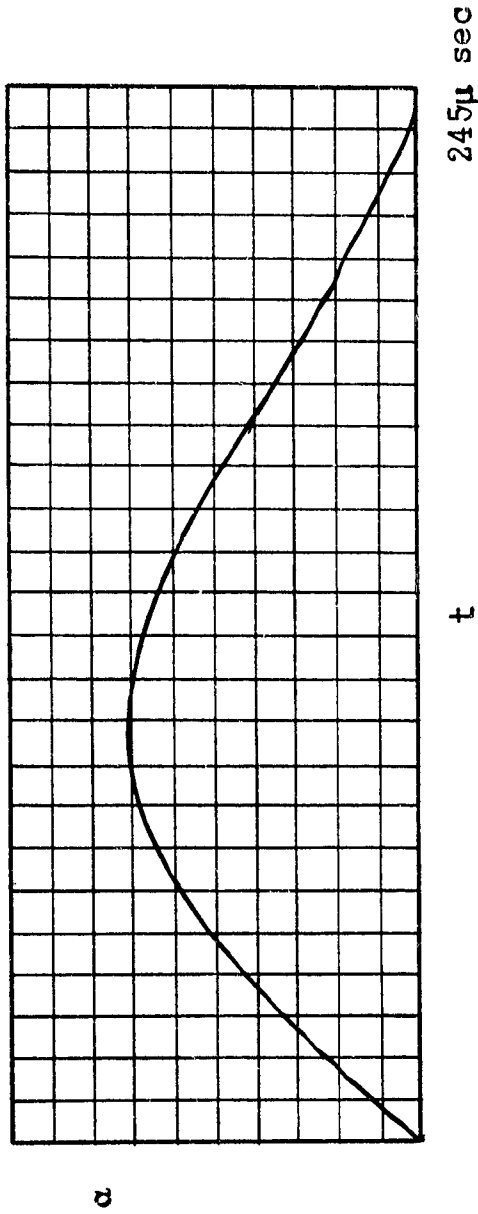


Figure 40

Ball impact -  $v_0 = 45$  cm/sec

(See Table 6)

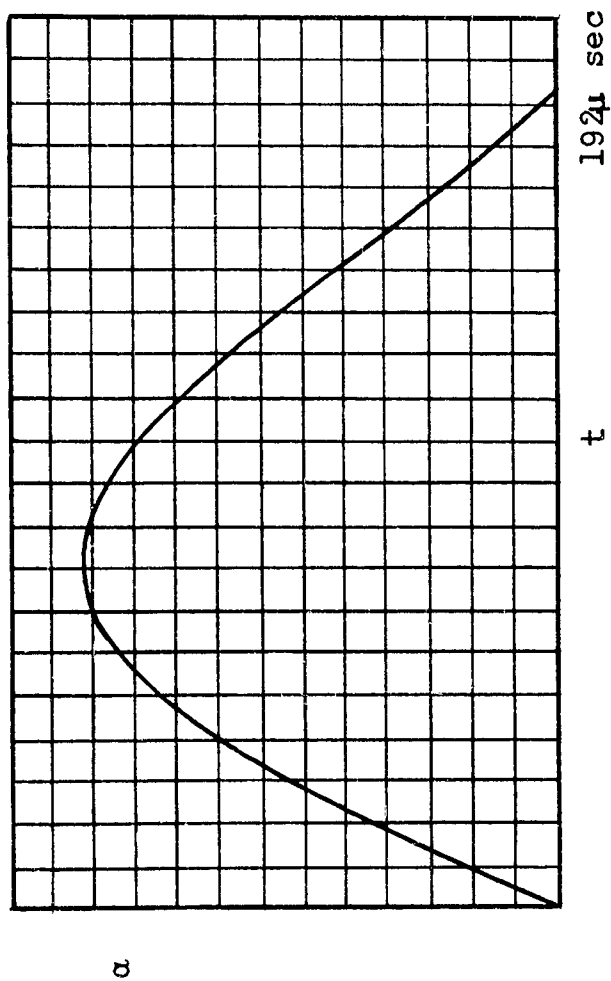


Figure 41

Ball impact -  $v_0 = 90 \text{ cm/sec}$

(See Table 6)

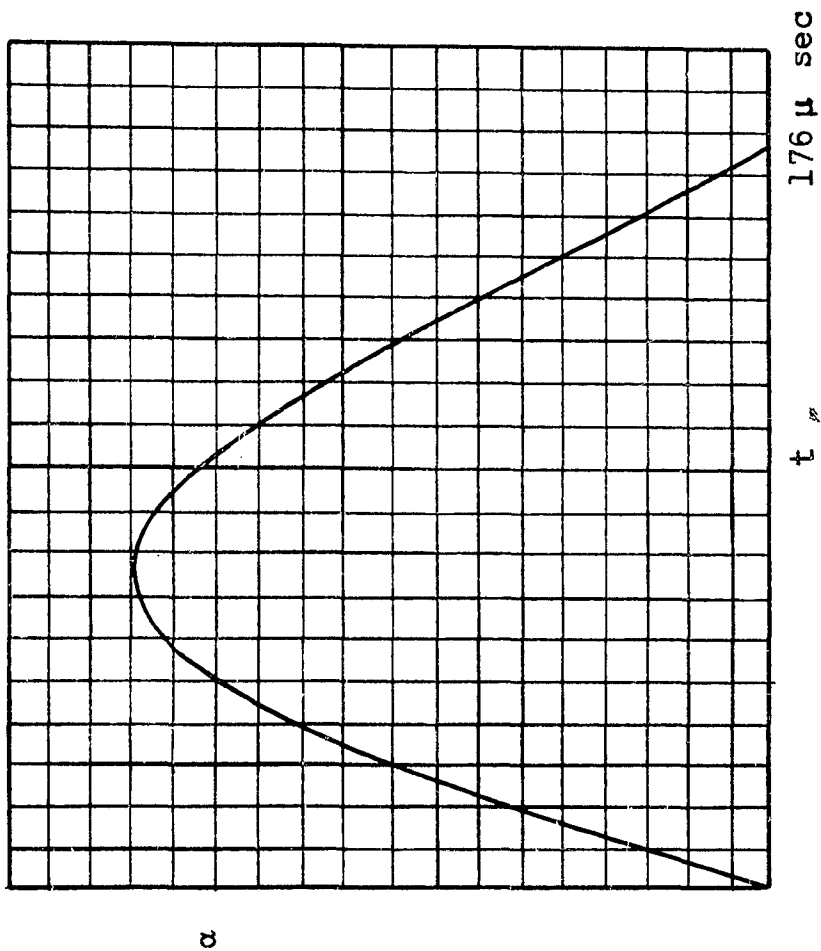


Figure 4.2

Ball impact -  $v_0 = 135$  cm/sec

(See Table 6)

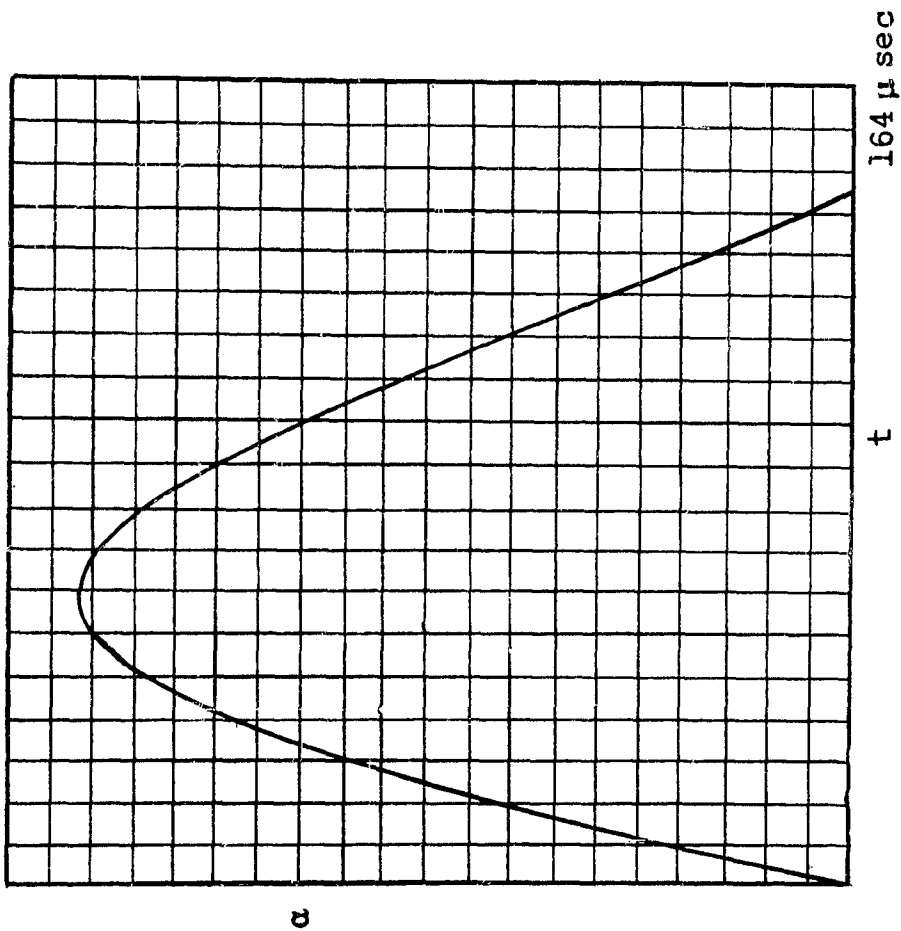


Figure 43

Ball impact -  $v_0 = 1.80$  cm/sec

(See Table 6)

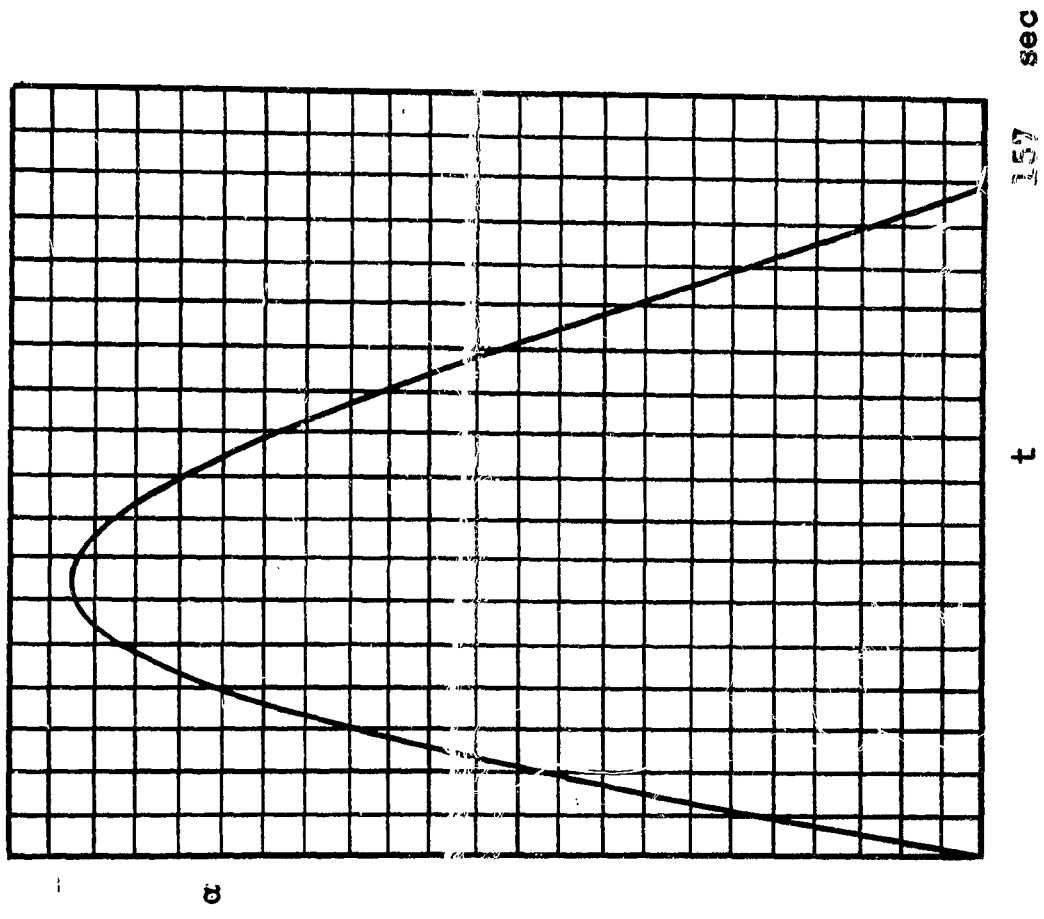


Figure 44

Ball impact  $v_0 = 220$  cm/sec

(See Table 6)

## APPENDIX B

### Rubber Specimen Recipes

The 1/2-inch by 1/2-inch rubber cylinders were fabricated in the Rubber Laboratories, Armour Research Foundation of Illinois Institute of Technology. They were made in an eight cavity mold of the following rubber compounds:

1. Hevea
2. Hycar OR-15
3. Neoprene GNA
4. GRS Artic (85 Butadiene/15 Styrene)
5. Butyl-25

The compounds were prepared on a two-roll 6 x 10-inch laboratory rubber mill with a front roll speed of 30 fpm and a speed ratio of back roll to front roll of 1.4 to 1. Cold water was circulated through both rolls during the mixing of the GRS, Butyl, Neoprene, and Hycar OR-15 compounds. No water was circulated during the mixing of the Hevea.

The formulas for the compounds are given in Table 7 and a summary of their physical properties is given in Table 8.

TABLE 7  
RUBBER SPECIMEN FORMULAS

<u>GRS (Artic)</u>		<u>Hycar OR-15</u>	
GRS (artic)	100	Hycar OR-15	100
Reogen	10	P-33	25
P-33	25	Diocetyl Adipate	30
Zinc Oxide XX78	5	Zinc Oxide XX78	5
Stearic Acid	2	Stearic Acid	1
Agerite Stalite	1	Agerite Stalite	1
H Teads	3	H Teads	3
D.P.G.	1	D.P.G.	1
<u>Neoprene</u>		<u>Butyl 25</u>	
Neoprene GNA	100	Butyl 25	100
L.C. MgO	3	P-33	25
P-33	25	Zinc Oxide XX78	5
Circo Lt. Process Oil	15	Mineral Oil (White)	1
Neozone D	1	Lime (CaOH)	5
Stearic Acid	1	Sulfur	2
Zinc Oxide XX78	5	Thiomex	1
		Polyac	0.5
		Akroflex C	2
<u>Natural Rubber</u>			
Smoked Sheets		100	
Reogen		10	
Zinc Oxide		5	
Stearic Acid		2	
Agerite Stalite		1	
P-33		25	
Methyl Teads		3	
D.P.G.		1	

TABLE 8  
 SUMMARY OF PHYSICAL PROPERTIES OF  
 RUBBER COMPOUNDS GIVEN IN TABLE 7

Stock	320°F	M500	T	E	S	Shore "A" Hardness
Hevea	10	600	2300	850	15	38
	20	710	2880	710	10	38
	30	725	2550	670	8	38
GRS (Artic)	30	215	270	565	10	38
Hycar OR-15	30	195	1280	945	13	31
Neoprene	30	965	2620	840	15	44
Butyl 25	30	-	365	285	0	43

M500 - Modulus at 500 per cent Elongation

T - Tensile Strength (psi)

E - Elongation (per cent)

S - Permanent Set at Break

## BIBLIOGRAPHY

## BIBLIOGRAPHY

- [1] "The Development of Pressure Waves During the Longitudinal Impact of Bars", by W. A. Prowse, The London, Edinburgh, and Dublin Philosophical Magazine, Series 7, Volume 22, (1936).
- [2] "On the Longitudinal Impact of Metal Rods with Rounded Ends", by J. E. Sears, Proceedings of the Cambridge Philosophical Society, Volume 14, (1908).
- [3] "On the Longitudinal Impact of Metal Rods with Rounded Ends", by J. E. Sears, Transactions of the Cambridge Philosophical Society, Volume 21, (1912).
- [4] "Experiments on the Duration of Impacts Mainly on Bars with Rounded Ends, in Elucidation of the Elastic Theory", by J. E. Wagstaff, Proceedings of the Royal Society of London, Series A, Volume 105, (1924), also see, London, Edinburgh, and Dublin Philosophical Magazine, Series 6, Volume 48, (1924).
- [5] "The Testing of Materials at High Rates of Loading", by G. I. Taylor, Journal of the Institution of Civil Engineers, London (1946).
- [6] "Alcuni risultati di prove dinamiche sui materiali", by Enrico Volterra, La Rivista del Nuovo Cimento, Volume IV, No. 1 (1948).
- [7] "Vibrations of Elastic Systems Having Hereditary Characteristics", by Enrico Volterra, Journal of Applied Mechanics, Volume 17, No. 4, (1950).
- [8] "On the Numerical Solutions of Integral Equations", by E. T. Whittaker, Proceedings of the Royal Society of London, Volume 94, Series A, (1918).
- [9] "The Calculus of Observations", by E. T. Whittaker and G. Robinson, Blackie and Son, London, (1924).
- [10] "A Method of Measuring the Pressure Produced in the Detonation of High Explosives or by the Impact of Bullets", by B. Hopkinson, Philosophical Transactions of the Royal Society of London, Series A, Volume 213, (1914).
- [11] "A Critical Study of the Hopkinson Pressure Bar", by R. M. Davies, Philosophical Transactions of the Royal Society of London, Series A, Volume 240, (1948).

- [12] "Longitudinal Wave Transmission and Impact", by L. H. Donnell, Transactions of the American Society of Mechanical Engineers, Volume 52, No. 22, (1930).
- [13] "The Mathematical Theory of Elasticity", by A. E. H. Love, Fourth edition, Dover Publications, New York, New York (1944).
- [14] "Über inners Reibung fester Körper, insbesondere der Metalle", by W. Voigt, Annalen der Physik, Volume 47, (1892).
- [15] "Zur Theorie der elastische Nachwirkung", by L. Boltzmann, Annalen der Physik, Volume 7, (1876).
- [16] "Physikalische Grundlagen der Festigkeitlehre", by T. von Kármán, Enzyklopädie der Mathematischen Wissenschaft, Section 4, Volume 11.
- [17] "Modern Operational Mathematics in Engineering" by R. V. Churchill, McGraw-Hill Book Company, Inc., New York (1944)
- [18] "Theorie und Anwendung der Laplace-Transformation", by G. Doetsch, Springer, Berlin (1937).
- [19] "The Propagation of a Disturbance in a Visco-Elastic and Visco-Plastic Bar", by I. N. Zverev. Translated by Graduate Division of Applied Mathematics, Brown University, Providence, R. I. Report to Office of Naval Research, NR-041-032. Contract N7onr-358, Task order 1. (January, 1951).
- [20] "Sur l'équation des ondes dans le domaine héréditaire", by H. Charles, Bulletin de la Société Royale des Sciences de Liège, Volume 20, No. 3, (1951).

Contributing personnel:

E. G. Volterra, Project Director

D. Muster, Project Engineer

R. A. Eubanks, Research Engineer

L. Tybur, Instrumentation Engineer

R. Balbert, Technician

R. A. Einweck, Technician

C. R. Olson, Technician

Respectfully submitted,

Mechanics Department

ILLINOIS INSTITUTE OF TECHNOLOGY



---

E. G. Volterra  
Professor of Mechanics